

**SURFACE COLOUR EFFECTS ON THE THERMAL BEHAVIOUR AND
MECHNICAL PROPERTIES OF HOT MIX ASPHALT**

**SURFACE COLOUR EFFECTS ON THE THERMAL BEHAVIOUR AND
MECHANICAL PROPERTIES OF HOT MIX ASPHALT**

By

ISLAM ABU-HALIMEH, B.ENG. (CIVIL ENGINEERING)

A Thesis

**Submitted to the School of Graduate Studies
In Partial Fulfillment of the Requirements
For the Degree**

Master of Applied Sciences M.A.Sc

McMaster University

© Copyright by Islam Abu-Halimeh, April 2007

ASTER OF APPLIED SCIENCES (2007) McMASTER UNIVERSITY
(Civil Engineering) Hamilton, Ontario

**TITLE: SURFACE COLOUR EFFECTS ON THE THERMAL
BEHAVIOUR AND MECHANICAL PROPERTIES OF
HOT MIX ASPHALT**

**AUTHOR: Islam Abu-Halimeh, B.Eng., (McMASTER
UNIVERSITY)**

**SUPERVISOR: Dieter F. Stolle, Ph.D., P.Eng (McMaster University,
Department of Civil Engineering, Hamilton, Ontario)**

NUMBER OF PAGES: 141

ABSTRACT

The focus of the study was to evaluate the effect of placing hydrated lime on the surface of asphalt concrete pavement. The study assesses the influence of hydrated lime on both the peak surface temperature as well as the temperature profile of the pavement with depth. The amount of lime that would yield the optimal temperature reductions without placing excess ineffective material was selected. To address the aforementioned goal, eight Superpave mix samples were prepared in the lab and compacted at the design compaction temperature to achieve a relatively consistent percent of air voids. All samples were compacted using a vibratory compactor to simulate real field construction procedures and conditions. To examine the effect of hydrated lime, surface temperatures as well as with-depth temperature measurements were made with an infrared camera, and thermocouples buried into the pavement, respectively. The same tests were performed at a field site with a newly laid down pavement. To minimize variables, the field Hot Mix Asphalt (HMA) pavement was of the same design as that used to prepare the lab samples.

The effect of temperature on the mechanical properties of HMA mixtures used in Ontario; namely Superpave SP12.5FC2 PG64-28, SP12.5FC2 PG70-28, SP19.0, and Stone Mastic Asphalt (SMA), was assessed. The mechanical properties studied include rutting susceptibility, fatigue resistance, and resilient modulus. Thirty two samples were prepared in the laboratory and compacted at the design compaction temperature and

percent air voids. For each mix, two samples were used to test rutting susceptibility, three samples were used to test fatigue resistance, and three samples were used to test the resilient modulus of the mixes. With regards to rutting, the samples were tested in the Asphalt Pavement Analyzer (APA) at four different temperatures in order to give a complete rutting versus temperature profile. Three samples of each mix were tested to measure the resilient modulus at different temperatures using the Nottingham Asphalt Tester (NAT). Lastly, the fatigue resistance for each mix was assessed in the NAT with each of the three samples tested at a different strain to provide a complete picture of the mix behaviour when subjected to fatigue. The stiffness characteristics of the newly laid down in-situ pavement was determined using the Light Weight Deflectometer (LWD).

Results indicate that placing 100g/m^2 of hydrated lime on the surface of the hot mix asphalt pavement was the optimum surface treatment while avoiding the placement of excess ineffective material. This level of surface treatment led to temperature reductions that significantly improved the mechanical properties of asphalt concrete. Using the increased resilient modulus, consistent with the temperature reductions, it was shown, by carrying out an analysis using KENLAYER, that the design life of a pavement could be increased from approximately 25 to 33 years, from 20 to 30 years and from 12 to 20 years corresponding to cool, intermediate and hot weather conditions, respectively.

ACKNOWLEDGEMENTS

In presenting this thesis, I would like to express my most sincere thanks and gratitude to the following individuals:

- My supervisor, Dr. Dieter Stolle for his guidance, support, and patience throughout this thesis.
- The President of John Emery Geotechnical Engineering Ltd (JEGEL), Dr. John J. Emery, for the project which involved a technology that had been developed by JEGEL, for his technical guidance and supervision throughout the course of my research, and also for his funding towards my Industrial *Natural Sciences and Engineering Research Council* of Canada (NSERC) Scholarship.
- Dr. Peijun Guo for the help he provided on theory during the course of the experimental work.
- Those associated with the Construction Materials and Testing Lab at JEGEL, and specifically Mr. Dawit Amar (Lab Manager), for their discussion and help with the actual preparation and testing of the specimens.
- Mr. Raymond Lau, Geotechnical & Material Testing Co-ordinator, Engineering & Works Section in the Transportation & Works Department at the City of Mississauga for his appreciated support in locating a field site and during field testing.

Finally, I would like to extend my heartfelt appreciation
with a special thank you to my family,

- Abdallah Abu-Halimeh (Father)
- Muna Hourani (Mother)
- Najat Abu-Halimeh (Older Sister)
- Mohammad Abu-Halimeh (Younger Brother)
- Nour Abu-Halimeh (Younger Sister)

and last but not least, to my wife Basma Qattous, for their support and encouragement towards my Engineering and Master's Degrees at McMaster University.

TABLE OF CONTENTS

CHAPTER 1. INTRODUCTION	1
1.1 Research Background	1
1.2 Lime As An Additive.....	3
1.3 Applications of Hydrated Lime in HMA Mixes	4
1.3.1 Anti-Stripping	4
1.3.2 Rutting.....	5
1.3.3 Aging.....	6
1.3.4 Fatigue Cracking.....	7
1.3.5 Fracture Toughness.....	8
1.3.6 Top-Down Cracking (TDC).....	9
1.3.7 Extended Benefits	10
1.4 Economics.....	10
1.5 Summary of Objectives.....	11
 CHAPTER 2. MIXES AND MATERIAL	 13
2.1 Introduction	13
2.2 Superpave SP12.5 FC2 PG64-28 and SP12.5 FC2 PG70-28	15
2.3 Superpave SP19	20
2.4 SMA.....	20
 CHAPTER 3. LABORATORY PAVEMENT SAMPLES.....	 26
3.1 Sample Preparation	26
3.2 Testing of Air Voids	29

TABLE OF CONTENTS (CONT'D)

CHAPTER 4. EFFECT OF HYDRATED LIME AMOUNT ON THE SURFACE TEMPERATURE OF HMA PAVEMENT	30
4.1 LABORATORY TESTING.....	30
4.1.1 Sample Preparation	31
4.1.2 Testing Apparatus: The FLIR Infrared Camera.....	34
4.1.3 Testing Procedures.....	35
4.1.4 Results.....	36
4.1.5 Discussion.....	39
4.2 FIELD TESTING.....	40
4.2.1 Site Preparation.....	41
4.2.2 Testing Setup and Procedures.....	42
4.2.3 Results.....	43
4.2.4 Discussion.....	43
4.3 METHOD OF ADDING HYDRATED LIME TO THE SURFACE OF HMA PAVEMENTS	46
CHAPTER 5. EFFECT OF HYDRATED LIME ON THE PROFILE TEMPERATURE OF HMA PAVEMENT	48
5.1 LABORATORY TESTING.....	48
5.1.1 Sample Preparation	49
5.1.2 Testing Procedures.....	52
5.1.3 Results.....	53
5.1.4 Discussion.....	54
5.2 FIELD TESTING.....	55
5.2.1 Site Preparation.....	56
5.2.2 Testing Procedures.....	58

TABLE OF CONTENTS (CONT'D)

5.2.3	Results.....	59
5.2.4	Discussion.....	60
CHAPTER 6. MECHANICAL PROPERTIES OF HMA MIXES.....		63
6.1	EQUIPMENT AND PROCEDURES.....	63
6.1.1	Nottingham Asphalt Tester (NAT)	63
6.1.1.1	Resilient Modulus Testing	65
6.1.1.2	Fatigue Resistance Testing	69
6.1.2	Light Weight Deflectometer (LWD)	71
6.1.3	Asphalt Pavement Analyzer (APA).....	75
6.2	SUMMARY OF RESULTS	79
6.3	RESILIENT MODULUS TESTING	81
6.3.1	Factors Affecting Resilient Modulus	81
6.3.2	Results and Discussion	83
6.4	EFFECTIVE SURFACE MODULUS FROM LWD TESTING.....	85
6.4.1	Analysis of Results	86
6.4.2	Results and Discussion	89
6.4.3	Effect of Hydrated Lime on Elastic Modulus of HMA Mixes	92
6.5	FATIGUE RESISTANCE TESTING.....	92
6.5.1	Results and Discussion	93
6.6	RUTTING RESISTANCE TESTING	97
6.6.1	Factors Influencing Rutting	98
6.6.2	Results.....	99
6.6.3	Discussion.....	102
6.6.4	Effect of Hydrated Lime on Rutting Resistance of HMA Mixes	106

TABLE OF CONTENTS (CONT'D)

CHAPTER 7. REAL WORLD APPLICATIONS OF HMA SURFACE MODIFICATION	108
7.1 PROCEDURES.....	108
7.2 RESULTS AND DISCUSSION	115
CHAPTER 8. CONCLUSIONS AND RECOMMENDATIONS	122
References.....	126
Appendix A.....	132
Appendix B	133
Appendix C	139

LIST OF FIGURES

1-1	<i>Left:</i> Hydrated Lime Production Cycle, <i>Right:</i> Hydrated Lime Sample	4
2-1	(A) SP12.5 FC2 PG64-28 Sample. (B) SP12.5 FC2 PG70-28 Sample. (C) SP19.0 Sample. (D) SMA Sample.....	14
3-1	Laboratory Samples Preparation Procedure.....	28
4-1	Placement of Hydrated Lime on the Surface of an HMA Pavement Sample	32
4-2	Large Patch/Pavement Grid As Is Encountered In-Situ.	33
4-3	<i>Left:</i> FLIR Thermacam Infrared Camera, <i>Right:</i> Example Infrared Thermal Image.....	35
4-4	Effect of Hydrated Lime Amount on Surface Temperature of HMA Laboratory Pavement with Time	37
4-5	Change in Surface Temperature between Black Unmodified Pavements and Those Modified with Different Hydrated Lime Amounts with Time.....	38
4-6	Peak Change in Surface Temperature between Black Unmodified Pavements and Those Modified with Different Hydrated Lime Amounts at Six Hours after Test Start.....	38
4-7	Field Testing Setup	41
4-8	Field Surface-Modified Pavement with 50, 100 and 150g/m ² of Hydrated Lime	41
4-9	Effect of Hydrated Lime Amount on Surface Temperature of Field HMA Pavement.....	44
4-10	Relationship between Laboratory and Field Site Surface Temperature Reduction for 100g/m ² of Hydrated Lime Dosage	45
4-11	Dry Hydrated Lime Application with Mechanical Spreader	46
5-1	Butt-Welded Unsheathed Micro-Temperature Thermocouple	50
5-2	Illustration of Thermocouples Configuration on a Laboratory Prepared Sample.....	50

LIST OF FIGURES (CONT'D)

5-3	Laboratory Sample Being Prepared for Temperature Profile Testing	52
5-4	Temperature Profile Laboratory Testing Apparatus	53
5-5	Peak Temperature Profiles of Laboratory Pavement That is Surface-Modified with Hydrated Lime at 0 and 100g/m ² Concentrations.....	54
5-6	Illustration of Thermocouples Configuration for Field Pavement.....	57
5-7	Thermocouples Placed into Black Unmodified and 100g/m ² Hydrated Lime Surface-Modified Field Pavement	58
5-8	Peak Temperature Profiles of Field Site Pavement That is Surface-Modified with Hydrated Lime at 0 and 100g/m ² Concentrations.....	59
5-9	Field Site versus Laboratory Temperature Profile Reduction.	62
6-1	The Nottingham Asphalt Tester (NAT)	64
6-2	Coring of HMA Samples	67
6-3	Resilient Modulus Testing Setup, Inside the NAT	68
6-4	(a): Fatigue Resistance Testing Setup, Inside the NAT, (b): Illustration of Specimen Failure in Fatigue	70
6-5	<i>Top Left:</i> LWD and Its Bluetooth Connection Ability <i>Left:</i> Screen Shot Of Sample Test Results <i>Top:</i> Deflections Measured with Three Sensors	72
6-6	Falling Weight Deflectometer (FWD)	73
6-7	Section of Traffic Lane Marked for Testing (Prior To Paving).....	74
6-8	<i>Left:</i> The Asphalt Pavement Analyzer (APA), <i>Right:</i> Testing Setup & Running Test Illustration	77
6-9	Preheating Of APA Testing Specimens Using A Curing Lamp	78
6-10	Effect of Temperature on Resilient Modulus of HMA Mixes	84
6-11	LWD-Mod Analysis Window	87
6-12	Relationship between Dynamic Poisson's Ratio and Temperature	88

LIST OF FIGURES (CONT'D)

6-13	In-Situ Effective Surface Modulus versus Surface Temperature	90
6-14	Effective LWD Stiffness versus Elastic NAT Resilient Modulus of The SP12.5FC2 PG64-28 HMA Mix	91
6-15	NAT Fatigue Endurance Testing of HMA Mixes.....	95
6-16	Rutting History of HMA Mixes at 70°C.....	101
6-17	Rutting Deformation of HMA Mixes With Temperature at 8000 Cycles	102
6-18	HMA Sample Tested for Rutting Resistance.....	102
7-1	KENLAYER Sample Analysis Window	110
7-2	Vertical Stress Measured at Bottom of HMA Layer for Black and 100g/m ² of Hydrated Lime Modified Pavement vs. Air Temperature.....	116
7-3	Vertical Stress Measured at Top of Subgrade Layer for Black and 100g/m ² of Hydrated Lime Modified Pavement vs. Air Temperature.....	117
7-4	Horizontal Strain Measured at Bottom of HMA Layer for Black and 100g/m ² of Hydrated Lime Modified Pavement vs. Air Temperature.	118
7-5	Vertical Strain Measured at Top of Subgrade Layer for Black and 100g/m ² of Hydrated Lime Modified Pavement vs. Air Temperature.....	119

LIST OF TABLES

1-1	Cost Summary of Surface Modification of HMA Mixes with Hydrated Lime.....	11
2-1	Superpave and SMA Ontario Traffic Categories.....	13
2-2	SP12.5FC2 PG64-28 Mix Design / Surface Course.....	18
2-3	SP12.5FC2 PG70-28 Mix Design / Surface Course.....	19
2-4	SP19.0 Mix Design / Base Course.....	21
2-5	SMA Mix Design / Surface Course.....	24
2-6	Comparison between SMA and Conventional HMA Mixtures.....	25
6-1	Summary of Resilient Modulus Data vs. Temperature of HMA Mixes.....	80
6-2	Summary of Rutting and Fatigue Life Data vs. Temperature of HMA Mixes.....	80
6-3	Relationship between Rutting Rates and Testing Temperature of Different HMA Mixes.....	105
6-4	Stiffness Rate of Change with Temperature for Different HMA Mixes.....	106
7-1	Actual Input Sets Corresponding To Different Summer Day Temperatures.....	112
7-2	Comparison between LTPPBind and Study Profile Temperatures for Different Hydrated Lime Concentrations (During hot summer day).....	113
7-3	Average Input Sets Corresponding To Different Summer Day Temperatures.....	113
7-4	Allowable Number of Load Repetitions for All Analysis Cases.....	121
7-5	Damage Analyses Results.....	121

CHAPTER 1

INTRODUCTION

The demands and reliance placed on roadways for mobility and commerce have increased substantially over the past 50 years. The highway network is not only the economic backbone of a country, but it also provides the only transportation access to a growing number of communities. To ensure that this mode of transportation remains cost effective, it is important that the design life of pavements is maximized. This thesis investigates a technology that is expected to prolong that service life of hot mix asphalt (HMA) pavement.

1.1 RESEARCH BACKGROUND

The transportation demands of the 21st century cannot be met by a 20th century road technology, mainly due to the dramatic increase in the volume and the weight of vehicular traffic. Pavement technology is being developed to deliver materials, design and testing innovations that result in the improved performance, safety, maintainability and sustainability of pavements. Superpave asphalt mix design is a new pavement design philosophy, but is complicated by many variables such as the temperature, which varies considerably over the year with changing seasons.

The temperature of an asphalt concrete pavement has a significant impact on its behaviour due to its viscoelastic/plastic nature. High summer temperatures reduce the asphalt concrete's resilient modulus and shear strength, which in turn decreases the resistance to the development of permanent deformations (rutting) under heavy vehicular loadings. Low winter temperatures, on the other hand, increase asphalt concrete resilient modulus and shear strength, together with the asphalt binder stiffness, leading to a reduction in the resistance to fatigue and temperature cracking. Technologies to reduce the in-service, hot-weather temperature of asphalt pavements, particularly near the surface where loading shear stresses are greatest, is of considerable technical and economical interest, which in turn contribute in a positive manner to maintaining a sustainable infrastructure. At this point in time, to improve pavement performance, asphalt cement is selected for a particular application taking into account the highest and lowest temperatures anticipated for each lift of the asphalt concrete pavement.

A practical asphalt technology, which has been used on runways at the Toronto Pearson International Airport, is investigated in this study, which lightens the surface colour of the pavement, thus, reducing the black body absorption and hot-weather temperature of a new HMA surface. The reduction in temperature improves the performance of the pavement by increasing stiffness and reducing rutting. Many methods and treatments are available for lightening the surface of the HMA, one of which is the placement of hydrated lime. This thesis investigates the beneficial effects of hydrated

lime on the properties of pavement as a result of its placement on the surface of a new HMA mix. In addition to carrying out tests, the study makes use of computer analysis to demonstrate the benefits of hydrated lime surface treatment with respect to reducing the stresses and strains at various points in the pavement structure, leading to increased resistance to fatigue cracking and rutting. In addition, the thesis includes a damage analysis completed to assess the effect of surface modification on the design life of the pavement.

1.2 LIME AS AN ADDITIVE

Commercially available hydrated lime contains at least 90% calcium hydroxide and has a pH of about 12.4. Figure 1-1 illustrates the hydrated lime production cycle and shows the resulting product. It is a fine-grained material with more than 85% of the material passes the #325 sieve (45 μ m sieve size). Being fine dramatically facilitates both mixing and coating efforts, and also contributes to a high speed of chemical activity.

The rationale for adding hydrated lime to asphalt mixes is often associated with the need to reduce moisture damage. Hydrated lime has the potential to positively influence the performance of asphalt pavements, well as their durability. The use of hydrated lime, for example, improves the ability of an asphalt concrete mixture to resist rutting, cracking and aging [Little and Epps, 2001]. Hydrated lime not only dramatically improves the hot mix asphalt (HMA) in these aspects when used alone, but also works

well when used in conjunction with other additives such as polymers, making the pavement system perform to the highest standards for many years.

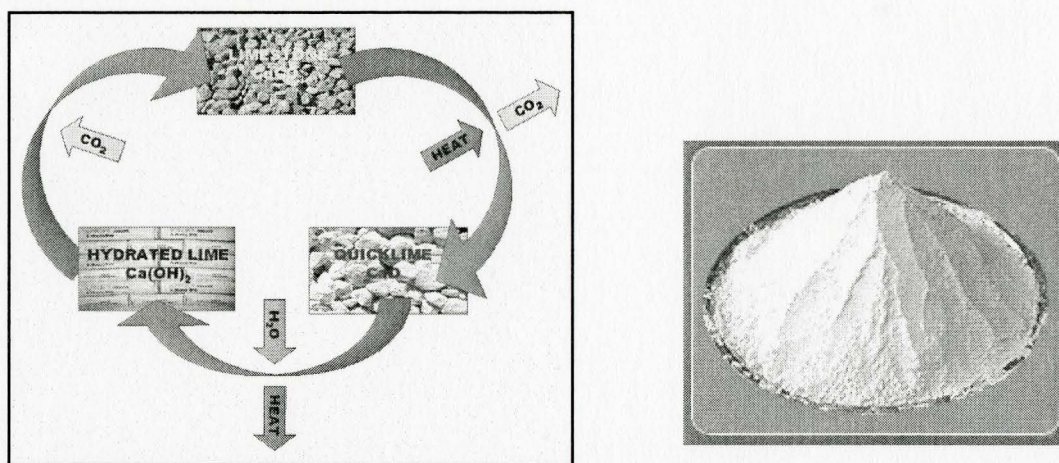


Figure 1-1: *Left: Hydrated Lime Production Cycle, Right: Hydrated Lime Sample* [National Lime Association, May 2004].

1.3 APPLICATIONS OF HYDRATED LIME IN HMA MIXES

The advantages of the use of hydrated lime in HMA mixtures are best demonstrated with regard to its positive effects on the properties of HMA.

1.3.1 Anti-stripping

Hydrated lime forms insoluble compounds that create very strong bonds between the asphalt binder and the aggregates, which act as barriers to stripping at all water pH levels

[Tarrer, 1996]. In addition, hydrated lime (0.5 to 2.0 percent by mass of HMA mix) tends to change the characteristics of the plastic fines contained in the marginal aggregates so that they are no longer plastic but act as agglomerates held together by a “pozzolanic cement” [Little, 1987]. This process is carried through mechanisms of cation exchange, agglomeration¹, and pozzolanic reactions² that reduce the ability of aggregate fines to attract and hold water. Having electropositive surface charge, and being made of 100% solids and 0% water, hydrated lime is highly attracted to asphalt cement (AC), which contributes to reducing the stripping potential of asphalt concrete.

1.3.2 Rutting

Rutting is best described as the permanent deformation of the asphalt concrete surface layer caused by traffic loading imparting stresses that cause the material to no longer behave in an elastic manner; in other words, strains are not recovered once loads are removed. Rutting, which mostly occurs at high temperatures, is due to a loss of stability of the asphalt mix, which in turn reduces the life of a pavement structure.

¹ Adherence of particles into a small mass due to moisture, static charge or chemical or mechanical binding [Hornby, 1974].

² Involve pozzolans: defined as siliceous or siliceous and aluminous materials, which possess little or no cementing properties, but chemically react with calcium hydroxide at normal temperatures in the presence of moisture to form compounds of high cementitious properties [Hornby, 1974].

Rutting is directly related to the stiffness of HMA. The stiffer the mix, the better it is in resisting rutting. Lime is a superior active mineral filler because of its ability to make HMA mixes stiffer, tougher, and hence more resistant to rutting. Hydrated lime particles tend to disperse throughout the HMA and react with the asphalt binder, which in turn contributes to increasing the dynamic modulus/stiffness of HMA.

The addition of hydrated lime (0.5 to 2% by mass) to the HMA generally increases the performance grade (PG) of the binder by as much as one full grade [National Lime Association, 2004]. Creep tests, performed on HMA mixes in Texas, clearly illustrate that the addition of hydrated lime has a positive effect on the high temperature stability of mixes. The study indicated that lime increases mixture stiffness at an early stage and becomes more stable over time [Little, 1994]. Increased stability produces an asphalt mix that is more resistant to rutting and other forms of permanent pavement deformation.

1.3.3 Aging

Beside the aforementioned benefits observed from the use of hydrated lime in HMA, it has also been observed that hydrated lime reduces the rate at which the asphalt cement oxidizes and hardens. Age hardening of asphalt cement is mainly due to the chemical reactions that take place between the asphalt binder and the environment. Highly polymer molecules present in the bitumen react with the environment, breaking

apart and contributing to increasing brittle pavement behaviour over time. The calcium hydroxide present in the hydrated lime and the highly polymer molecules chemically react together to inhibit the polymer molecules from reacting with the environment. The addition of hydrated lime alters the oxidation kinetics of the asphalt cement and interacts with oxidation products present in the binder, which in turn reduces their deleterious effects. Age hardening effects are reduced more at high temperatures than at low temperatures. Consequently, lime-modified asphalt cement remains flexible and protected from brittle cracking for periods longer than it would without the addition of hydrated lime. A study conducted at the Western Research Institute (WRI) shows that age hardening of asphalt can be reduced by the addition of as little as 0.5% of hydrated lime by dry weight [Petersen, Plancher and Harnsberger, 1987].

1.3.4 Fatigue Cracking

Although stiffening the HMA with hydrated lime makes it able to resist rutting, one could assume that it would cause the binder to become too brittle at low temperatures. Even though hydrated lime increases the stiffness of the HMA at low temperatures, it is not nearly as significant as the beneficial effect at high temperatures.

Asphalt concrete cracking is not only a result of aging, but also depends on mechanical causes including fatigue at low temperature. The use of hydrated lime not only stiffens the pavement but also improves the fatigue characteristics and reduces

cracking. Cracks start as tiny micro-cracks at either the top or the bottom of the pavement layer and later join together after propagating to form macro-cracks due to repeated traffic loadings. These micro-cracks are interrupted by the tiny hydrated lime particles and are deflected. It has been found that lime reduces cracking more than inactive fillers because of the chemical reaction that occurs between the calcium hydroxide in the lime and the polar molecules in the asphalt cement, which in turn increases the effective volume of the lime particles by surrounding them with large organic chains [Lesueur and Little, 1999]. Therefore, lime is a superior additive because of its ability to intercept and deflect micro-cracks, preventing them from growing into macro-cracks that can cause major structural failure of the pavement.

1.3.5 Fracture Toughness

Fracture toughness is best described as the amount of energy used to fracture a material. In addition to hydrated lime increasing the stiffness of the asphalt binder at high temperatures, the fracture toughness is dramatically increased due to the increased tensile strength of the lime-modified asphalt cement. The lime-modified asphalt cement demonstrates a greater tendency to dissipate energy by allowing the material to deform more at low temperatures, when compared to that of the unmodified cement.

1.3.6 Top-Down Cracking (TDC)

Top-down cracking of asphalt pavement has become a growing concern that must be dealt with at the design, construction, maintenance, and resurfacing stages of long-life asphalt pavements. This cracking mode is related to the tensile and shear stresses associated with temperature variations, stiffness gradients, and construction problems such as premature age hardening of the asphalt binder, as well as other factors. Top-down cracking initiates at the surface of the pavement and then propagates downwards. Such cracks are induced by various mechanisms, one of which is large drops in temperature that causes tensile stresses to build up within the asphalt surface course layer. These stresses later exceed the tensile strength of the mixture leading to rupture.

Even though highly advanced pavement design methods to deal with top-down cracking are currently being developed, the most effective way of addressing this concern is to enhance the mechanical properties of asphalt materials. To overcome pavement failures due to TDC, designers consider the use of softer binders that are less prone to aging as part of the solution. To reduce the rate of oxidation and age hardening of asphalt binders, the use of hydrated lime is highly recommended as it positively alters the oxidation kinetics of the asphalt cement and interacts with oxidation products present in the asphalt cement to minimize the negative effects of these products.

1.3.7 Extended Benefits

Dark colours affect the surrounding temperature, the amount of energy used for cooling/air conditioning, and the habitability of cities. During the summer, dark colours such as the surface of the asphalt pavements get heated from the sun and retain the thermal energy. Pavements radiate some of this energy making the cities a lot hotter, which in turn raises the summertime cooling demand.

The working hypothesis in this thesis is that, with the use of hydrated lime in pavement mixes, pavement surfaces become lighter in colour, which in turn contributes to lowering the amount of energy absorbed and held by the pavements. Consequently, cities should become less hot, reducing the amount of energy used in cooling. From a sustainability point of view, the work of this study also contributes to reducing the temperature of the run-off water, and hence protecting the habitat.

1.4 ECONOMICS

Economics play an important role in our daily lives, and therefore, any new technology to be implemented must be economical on a life-cycle cost basis. Table 1-1 summarizes the cost of placing hydrated lime on the surface of HMA mixtures.

Table 1-1: Cost Summary of Surface Modification of HMA Mixes with Hydrated Lime.

Category	Price (Canadian Dollars)
Cost of Hydrated Lime in Greater Toronto Area (GTA)	\$165/ton
Typical Hourly Rates on Construction Sites in GTA	\$200/hour ¹
Category	Price (Canadian Cents, ¢) per m ²
Cost of hydrated lime including delivery	1.7 ≈ 2
Construction cost	5 ²
Total cost	8.5 ³

Notes:

1. Based on two workers per equipment.
2. Based on 4000 m²/hour.
3. Price includes 20% contingency

1.5 SUMMARY OF OBJECTIVES.

An asphalt technology, which has been used in off-road applications, hypothesizes that lightening the surface colour of new pavement surfaces, that are originally very black before aging to a grayer colour, reduces the black body absorption and hence the summer temperature of the surface. One method available for lightening the surface of HMA to improve its performance is the addition of hydrated lime, which is currently thought to be the most suitable choice as a surface treatment.

Previous studies have been conducted to evaluate the impact of adding various hydrated lime amounts to HMA mixes on non-thermally affected mechanical properties.

The primary focus of the research reported in this thesis was to study the effect of placing different amounts of hydrated lime on the surface of asphalt concrete pavement and assess their influence on both the surface temperature as well as the temperature profile of the pavement with depth. An important outcome was to determine an optimum level of hydrated lime addition.

A further objective of the study was to assess the effect of temperature on the mechanical properties of hot mix asphalt mixtures used in Ontario; namely Superpave SP12.5FC2 PG64-28, SP12.5FC2 PG70-28 and SP19, and Stone Mastic Asphalt (SMA). The mechanical properties studied include rutting susceptibility, fatigue resistance, and the resilient modulus of the HMA mixtures in hand.

CHAPTER 2

MIXES AND MATERIALS

2.1 INTRODUCTION

Asphalt concrete consists of a bituminous binder, coarse and fine aggregate, and additives occasionally used to improve the engineering properties of the material. Mix design involves determining an optimum asphalt binder content for a desired aggregate structure to meet prescribed physical properties of the material both, from the aggregate and asphalt binder perspective. The selection of different mixes for different projects is

Table 2-1

Superpave and SMA Ontario Traffic Categories [Ontario Provincial Standards Specifications (OPSS) 1003 Table 3 and OPSS 1151 Table 1].

Ontario Traffic Category	20-Year Design ESALS (Million) – Note 1	Typical Applications
A	< 0.3	Low volume roads, parking lots, driveways, and residential roads.
B	0.3 to < 3.0	Minor collector roads.
C	3.0 to < 10	Major collector and minor arterial roads.
D	10 to < 30	Major arterial roads and transit routes.
E	> 30	Freeways, major arterial roads with heavy truck traffic, and special applications such as truck and bus climbing lanes or stopping areas.
Note 1: Equivalent single axle load (ESAL) for the projected traffic level expected in the design lane over a 20-year period, regardless of the actual design life of the pavement.		

based on required performance, which takes into account the availability of materials and the climate and the traffic conditions of the geographic area that the asphalt mixes are intended to serve in. Within the Superpave mix design context in Ontario, traffic level, also referred to as traffic condition, is categorized by the use of an alphabetical designation presented in Table 2-1.

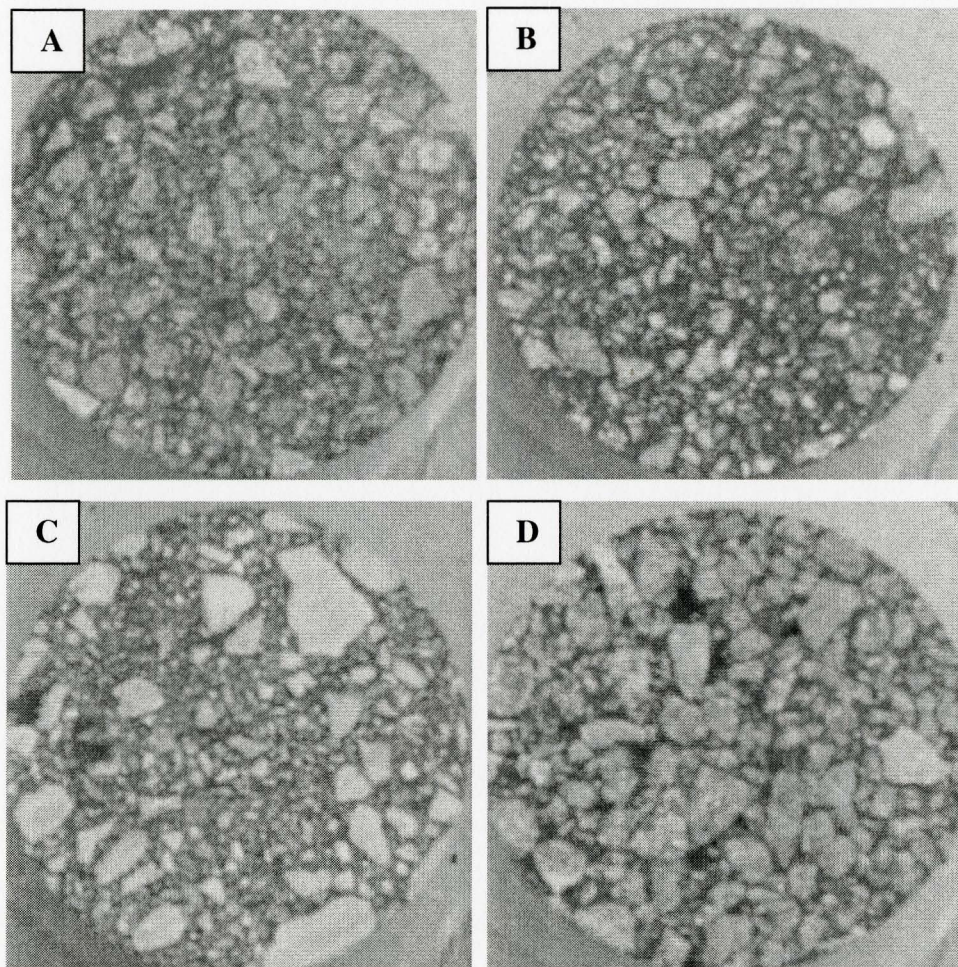


Figure 2-1: (A) SP12.5 FC2 PG64-28 Sample. (B) SP12.5 FC2 PG70-28 Sample. (C) SP19.0 Sample. (D) SMA Sample.

The purpose of this chapter is to introduce the different HMA mix designs that were used for this study; namely Superpave SP12.5FC2 PG64-28 and PG70-28, Superpave SP19.0 and Stone Mastic Asphalt (SMA). According to nomenclature, SP12.5FC2 PG64-28 indicates that the maximum nominal size aggregates used is 12.5mm, the mix has frictional characteristics for both coarse and fine aggregates (FC2) and PG64-28 meaning that the binder is designed to perform over a range bounded by a maximum and minimum pavement temperatures of 64°C and -28°C, respectively. Figure 2-1 compares the appearance of these asphalt concrete designs, which are commonly encountered in the Greater Toronto Area (GTA). Since Superpave mixtures and design procedures are starting to take over conventional HMA mixtures, Superpave mix types were chosen for the study. The mix designs that were considered allowed for an assessment of the effect of asphalt concrete design and different performance grades (PG) on the mix, as well as the impact of hydrated lime surface modification on the mechanical and albedo¹ properties.

2.2 SUPERPAVE SP12.5 FC2 PG64-28 and SP12.5 FC2 PG70-28

What differentiates the different asphalt cement grades is the temperature range over which the performance requirements are to be met. The requirements, being target physical properties, are directly related to field performance. PG64-28 for example

¹ Albedo is a unitless measure of a surface or body's reflectivity [Wikipedia Encyclopedia, 2006].

indicates that the binder has been designed to resist rutting and shoving distresses up to 64°C and at the same time resist low temperature cracking at temperatures with a value as low as -28°C. The high and low temperature designations of bituminous performance grades extend both directions in six-degree increments. The engineer selects a binder grade based on environment (historical temperature data), road classification, traffic level, binder cost and availability. In southern Ontario, which is within Zone III, PG64-28 is recommended for slow moving traffic and highways. PG70-28 on the other hand is recommended for roadways with a high percentage of heavy truck traffic at slow speeds and frequent stops and starts within the same zone.

Superpave 12.5 FC2, which is similar to the traditional Dense Friction Coarse (DFC) mix according to Ontario Provincial Standards Specifications (OPSS) 1150, is a surface mix for use on Traffic Category D and E roads. In other words, the mix can be used for major arterial roads with heavy truck traffic, transit routes, freeways and special applications such as truck and bus climbing lanes as well as for stopping areas.

The mix, at both performance grades (i.e. PG64-28 and PG70-28), provides superior rutting and skid resistance through a proper selection of aggregates. When comparing the SP12.5 FC2 mixtures at both grades, PG70-28 is more resistant to high temperature distresses such as rutting and shoving. On the other hand, both mixtures are

seen to equally resist temperature cracking since both HMA mixtures can withstand a minimum pavement temperature of -28°C .

A summary detailing the mix designs is presented in Table 2-2 for the SP12.5 FC2 PG64-28 mix and in Table 2-3 for the SP12.5 FC2 PG70-28 mix.

In addition to the laboratory testing, field tests were performed to see how well laboratory measurements represent what is observed in the field. The field site pavement was similar in mix design to the SP12.5 FC2 PG64-28 mixture tested in the laboratory, with the only difference being the AC content. The bitumen content was 4.7% in the laboratory whereas it was 5.2% in the field.

Table 2-2: SP12.5FC2 PG64-28 Mix Design / Surface Course [JEGEL Data Sheet, 2005]

MIX FORMULA – GRADATION PERCENT PASSING*																		
% A.C / Sieve Sizes (mm)	% A.C	53.0	37.5	25.0	19.0	16.0	12.5	9.5	6.7	4.75	2.36	1.18	0.600	0.300	0.150	0.075		
Job Mix Formula (JMF)	4.7	100.0	100.0	100.0	100.0	100.0	98.9	88.9	62.2	52.1	41.6	29.5	21.0	14.0	9.0	4.9		
Superpave Volumetrics		REQUIRED		SELECTED				% CA #1		53.0		% RAP		-				
N _{des}		75		75				% CA #2		-		% A.C RAP		-				
N _{ini} (% Gmm)		≤ 89.0		87.5				% CA #3		-		Gmb		2.541				
N _{max} (% Gmm)		≤ 98.0		97.4				% FA #1		23.6								
Air Voids (%) @ N _{des}		4.0		4.0				% FA #2		23.5		Gmm		2.646				
VMA (%)		13.0		15.2				% FA #3										
VFA (%)		Minimum	65.0		74.0			Composite Gsb						2.856				
		Maximum	75.0															
Dust Proportion		Minimum	0.6		1.1			ASPHALT CONTENT										
		Maximum	1.2					SUPPLIER		AC GRADE								
Tensile Strength Ratio, %		80.0% Minimum		82.7		-						PG 64 - 28						
Asphalt Film Thickness		N/A		8.2		ADDITIVE												
Traffic Category		C		C		SUPPLIER						TYPE		AS % OF AGG.				
						-						Hydrated Lime		1.0				
AGGREGATE TYPE		AGGREGATE SOURCE / INVENTORY NO.					AGGREGATE TYPE		AGGREGATE SOURCE / INVENTORY NO.									
COARSE AGGREGATE #1		DFC CA					FINE AGGREGATE #2		Unwashed Fines (6.35 mm minus)									
		-		-					-		-							
COARSE AGGREGATE #2		-					FINE AGGREGATE #3		-									
		-		-					-		-							
COARSE AGGREGATE #3		-					RAP #1		-									
		-		-					-		-							
FINE AGGREGATE #1		Manufactured Sand					RAP #2		-									
		-		-					-		-							
AGG. TYPE	Gsb	Gsa	ABS. (%)	AGGREGATE GRADATION (Sieve Sizes in mm) – PERCENT PASSING														
				53.0	37.5	25.0	19.0	16.0	12.5	9.5	6.7	4.75	2.36	1.18	0.600	0.300	0.150	0.075
CA #1	2.874	2.910	0.125	100.0	100.0	100.0	100.0	100.0	98.8	89.7	29.5	11.5	6.1	4.9	4.0	2.2	1.0	0.4
CA #2																		
CA #3																		
FA #1	2.807	2.834	0.342	100.0	100.0	100.0	100.0	100.0	100.0	100.0	100.0	100.0	93.5	61.2	43.4	27.7	17.1	7.5
FA #2	2.864	2.911	0.560	100.0	100.0	100.0	100.0	100.0	100.0	100.0	98	95.9	68.7	48.7	35.3	25.0	17.2	10.5
FA #3																		
RAP CA																		
RAP FA																		

Table 2-3: SP12.5FC2 PG70-28 Mix Design / Surface Course [JEGEL Data Sheet, 2005]

MIX FORMULA – GRADATION PERCENT PASSING*															
% A.C / Sieve Sizes (mm)	%A.C	37.5	25.0	19.0	16.0	12.5	9.5	6.7	4.75	2.36	1.18	0.600	0.300	0.150	0.075
Job Mix Formula (JMF)	4.6	100.0	100.0	100.0	100.0	98.1	79.1		53.2	47.7	31.2	20.8	13.1	7.4	3.9

Gyrations:

N ini = 9

N des = 125

N max = 205

Superpave Volumetrics		REQUIRED	SELECTED
N _{des} (% Gmm) / V%		96.0 / 4.0	96.0 / 4.0
N _{ini} (% Gmm)		≤ 89.0	88.2
N _{max} (% Gmm)		≤ 98.0	96.5
VMA (%)		14	15.0
VFA (%)	Minimum	65.0	73.3
	Maximum	75.0	
Dust Proportion	Minimum	0.6	0.9
	Maximum	1.2	
Tensile Strength Ratio, %		80.0% Minimum	84.1
Traffic Category		E	E

ASPHALT CEMENT	
SUPPLIER	AC GRADE
-	PG 70 – 28

AGGREGATE TYPE	AGGREGATE SOURCE / INVENTORY NO.		AGGREGATE TYPE	AGGREGATE SOURCE / INVENTORY NO.	
COARSE AGGREGATE #1	DFC Stone		FINE AGGREGATE #2	Modified Blend Sand	
	-	-		-	-
COARSE AGGREGATE #2	-		FINE AGGREGATE #3	-	
	-	-		-	-
FINE AGGREGATE #1	Washed Blend Sand		RAP #1	-	
	-	-		-	-

ADDITIVE		
SUPPLIER	TYPE	AS % OF AGG.
-	N/A	-

AGG. TYPE	AGG. SPECIFIC GRAVITY	AGG. ABS. (%)	AGGREGATE GRADATION (Sieve Sizes in mm) – PERCENT PASSING												
			37.5	25.0	19.0	16.0	12.5	9.5	4.75	2.36	1.18	0.600	0.300	0.150	0.075
CA #1	3.043	0.4	100.0	100.0	100.0	100.0	96.0	57.0	3.6	1.5	1.3	1.3	1.2	1.2	0.8
CA #2															
FA #1	2.896	1.1						100.0	100.0	82.2	50.4	32.7	21.7	13.6	7.1
FA #2	2.904	0.5						100.0	100.0	93.2	60.5	39.3	23.0	11.1	4.5
FA #3															
RAP CA															
RAP FA															

* FINES RETURNED TO MIX (1.0%)

REMARKS

1. The specimens were compacted with SGC @ 155°C (= Recompression Temperature).
2. No SSD air voids correction is required.
3. Weight required for 115mm Height of SGC Specimen = 5260 g.
4. The absorption of water is 0.3% < 2.0%, hence, no sealing of specimen is required.
5. AC Extraction by Solvent or Ignition.

2.3 SUPERPAVE SP19

Superpave 19.0, a binder mix for use on Traffic Category A, B, C, and D roads, is similar to the traditional HL 4, HL 8, and HDBC mixes according to OPSS 1150. SP19, being used in southern Ontario, employs a PG58-28 asphalt cement and is primarily used for low volume facilities such as parking lots, driveways, and residential streets. It can also be used for major and minor collector roads, major and minor arterial roads, and transit routes. A summary of mix design details is presented in Table 2-4.

2.4 STONE MASTIC ASPHALT (SMA)

SMA, which is considered to be a high performance mix in Ontario, is known for its rut, skid, and fatigue cracking resistance. In addition, SMA is known for its durability through its high AC content. SMA is commonly used as a wearing or surface course for divided highways and high-volume roadways in both intermediate and surface courses.

Stone Mastic Asphalt (SMA) is a gap-graded dense asphalt mix with approximately 3 percent air voids. Proportionally, these mixes contain a large amount of 100% crushed coarse aggregate and a rich enhanced asphalt cement/filler matrix. The coarse aggregate, through point-to-point contact, forms a high-stability skeleton. The binder mastic consists of high AC content, cellulose or mineral fibers, and a high percentage of mineral filler. SMA mixes appear to be stickier than conventional HMA

Table 2-4: SP19.0 Mix Design / Base Course [JEGEL Data Sheet, 2005]

MIX FORMULA – GRADATION PERCENT PASSING*																		
% A.C / Sieve Sizes (mm)	% A.C	53.0	37.5	25.0	19.0	16.0	12.5	9.5	6.7	4.75	2.36	1.18	0.600	0.300	0.150	0.075		
Job Mix Formula (JMF)	4.5	100.0	100.0	100.0	97.0	90.3	84.6	69.8	56.2	50.0	42.6	29.5	19.7	11.6	6.5	4.4		
Superpave Volumetrics		REQUIRED		SELECTED														
N_{des}		75		75														
N_{ini} (% Gmm)		≤ 89.0		87.5														
N_{max} (% Gmm)		≤ 98.0		97.3														
Air Voids (%) @ N_{des}		4.0		4.0														
VMA (%)		13.0		13.75														
VFA (%)	Minimum	65.0		70.0														
	Maximum	75.0																
Dust Proportion	Minimum	0.6		1.1														
	Maximum	1.2																
Tensile Strength Ratio, %		80.0% Minimum		89.9														
Asphalt Film Thickness		N/A		8.3														
Traffic Category		C		C														
AGGREGATE TYPE		AGGREGATE SOURCE / INVENTORY NO.					AGGREGATE TYPE		AGGREGATE SOURCE / INVENTORY NO.									
COARSE AGGREGATE #1	19 mm Clear					FINE AGGREGATE #2	-											
	-	-					-	-										
COARSE AGGREGATE #2	9.5 mm Stone					FINE AGGREGATE #3	-											
	-	-					-	-										
COARSE AGGREGATE #3	-					RAP #1	12.5 mm RAP											
	-	-					-	-										
FINE AGGREGATE #1	High stability Sand					RAP #2	-											
	-	-					-	-										
AGG. TYPE	Gsb	Gsa	ABS. (%)	AGGREGATE GRADATION (Sieve Sizes in mm) – PERCENT PASSING														
				53.0	37.5	25.0	19.0	16.0	12.5	9.5	6.7	4.75	2.36	1.18	0.600	0.300	0.150	0.075
CA #1	2.662	2.711	0.678	100.0	100.0	100.0	78.0	40.0	12.1	1.6	1.4	1.2	1.0	0.8	0.6	0.4	0.2	0.1
CA #2	2.653	2.709	0.781	100.0	100.0	100.0	100.0	100.0	97.5	57.2	17.8	2.3	1.6	1.3	1.2	0.9	0.8	0.6
CA #3																		
FA #1	2.777	2.839	0.782	100.0	100.0	100.0	100.0	100.0	100.0	100.0	100.0	99.7	84.1	53.2	31.2	16.3	7.0	3.3
FA #2																		
FA #3																		
RAP CA	2.685	2.751	0.897	100.0	100.0	100.0	100.0	100.0	99.0	87.1	71.6	61.5	49.9	41.5	32.7	19.6	11.0	7.5
RAP FA	2.642	2.712	0.915															

* FINES RETURNED TO MIX (1.5%)

REMARKS

- The pass 4.75mm portion of the blend gradation has been adjusted for fines returned to the mix.
- The specimens were compacted with SGC @ 138°C (= Recompression Temperature).
- No SSD air voids correction is required.
- Weight required for 115mm Height of SGC Specimen = 4800 g.
- The absorption of water is < 1.0%, hence, no sealing of specimen is required.
- Total AC in the mix = 4.5%; AC from RAP = 0.8% and New AC = 3.7%

mixes due to the addition of polymer-modified asphalt cement. A typical mix consists of 70% coarse aggregates, 8% limestone filler, 17% fine aggregates, 6% polymer modified PG70-28 AC, and 0.3% cellulose fiber.

Frequently, a bumped or double bump high temperature grade of performance graded AC is used. The bitumen used for instance is bumped up one grade from PG58-28 to PG64-28 or twice to PG70-28. The mortar component of the mix is critical to mix durability and satisfactory retention of the asphalt cement during transport and placement. The mortar is generally made up of asphalt cement, mineral filler, and cellulose fiber. Mineral fillers and cellulose fibers are commonly added to form a stiff mortar and prevent drain down of the AC. The in-place air voids of the mix are kept low to achieve a high impermeability of the compacted mix to water.

SMA mixes cool rapidly on the road and therefore, compaction must be completed in the shortest time possible. This is normally done using static steel drum rollers as vibratory rollers may crush some of the coarse aggregate particles, whereas rubber tired rollers tend to pull out some of the fine material, causing minor flushing of the mix. SMA mixes are generally not tender and therefore, rollers should be placed on the hot mat and kept close to the screed to ensure optimal compaction before the mix cools.

It is estimated that the SMA mix costs 30 percent more than the conventional HMA mixes, but it may last twice as long and hence require less maintenance with a correspondingly lower life-cycle cost. A summary of mix design details is presented in Table 2-5.

Table 2-5: SMA Mix Design / Surface Course [JEGEL Data Sheet, 2005]

MIX FORMULA – GRADATION PERCENT PASSING*														
% A.C / Sieve Sizes (mm)	% A.C	25.0	19.0	16.0	12.5	9.5	6.7	4.75	2.36	1.18	0.600	0.300	0.150	0.075
Job Mix Formula (JMF)	5.8	100.0	100.0	100.0	99.8	74.2	39.9	24.4	18.9	16.1	14.1	11.7	9.4	8.0
Superpave Volumetrics			REQUIRED		SELECTED			% CA #1		85.0		% RAP		-
% Voids			4.0		4.0			% CA #2		-		% A.C RAP		-
TSR			70% min		80.8			% CA #3		-		RAP PEN		N/A
Drain Down (%)			0.3 max		0.00			% FA #1		9.3		BRIQ. BRD		2.489
VCA _{mix}			< VCA _{DRC}		38.5 < 54.6			% FA #2		5.7		MRD		2.592
% VMA (min)			17.0		18.3			% FA #3		-		Gb		2.870

ASPHALT CEMENT	
SUPPLIER	AC GRADE
-	PG 70 – 28 P

ADDITIVE		
SUPPLIER	TYPE	AS % OF MIX
-	Cellulose	0.3
-	Hydrated Lime	1.0 (% of Agg.)

AGGREGATE TYPE	AGGREGATE SOURCE / INVENTORY NO.		AGGREGATE TYPE	AGGREGATE SOURCE / INVENTORY NO.	
COARSE AGGREGATE #1	DFC CA		FINE AGGREGATE #2	Mineral Filler	
	-	-		-	-
COARSE AGGREGATE #2	-		FINE AGGREGATE #3	-	
	-	-		-	-
COARSE AGGREGATE #3	-		RAP #1	-	
	-	-		-	-
FINE AGGREGATE #1	Unwashed Fines (6.35 mm minus)		RAP #2	-	
	-	-		-	-

AGG. TYPE	BULK RELATIVE DENSITY	ABS. (%)	AGGREGATE GRADATION (Sieve Sizes in mm) – PERCENT PASSING												
			25.0	19.0	16.0	13.2	9.5	6.7	4.75	2.36	1.18	0.600	0.300	0.150	0.075
CA #1	2.881	0.43	100.0	100.0	100.0	99.8	69.7	29.5	11.5	6.1	4.9	4.0	2.2	1.0	0.4
CA #2															
CA #3															
FA #1	2.864	0.56	100.0	100.0	100.0	100.0	100.0	98.0	95.9	68.7	48.7	35.3	25.0	17.2	10.5
FA #2	2.721	2.30	100.0	100.0	100.0	100.0	100.0	100.0	100.0	100.0	100.0	100.0	100.0	90.0	82.0
FA #3															

* FINES RETURNED TO MIX (2.0%)

REMARKS

1. The pass 4.75mm portion of the blend gradation has been adjusted for fines returned to the mix.
2. The specimens were compacted with SGC (100 gyrations) @ 150°C (= Recomaction Temperature).
3. No SSD air voids correction is required.
4. Weight required for 115mm Height of SGC Specimen = 4800 g.
5. Dry Rodded Density of Coarse Aggregate (AASHTO T19) = 1569 kg/m³.

Table 2-6 compares SMA and conventional HMA. One observes that Stone Mastic Asphalt mixes better resist shear as a result of the high degree of interlocking between the aggregates, which improves stability against rutting. At the same time, SMA is much better than a conventional HMA mix with regard to abrasion resistance and durability. SMA is known for its lower stiffness at low temperatures and higher stiffness at high temperatures, which makes it highly resistant to both fatigue cracking and rutting. Due to its enhanced performance, SMA is commonly used in heavy truck traffic areas and freeways.

Table 2-6

Comparison between SMA and Conventional HMA Mixtures [4G03: Pavement Design Course Notes, 2005].

Property / Feature	Ranking of SMA compared to conventional HMA
Shear Resistance	Much Better
Abrasion Resistance	Much Better
Durability	Much Better
Load Distribution	Somewhat Less
Cracking Resistance	Better/Much Better
Skid Resistance	Better
Water Spray	Equal/Better
Light Reflection	Better
Noise Reduction	Equal/Better
Public Recognition	Much Better

CHAPTER 3

LABORATORY PAVEMENT SAMPLES

Laboratory testing was performed to ensure a controlled, consistent environment and to avoid temperature fluctuations and the destructive testing of in-situ pavement. In addition, research is generally a lengthy process and therefore, laboratory testing is often performed before testing in the field. Laboratory testing was conducted on samples that were prepared using the same HMA mix as that placed in the field. To simulate real field conditions, the samples were prepared to the same specifications and using similar methods as those in the field. Compaction of the samples, for instance, was done using the Asphalt Vibratory Compactor (AVC), which simulates the role of a vibratory steel-wheeled roller that usually makes the first compaction run on an in-situ pavement. Once laboratory testing was completed, in-situ testing was performed to assess how well laboratory measurements represent what is observed in the field.

3.1 SAMPLE PREPARATION

Superpave HMA brought to John Emery Geotechnical Engineering Limited (JEGEL) for testing were used for the preparation of laboratory samples. This helped avoid lengthy mixing periods and the high mixing accuracy required to generate mixtures with properties similar to those of the field HMA. The pre-mixed hot mix was

reheated for 30 minutes using a microwave in order to make it more workable for the fabrication of specimens. Depending on the targeted Maximum Theoretical Relative Density (MRD) of the mix, the desired final height of the sample (i.e. 78mm), and the percent voids being targeted ($5 \pm 2\%$ according to OPSS310 *Field Requirement for Compaction*), asphalt concrete amounts needed for the individual samples were calculated¹ and the correct quantities were then placed in pans and covered with aluminum foil to prevent excessive heating and age hardening of the mix. Depending on the compaction temperature provided on the mix design sheet for that specific mix, the pans containing the material were then placed in the oven at a temperature that was 5°C higher than that required for compaction. Given that the hot mix must be compacted above a threshold temperature, this higher temperature took into account heat loss during the transfer of the material from the pans to the compaction mould and then to the compactor itself. While in the oven, the temperature of the material was monitored using a temperature gauge inserted into the material through the aluminum foil covering the pans. While transferring the mould to the compactor, two digital thermocouples were inserted into the material to monitor the average temperature to make sure that it was above that required for the compaction of the material as specified on the mix design sheet.

An Asphalt Vibratory Compactor (AVC), which has two vibrators placed on top

¹ Refer to Appendix A for a sample calculation.

of a compaction plate, was used for compaction. The compaction mould was designed to give samples that were 300mm in length and 125mm in width, with AVC compaction plate height location being adjusted to yield a sample height of 78mm. Samples were compacted in 6 alternating cycles that were of 25 seconds duration each. To ensure uniform compaction and hence height of sample, the compaction mould was rotated 180 degrees after every cycle to yield 3 alternate cycles applied on each of the two

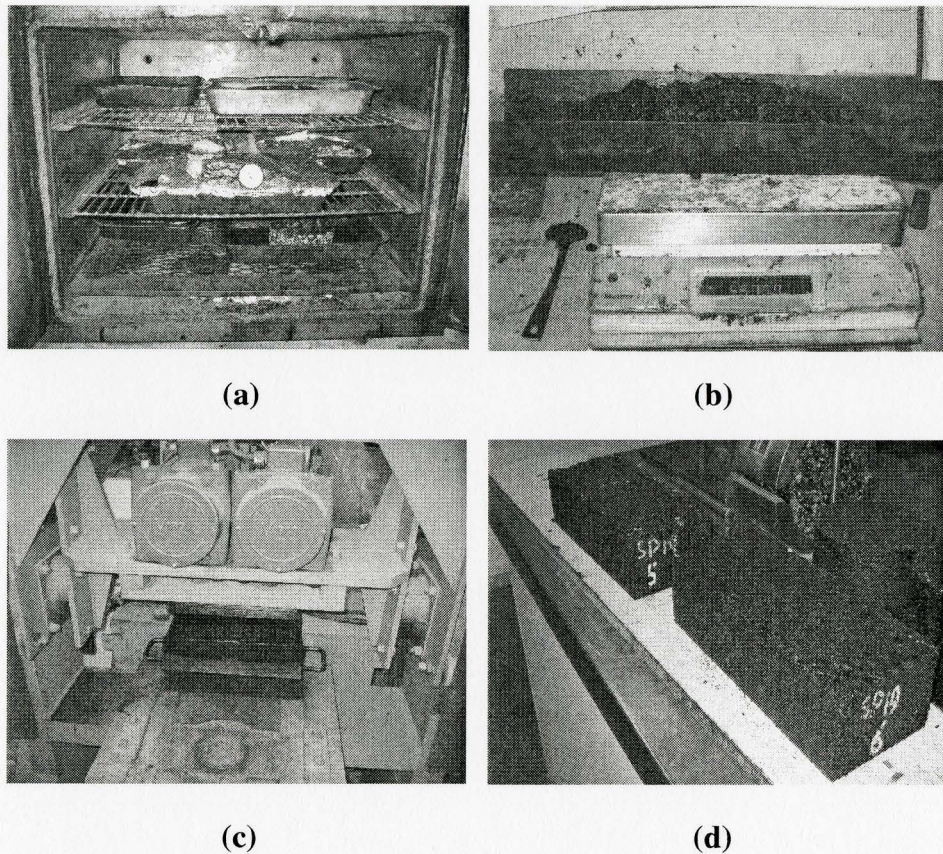


Figure 3-1: Laboratory Samples Preparation Procedure. [(a): Reheating of Premixed Hot Mix, (b): Weighing of the Hot Material, (c): Compacting in a Mould Using an AVC, (d): Compacted Samples Left to Cool on a Flat Surface].

orientations of the sample being compacted. Once compacted, samples were then placed to cool on a rigid flat surface to maintain their shape and not get distorted. Figure 3-1 illustrates the stages for sample preparation.

After determining the total number of samples needed for each mix type for the entire study, the complete set of samples were fabricated before the start of testing. This was done to ensure consistency in the preparation of the samples. Once the samples cooled, they were stored on a flat clean surface and covered to prevent dust collection on their surface until they were ready to be tested.

3.2 TESTING OF AIR VOIDS

Percent air voids was assumed not to play a significant role in this study. Nevertheless, targeted percent air voids of the samples was kept to approximately 5% in order to maintain consistency between samples and to ensure that this assumption was not a factor in the interpretation of results.

Percent air voids was determined in accordance to ASTM D3203-94 [ASTM International, 1994] and AASHTO T 269. A complete set of the procedural instructions is found in Appendix B.

CHAPTER 4

EFFECT OF HYDRATED LIME AMOUNT ON THE SURFACE TEMPERATURE OF HMA PAVEMENT

This chapter describes the placement of hydrated lime on the surface of hot mix asphalt (HMA), and its impact on surface temperature. Once different lime concentrations were assessed for their effect on the surface temperature reduction, an optimum level was selected. Laboratory results were supported by in-situ test measurements on surfaces that were tested using the same strategies developed in the laboratory.

4.1 LABORATORY TESTING

The effect of adding hydrated lime to HMA mixes has been found to be positive in improving their mechanical properties, specifically reducing stripping susceptibility of moisture susceptible mixes. Considerable attention has been given to issues related to impact of lime on the mechanical properties of hot mix asphalt mixtures, but not much attention has been given to its impact on the thermal behaviour of asphalt concrete, which strongly influences the mechanical properties of HMA.

Asphalt mixes are usually black, and therefore blackbody absorption is important. HMA mixtures absorb a large amount of radiation by the sun and surroundings, as well as

radiate stored energy, particularly at night. HMA mechanical properties are strongly influenced by the temperature of the pavement surface, as a result, high temperatures, as will be discussed later in the thesis, strongly influence the rutting resistance of HMA mixes, their stiffness, as well as other mechanical properties. Hydrated lime, which is considered to be a suitable treatment that is chemically compatible with AC, was used to lighten the surface of the SP12.5FC2 PG64-28 pavement to help reduce the radiation absorption and the surface temperature. Different amounts of hydrated lime; namely 20g, 35g, 50g, 70g, 100g, 125g and 150g per m² of pavement surface area, were applied to the surface to assess the influence of lime coverage rate. The objective was to determine an optimum hydrated lime amount that maximizes the influence on temperature reduction without wasting material.

4.1.1 Sample Preparation

The optimum hydrated lime amount to be placed on the surface of the pavement was not known a priori, and therefore, had to be determined as a first step in the study. Given the small surface area of the samples to be modified, which was less than one square meter, it was possible to tightly control the amount of hydrated lime applied to the surface. The hydrated lime amounts, in powder form, were weighed using a digital scale. Thereafter the required amount of material was spread on the surface of the pavement samples using a brush to guarantee uniformity and homogeneity. As shown in Figure 4-1, only a portion of the surface was modified with hydrated lime to avoid loss of material

along the edges of the sample and hence produce inaccurate results, which could have occurred if the surface had been completely modified. To ensure the exact coverage, the modified area was ‘fenced’ with masking tape before spreading the lime and once the modification was completed, the tape was removed and finishing ‘compaction’ was performed using the semi-rubber roller (Figure 4-1) built for this study. The intent of the semi-rubber painting roller was to force the lime to penetrate a few millimeters into the pavement. To prevent the hydrated lime from sticking to the roller and hence alter the hydrated lime surface concentration, the roller was covered with smooth scotch tape prior to compaction. The laboratory compaction was performed to simulate what happens in

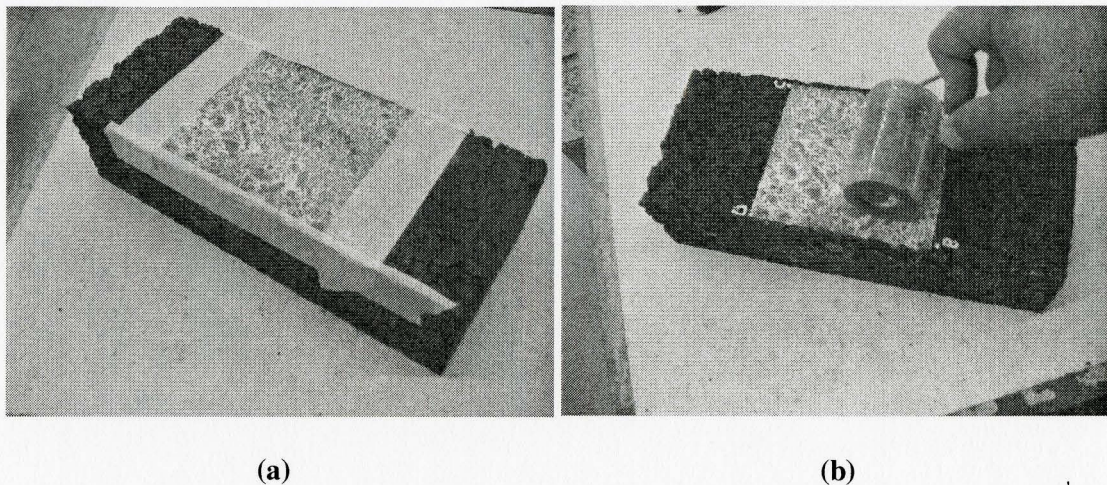


Figure 4-1: Placement of Hydrated Lime on the Surface of an HMA Pavement Sample.
[(a): Hydrated Lime on Sample Surface after Confining Area with Masking Tape,
(b): Compacting Lime with Semi-Rubber Roller after Removal of Masking Tape].

the field during construction. On site, hydrated lime should be spread on the surface after the initial rolling of the pavement. Once this is done, the finishing rubber wheel roller would make the final compaction, forcing the hydrated lime into the pavement for better hydrated lime-AC contact and hence better performance.

Once a sample was ready, it was placed in the centre of a group of similar prisms and made part of a larger pavement grid as shown in Figure 4-2. Due to the ease of losing hydrated lime with a light summer wind, only the center sample was carefully prepared inside the laboratory. The remaining uncovered portion of the sample being tested as well as the surrounding samples were then covered by roughly the same hydrated lime surface concentration to minimize the impact that the adjacent unmodified prisms would have on

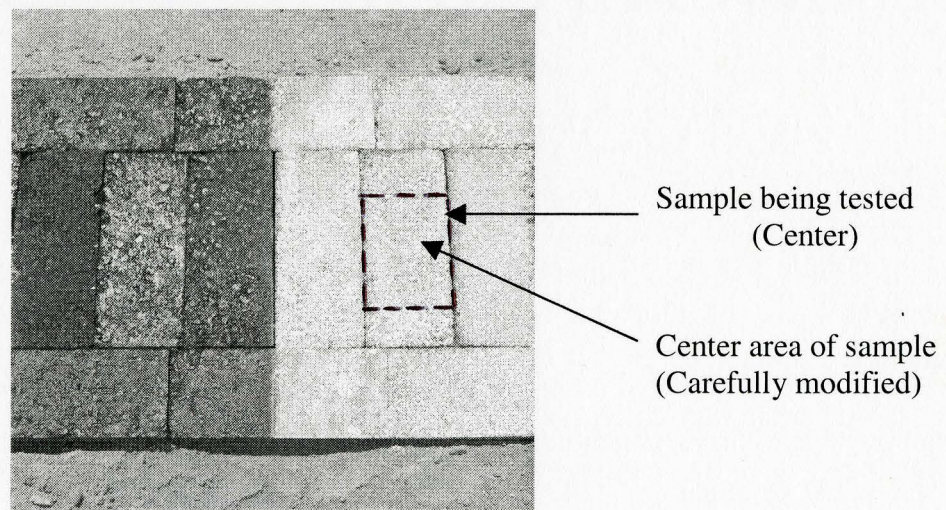


Figure 4-2: Large Patch/Pavement Grid As is Encountered In-Situ.

the test specimen. In other words, the objective was to have the test specimen in the middle of a larger test area.

4.1.2 Testing Apparatus: The FLIR Infrared Camera

Thermal energy, which is sometimes referred to as infrared energy, is the electromagnetic energy that cannot be detected by a human eye due to its long wavelength. It is also that part of the electromagnetic spectrum that we perceive via heat transfer. Everything with a temperature above absolute zero emits heat, which means that it may be tracked and measured via thermography.

Thermography is known as the technique of detecting and measuring the thermal energy emitted from an object. Infrared cameras, which translate the invisible infrared spectrum into thermal images that are seen and tracked via thermography, are highly advanced tools capable of performing such a task. As the temperature of an object increases, more infrared radiation is emitted, which can be detected by an infrared camera such as the FLIR ThermoCAM shown in Figure 4-3. This camera was used for measuring the HMA surface temperatures in this study.

To measure the temperature of a certain point on an object, the window cursor is placed on that point. Once the user is satisfied, the image is recorded and saved for reporting purposes. In addition to the actual hardware, the FLIR infrared camera is

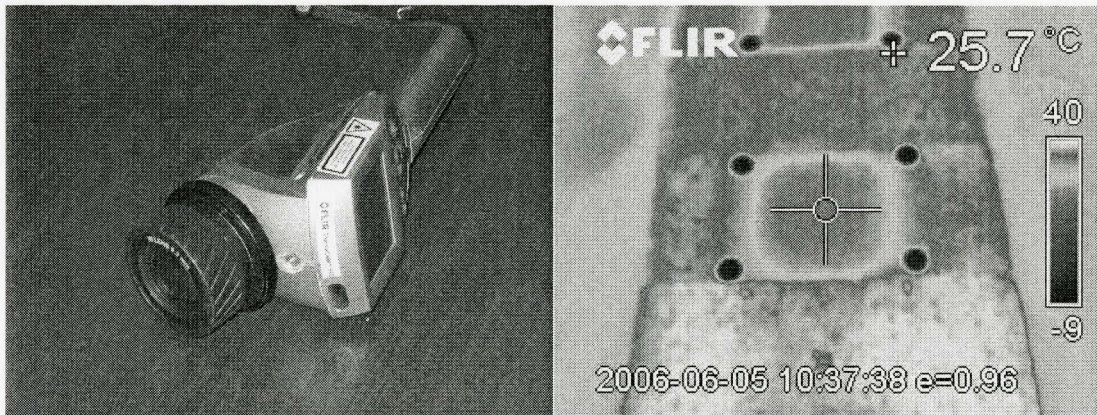


Figure 4-3: *Left:* FLIR Thermacam Infrared Camera, *Right:* Example Infrared Thermal Image.

accompanied by a Quickview software, which allows the user to read the temperature anywhere on the image using the cursor once the image is saved and transferred to a computer and used for further analysis. The camera was used during both laboratory and field testing.

4.1.3 Testing Procedures

As mentioned previously, the sample being tested was placed in the middle of a grid of prisms that had similar surface conditions, mix design and air voids. The lime-modified area was made large enough to reduce the edge effect due to adjacent black surface. Dry sand was placed along the outside perimeter of the pavement grid and made level with the pavement surface to reduce the amount of heat transfer between the pavement and the ambient air along the edges. Not only along the sides, but a 25mm

thick dry sand layer representing a subgrade was also placed under the pavement grid to simulate field conditions.

Referring to Figure 4-1, the surface temperature readings were taken at the center in order to capture most representative results. The test setup was placed outside in the sun and surface temperature readings using the FLIR infrared camera were normally taken every 15 minutes for the first 1.5 hours and then every half an hour for the remainder of the test, which usually ended shortly after the temperature of the black surface reached its peak value. Although extreme care was taken to prepare the surface that was monitored over time, readings of adjacent surfaces, which were covered with similar levels of hydrated lime, were found to be the same as those observed on the sample being monitored.

4.1.4 Results

Testing took place at a parking lot outside JEGEL, which is located in Toronto. To avoid the impact of weather fluctuations from coming into play, the different hydrated lime concentrations were all assessed during the same day on May 29th, 2006, which was a brightly sunny day with a clear sky.

Evaluating the effect of the different hydrated lime amounts was a lengthy process, requiring continuous measurement for a period of approximately 7 hours. Once

the entire set of different hydrated lime concentrations was evaluated, the results were organized and plotted in Figures 4-4, 4-5 and 4-6.

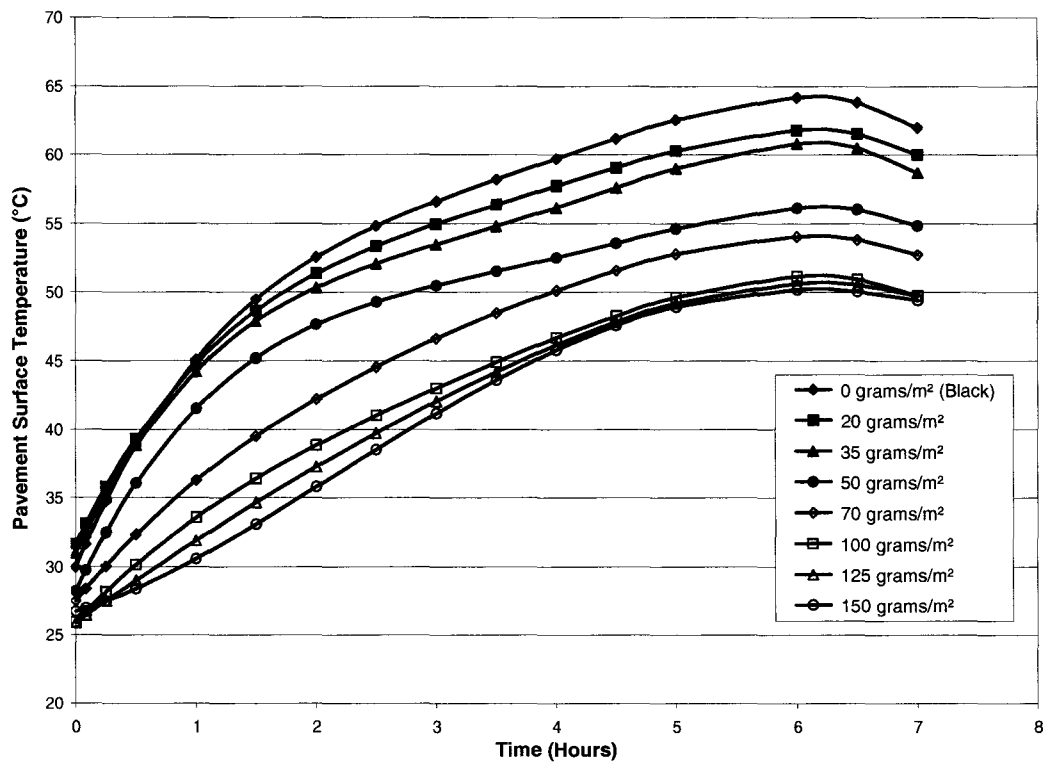


Figure 4-4: Effect of Hydrated Lime Amount on Surface Temperature of HMA Laboratory Pavement with Time.

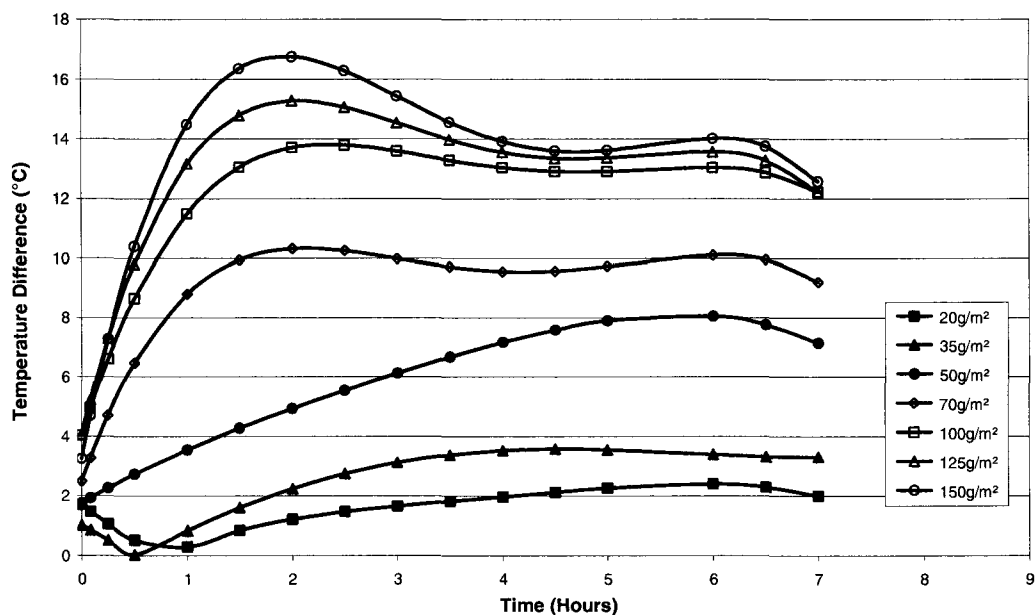


Figure 4-5: Change in Surface Temperature between Black Unmodified Pavements and Those Modified with Different Hydrated Lime Amounts with Time.

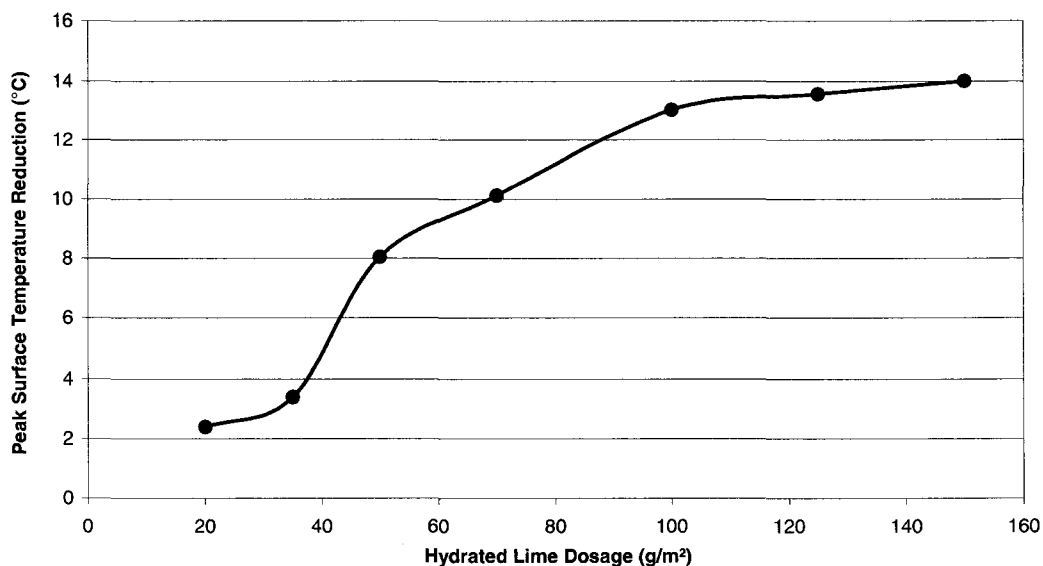


Figure 4-6: Peak Change in Surface Temperature between Black Unmodified Pavements and Those Modified with Different Hydrated Lime Amounts at Six Hours after Test Start (Figure 4-4).

4.1.5 Discussion

As shown in Figure 4-4, the more lime that is applied to the surface, the lower the surface temperature, as one might expect. This is due to making the surface lighter and thus decreasing the energy absorption property. One, however, also observes that there is an upper limit, above which relatively little change in temperature occurs, regardless of the extra lime placed on the surface; see Figures 4-5 and 4-6. That is to say, increasing the hydrated lime concentration above 100g/m^2 did not substantially further reduce the surface temperature. Therefore, placing additional lime on the surface could be considered excessive from an economic and environmental point of view.

When compared to unmodified newly paved asphalt, and referring to Figures 4-4, 4-5 and 4-6, 100g/m^2 of hydrated lime maybe considered to be an optimal choice with a peak temperature reduction from 64.2 to 51.2°C during a summertime air temperature of 34.3°C , which in our case occurred six hours after starting the test. This is a reduction of 13 celsius degrees ($^\circ\text{C}$). This reduction, as mentioned before, is at peak temperatures but according to Figure 4-5, the maximum temperature difference using 100g/m^2 of hydrated lime was approximately 14°C . Even though the use of 125 and 150g/m^2 of hydrated lime during peak temperatures caused further reductions of 0.6 and 1.0°C , respectively, the marginal decrease in temperature would likely not contribute to sufficient improvement in performance to justify the additional hydrated lime added.

Referring to Figure 4-5, and specifically for the cases of 20g and 35g/m² hydrated lime, the temperature difference shown by the curves decreased for the first hour and then started to increase again. The unexpected decrease is relatively small in magnitude, and maybe explained by the variation in the accuracy and sensitivity of the thermocouples used, and the possibility that some of the lime escaped with wind.

The black body of asphalt pavements has a negative impact on the pavement performance during the summer, due to the high pavement temperatures. On the other hand, the black surface of the pavement is considered to be beneficial during Canadian icy winter conditions. Although beyond the scope of this study, the impact of modifying the surface temperature of pavements should be addressed during winter conditions.

4.2 FIELD TESTING

Field testing at a site with newly placed pavement was performed to confirm that the laboratory surface temperature measurements represent what is observed in the field. The in-situ testing site was located at the South-West corner of Erin Mills Parkway and Dundas Street in Mississauga, Ontario. The tests performed in the field were the same as those performed in the parking lot at the laboratory. To reduce the number of variables coming into the analysis, the in-situ hot mix asphalt pavement, being SP12.5FC2 PG64-28, was of the same design as that used in the laboratory.

4.2.1 Site Preparation

Once the new pavement was laid down and before traffic was allowed to drive on it, a test area, shown in Figure 4-7, was reserved and delineated for this study. The test patches were chosen to be 700mm x 800mm to ensure that representative results could be obtained. Four areas, as shown in Figure 4-7, were allocated for testing. The control area was black with the second, third, and fourth areas, shown in Figure 4-8, being surface-

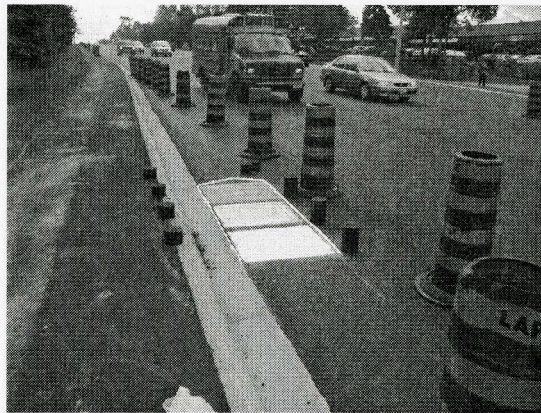


Figure 4-7: Field Testing Setup

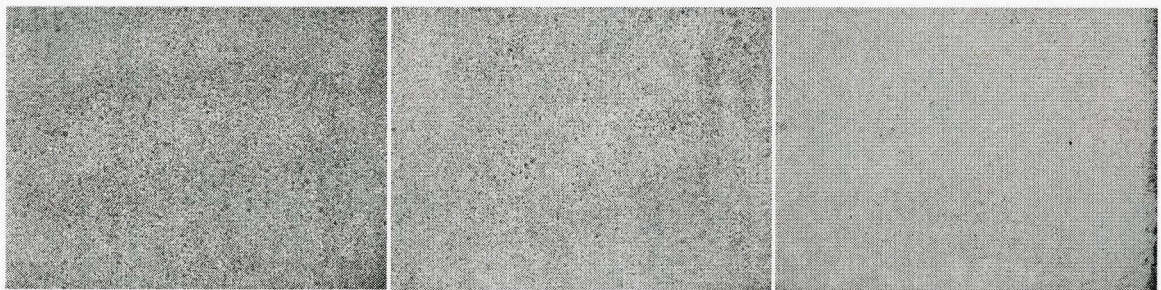


Figure 4-8: Field Surface Modified Pavement with 50, 100 and 150g/m² of Hydrated Lime [From Left to Right].

modified with 50g/m^2 , 100g/m^2 and 150g/m^2 concentrations of hydrated lime, respectively. Similar to the procedure adopted in the laboratory, the hydrated lime amounts were weighed using a digital scale. The material was then spread on the surface of the pavement using a brush, after which the laboratory hand-made rubber wheel paint roller was used to compact the lime and force it to penetrate a couple of millimeters into the pavement structure. Due to the fact that traffic could not be blocked for a long time, only three representative hydrated lime concentrations per surface area were applied to the pavement surface for later comparison with laboratory results.

4.2.2 Testing Setup and Procedures

Being located on an incline, there was a chance of drainage water flowing onto the test areas during a rainfall. Therefore besides covering the entire setup with a tarp during the night, the test areas were surrounded with silicon to prevent any water leakage onto the patches, which could affect the lime coverage. Testing was carried out during a clear sunny day in August to assure quality results. Surface temperatures were recorded using the FLIR infrared camera shown in Figure 4-3. Measurements were generally taken and recorded every 15 minutes for the first 1.5 hours and then every half an hour for the remainder of the test, which usually ended shortly after the temperature of the black surface reached its peak value. The surface temperature readings were taken at the center of the test areas in order to provide representative results and minimize the influence of edge effects.

4.2.3 Results

Being in an area of high traffic volume, the tests were all completed in one day. The test duration was approximately 5 hours during a summer day, which was at a maximum ambient air temperature of 36.6°C. The different lime concentrations were all assessed together for their influence to avoid weather variations that might have occurred had each patch been tested separately. Once the testing was completed, the results were organized and plotted, as summarized in Figure 4-9.

4.2.4 Discussion

As shown in Figure 4-9, the reduction in the surface temperature of the asphalt pavement increases with an increase in the amount of hydrated lime placed on the surface. As observed previously, surface temperature increases during the course of the day. Unlike the controlled case in the laboratory, one observes a greater temperature difference between surfaces covered with 100 and 150 g/m², respectively. In the laboratory setting, the maximum temperature difference between the above-mentioned lime concentrations was 2 celsius degrees whereas in the field, the difference is 4 degrees as seen in Figure 4-9. This maybe due to a small amount of lime that escaped while spreading it on the surface of the pavement, which was modified with 100g/m². This did not happen at the laboratory due to the fact that the surface of the sample to be tested was carefully modified inside the laboratory before it was taken out and placed at the center

of the pavement grid. The temperature difference could also be due to the differences in environmental conditions such as the amount of air blowing across the surface.

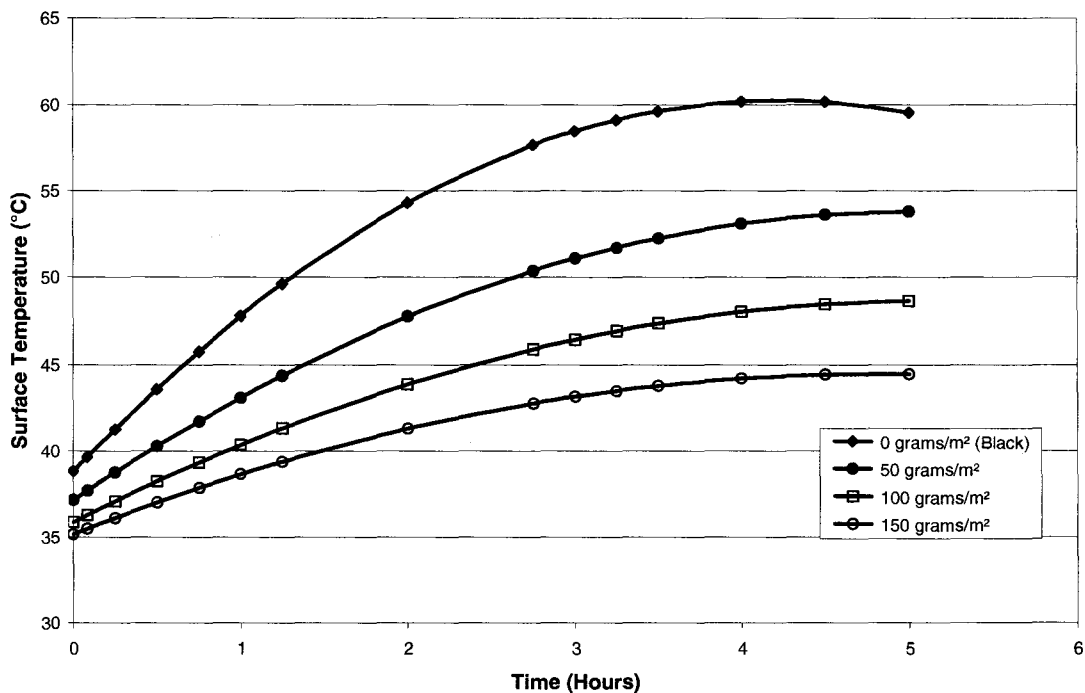


Figure 4-9: Effect of Hydrated Lime Amount on Surface Temperature of Field HMA Pavement.

It should be noted that the air temperature recorded during laboratory testing was 34.3°C, whereas during in-situ testing, it was 36.6°C. Taking into account the above-mentioned possible contributors to the error encountered and in spite of the in-situ results, it was still felt that 100g/m² of hydrated lime was an optimum application level.

As shown in Figure 4-10, which relates the surface temperature reductions from the laboratory and field site settings with each point corresponding to a specific black

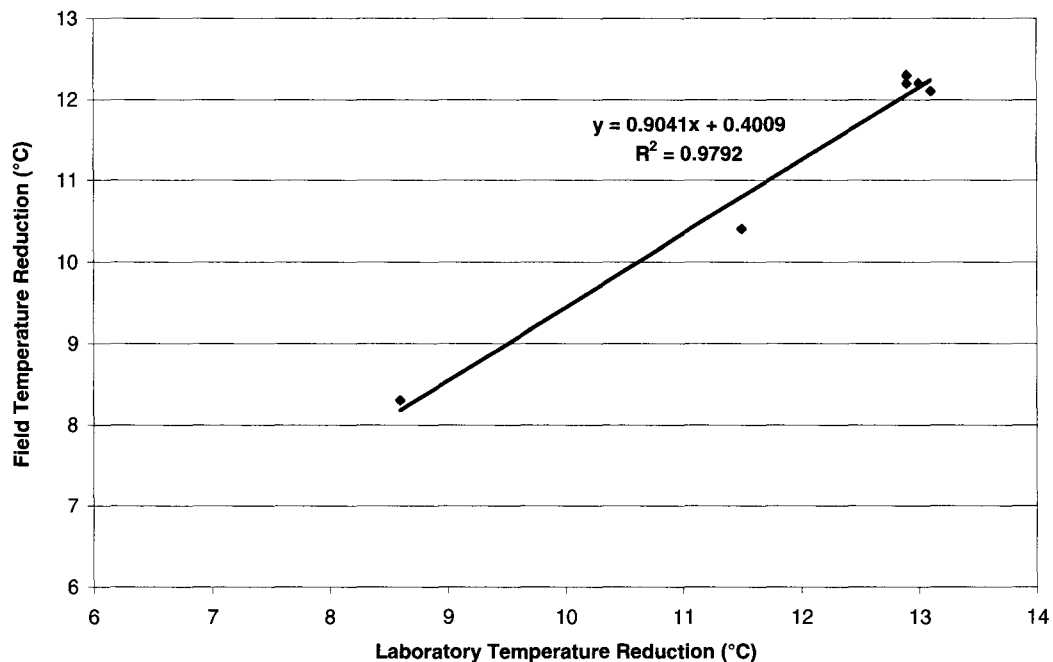


Figure 4-10: Relationship between Laboratory and Field Site Surface Temperature Reduction for 100g/m^2 of Hydrated Lime Dosage

body temperature, it is evident that there is a strong linear correlation between the two sets of readings (i.e. $R^2 = 0.988$). This means that one can further assess the influence of 100g/m^2 of hydrated lime on the surface of the pavement in a laboratory environment over a broad range of conditions without the need for further field site verification of results.

4.3 METHOD OF ADDING HYDRATED LIME TO THE SURFACE OF HMA PAVEMENTS

Although construction procedures are not part of this thesis, it is worth mentioning the method of placing hydrated lime on the surface of an in-situ pavement.

In practice, hydrated lime should be uniformly spread at the specified amount per surface area of asphalt pavement using a suitably equipped truck, similar to that shown in Figure 4-11. It should not be spread under windy conditions to prevent excessive dusting. The equipment often used for the application of hydrated lime includes self-unloading bulk tanker trucks, which are most efficient for transporting and spreading of hydrated

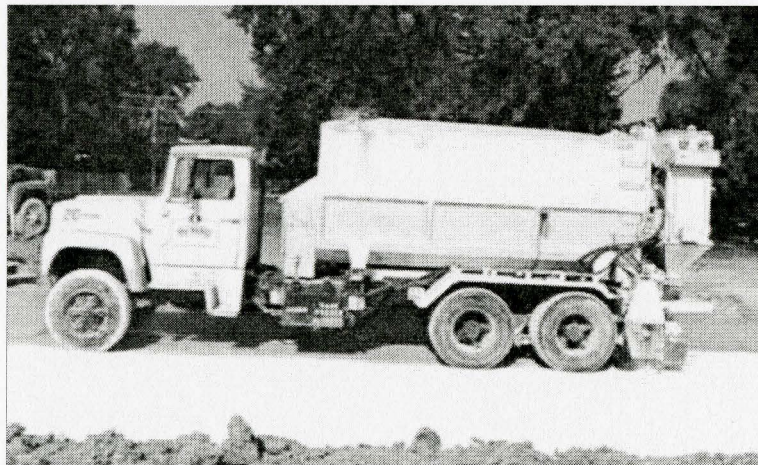


Figure 4-11: Dry Hydrated Lime Application with Mechanical Spreader.
[National Lime Association, May 2004]

lime because no rehandling is involved once the hydrated lime is placed into the tanker. Unloading of hydrated lime is conducted pneumatically or by one or more integral screw conveyors. Spreading, on the other hand, is accomplished by a mechanical spreader attached to the rear, or through metal downspouts or flexible rubber boots extending from each conveyor or air line.

If live bottom trailers are used, the bodies should be enclosed to prevent dusting during transit to the job and during spreading. Spreading from live bottom trailers should be conducted by means of a mechanical spreader attached to the rear. Tailgate spreading of hydrated lime and leveling with a grader are not recommended [National Lime Association, September 2003].

CHAPTER 5

EFFECT OF HYDRATED LIME ON THE TEMPERATURE PROFILE OF HMA PAVEMENT

This chapter describes the impact of hydrated lime on the temperature profile once the lime is placed on the surface of hot mix asphalt (HMA). Laboratory results were supported by in-situ test measurements on surfaces that were tested using the same strategies developed in the laboratory.

5.1 LABORATORY TESTING

The surface of an HMA mix is continuously in direct contact with the ambient air, and therefore has a tendency of experiencing either a temperature reduction or increase. Due to thermal equilibrium, the hotter objects tend to lose heat to the colder objects to create a balance. Equilibrium not only takes place between objects, but also within an object itself. A reduction in surface temperature of HMA mix would cause heat to move from within the structure to the surface to restore the temperature balance. Consequently, surface modification of HMA mixtures with hydrated lime not only affects the surface temperature but also affects the temperature within the pavement. The effect of placing hydrated lime on the surface of HMA mixes was found to reduce the surface temperature of pavement, which is expected to improve the mechanical properties of the asphalt concrete and its performance.

As indicated in Chapter 4, the optimum amount of hydrated lime was found to be approximately 100g/m^2 . Given this surface dosage, the next step was to evaluate the temperature reduction with depth, and therefore generate a temperature profile within the SP12.5FC2 PG64-28 pavement as a result of this surface modification.

5.1.1 Sample Preparation

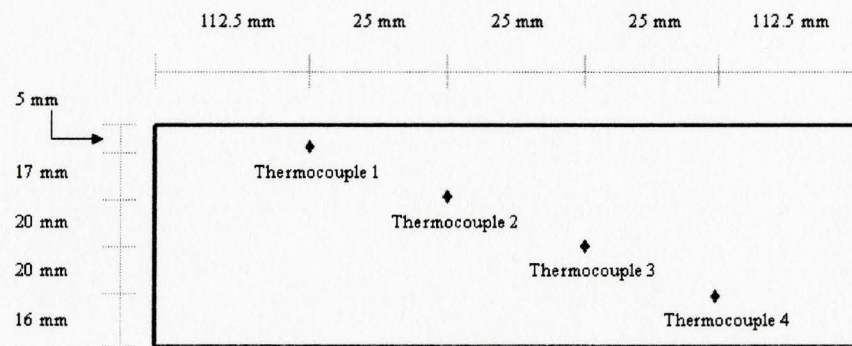
The fine-gauge temperature measuring device, the Butt-welded unsheathed micro-temperature thermocouples from Omega Canada shown in Figure 5-1, was chosen to measure the temperature profile of the SP12.5 FC2 PG64-28 pavement structure. This device, which is 0.25mm (0.010 inch) in diameter and 305mm (12 inches) long, consists of two metal wires; one made of constantan¹ whereas the other copper. Both wires are connected together at their tips by welding. The welded tip is where the measurement takes place at the time of contact. Both wires of each thermocouple were insulated prior to installing them into the specimens to avoid contact at a point other than the tip where temperature was to be measured. Being fine gauged, it was possible to insert the wires into 3.2mm (1/8") in diameter fine drilled openings in the pavement, which made it possible to minimize the amount of heat loss. Samples were drilled from the side, halfway through the width (125mm), which corresponded to roughly 62.5mm, as shown

¹ Constantan is an alloy usually consisting of 55% of copper and 45% of nickel ($\text{Cu}_{55}\text{Ni}_{45}$). It has high electrical resistance and a very low temperature coefficient [Wikipedia, 2007].

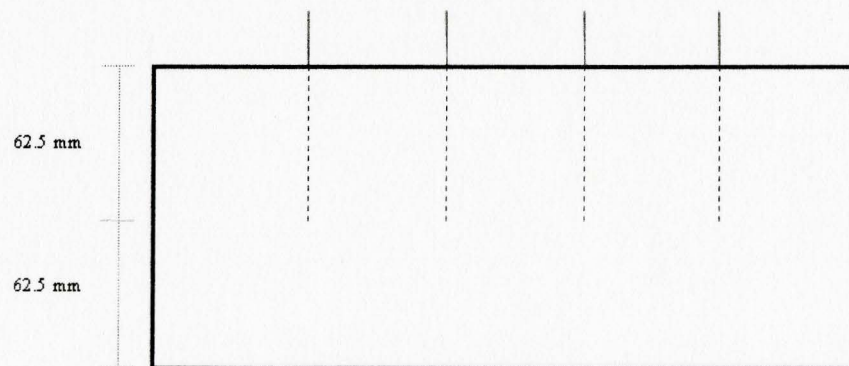
in Figure 5-2 (b). The reason for placing the thermocouples centrally along the width of the samples was to ensure that representative body measurements of temperature could be



Figure 5-1: Butt-Welded Unsheathed Micro-Temperature Thermocouple [Omega Canada, 2002].



(a) Side view of sample.



(b) Top view of sample.

Figure 5-2: Illustration of Thermocouples Configuration on a Laboratory Prepared Sample.

made in the area that was modified with hydrated lime as described in the “Sample Preparation” Section of Chapter 4.

To reduce the number of factors coming into the analysis, the sample used for assessing the effect of 100g/m^2 of hydrated lime on the surface temperature was also used for determining the temperature profile. Before drilling, samples were placed in a freezer for 2 hours in order to bring down the pavement temperature to 4°C , which was necessary to reduce the possibility of pulling the AC and separating it from the aggregates while drilling. Four thermocouples were placed at various pre-selected distances measured down from the top surface of the specimen. Figure 5-2 shows the target depths and the configuration in accordance to the Long-Term Performance Program (LTPP) guidelines. The guidelines suggest that the thermocouples are not to be inserted above one another along a vertical line, which implies that a lateral spacing forming a V-shape pattern was kept between the thermocouples. Staggering the thermocouples reduced the effect that each thermocouple had on its neighbours. According to LTPP, a lateral spacing of 20-30mm is recommended. The lateral spacing between the thermocouples chosen for this study was an average of 25mm measured centre to centre.

Vertical heat transfer through the pavement is not one-dimensional, but rather two-dimensional. This is to say, not only does the heat move vertically, it also flows

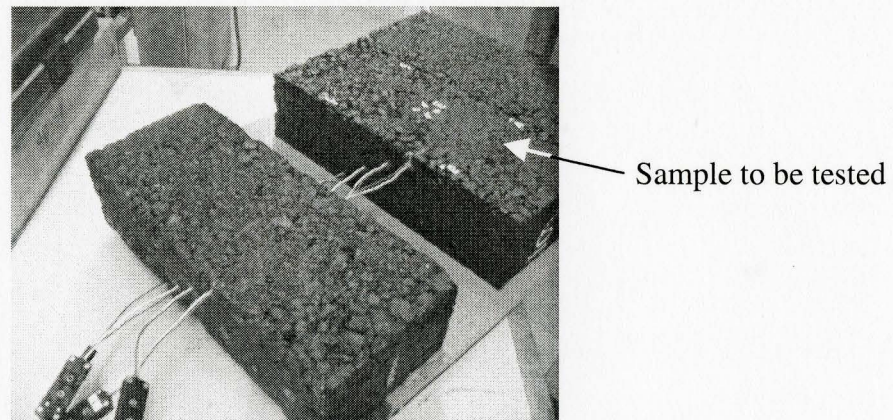


Figure 5-3: Laboratory Sample Being Prepared for Temperature Profile Testing.

horizontally. As a result, those areas of the surface not modified with hydrated lime, can act as a heat sink contributing to horizontal flow of heat. In order to reduce this effect on measurements and obtain more reliable readings, the lime-modified area was made large enough ($450 \times 550\text{mm}^2$) using a number of samples to form a pavement grid as shown in Figure 5-4. The sample being tested was placed at the centre of the grid.

5.1.2 Testing Procedures

Once the sample being tested was placed at the centre of the pavement grid, thermocouples were passed through the surrounding samples and placed tightly into the sample located at the centre. Besides being more representative of field conditions, the surrounding samples were covered with approximately the same dosage of hydrated lime

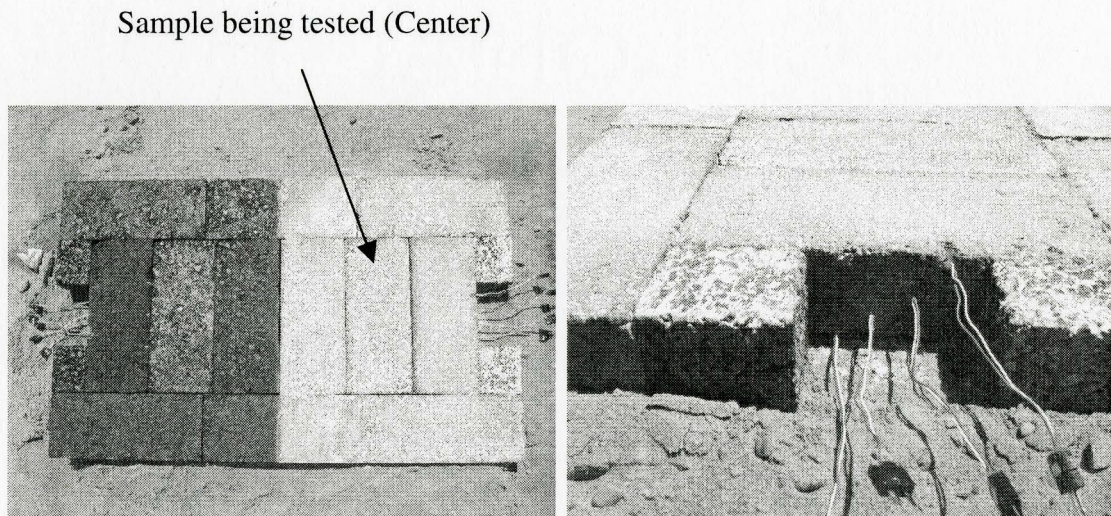


Figure 5-4: Temperature Profile Laboratory Testing Apparatus.

to reduce the potential for horizontal heat transfer. The test setup was placed outside under sunlight and temperature readings using a 12-channel data logger were generally taken every 15 minutes for the first 1.5 hours and then every half an hour for the remainder of the test, which usually ended shortly after the temperature of the black surface reached its peak value, similar to the procedure adapted in Chapter 4.

5.1.3 Results

Pavement temperature profiles, corresponding to peak surface temperature at 6 hours, were obtained for the case of no lime on a new pavement, which acted as a control for comparison reasons, and secondly for the case in which 100g/m^2 of hydrated lime was applied to the surface. Test results corresponding to the two cases are shown in Figure

5-5 with the measurements made with respect to time are summarized in Appendix C. It is clearly observed that a temperature reduction occurs over the entire 78mm sample depth. It should be noted that typical pavements have thicknesses varying from 150 to 200mm. As a result, 78mm would correspond to the upper zone of asphalt concrete; i.e. within the surface course.

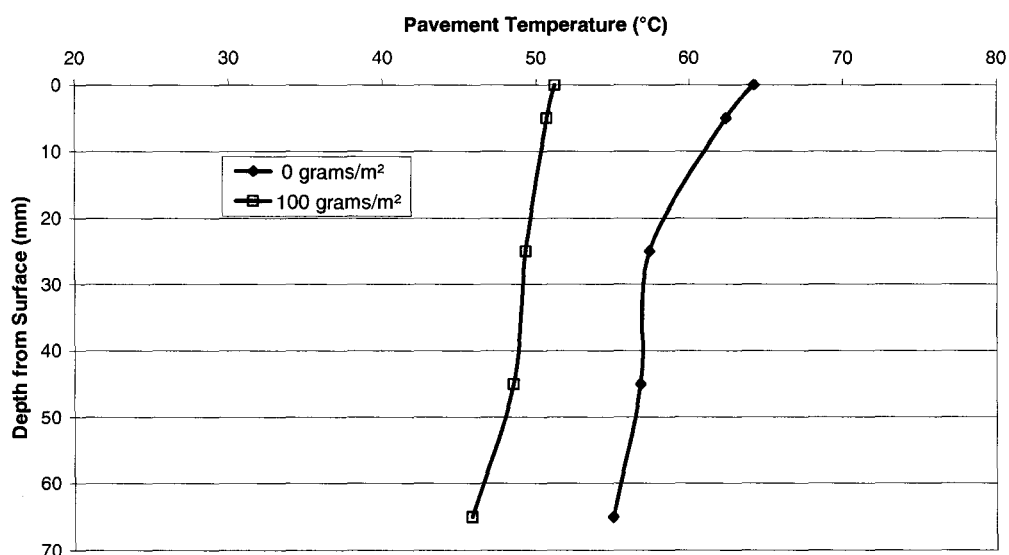


Figure 5-5: Peak Temperature Profiles of Laboratory Pavement That is Surface-Modified with Hydrated Lime at 0 and 100g/m² Concentrations.

5.1.4 Discussion

HMA mechanical properties are strongly influenced by temperature. There is a tendency for the rutting resistance of HMA mixes and their stiffness to decrease as temperature increases, as indicated previously. Hydrated lime was used to lighten the

surface colour of the pavement to help increase the albedo, which in turn reduces the surface temperature and hence enhances the pavement's performance.

As explained earlier, an increase in the amount of hydrated lime applied to the HMA surface increased the reflectivity, thus lowering the temperature both at the surface and also with depth. Since an optimum amount of hydrated lime modification of the pavement surface was found to be approximately 100g/m^2 , comparisons of temperature profiles were only carried out for specimens having this dosage and the control. Referring to Figure 5-5, the general trend, as one might expect, is for temperature to decrease as one moves away from the surface and deeper into the asphalt layer. It is clearly shown that the maximum temperature, which occurred at the surface, decreased from roughly 64.0 to 51.0°C , corresponding to hot summertime temperature conditions. The reduction in temperature was seen to be the maximum on the surface and to decrease as one moves deeper into the pavement. It should be noted that deeper in the asphalt layer, the temperature may not have reached steady-state conditions.

5.2 FIELD TESTING

To determine how representative laboratory specimens are with regard to modeling in-situ conditions, parallel field testing was performed following the same techniques developed in the laboratory. To reduce the effect of factors coming into the

analysis, the field hot mix asphalt pavement, being SP12.5FC2 PG64-28, was of the same design as that used for the laboratory testing.

5.2.1 Site Preparation

As mentioned in Chapter 4, four 700mm x 800mm patches located at the South West corner of Erin Mills Parkway and Dundas Street in Mississauga, Ontario, were allocated for testing. Similar to Chapter 4, comparisons are made only between the control and the surface covered by 100g/m² of hydrated lime to evaluate its influence on the temperature profile besides the control dosage.

As for the laboratory-prepared specimens, both profile and surface temperature readings were taken at approximately the centers of the test areas in order to yield representative results. In the field, temperature profile testing thermocouples were however located at depths different than those corresponding to the laboratory samples, the reason being that the samples in the laboratory were 78mm thick whereas the field surface course was only 50mm thick. To obtain readings representing a broad range of depths, the thermocouples in-situ were located at 10mm and 30mm from the surface, as shown in Figure 5-6. According to LTPP, a V-shape staggering of thermocouples is suggested, therefore a 100mm staggering was implemented to ensure accurate readings and minimize the influence of readings on one another.

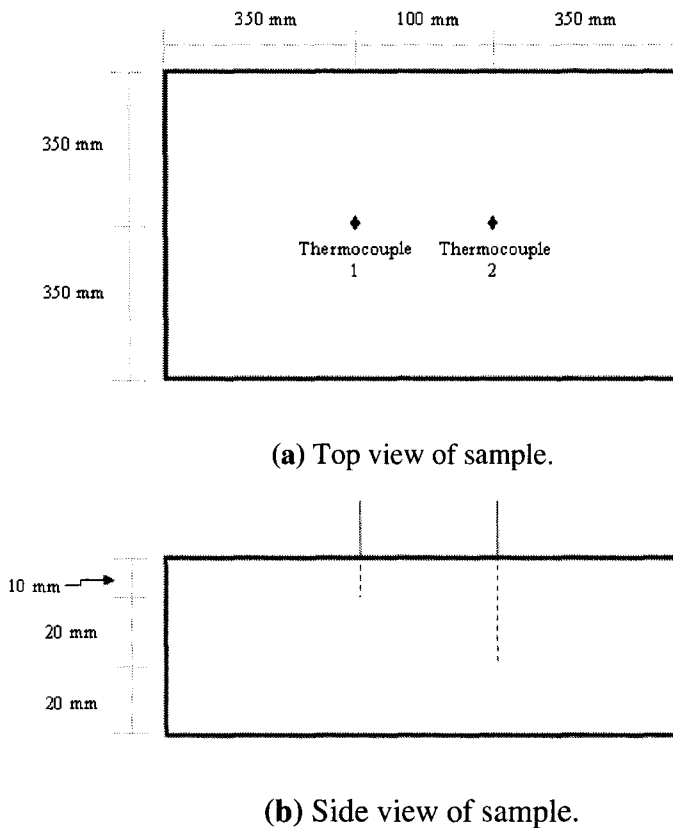


Figure 5-6: Illustration of Thermocouples Configuration for Field Pavement.

Thermocouples were inserted from the side of the laboratory specimens, whereas in the field, they had to be inserted vertically from the top, as shown in Figures 5-6 and 5-7, since the pavement had already been placed before arriving on site. In addition, the thermocouples would not have been at the correct depth and could have been damaged had they been placed before compaction and during construction.

To install the thermocouples, a drill bit of the same size as that used in the laboratory was used to drill holes from the surface and vertically downwards. The objective was to drill a hole that would be tight around the thermocouples once they are installed into the pavement in order to reduce heat transfer losses. To further reduce losses, the holes were blocked with non-heat conductive silicon once the thermocouples have been installed.

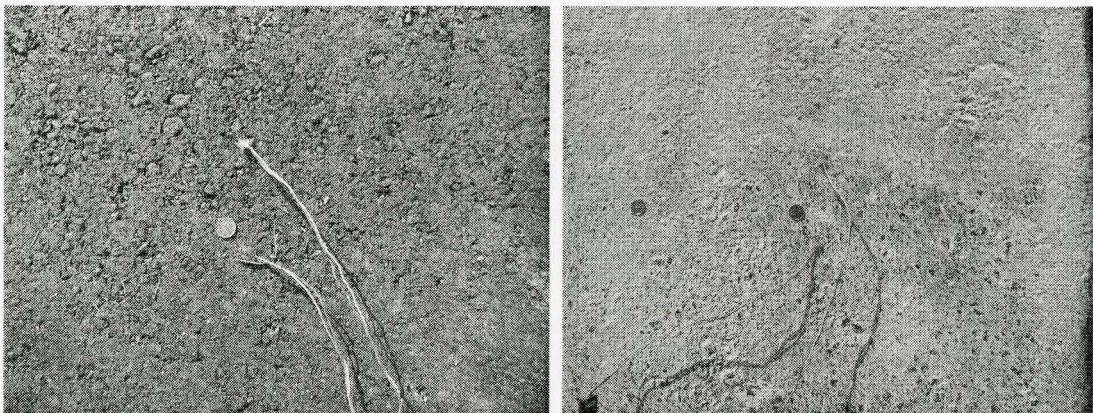


Figure 5-7: Thermocouples Placed into Black Unmodified and 100g/m² Hydrated Lime Surface-Modified Field Pavement.

5.2.2 Testing Procedures

To be able to correlate laboratory and in-situ test results, the procedures and equipment adopted for the laboratory testing were also used in the field. Once the testing setup was ready, temperature readings using the a 12-channel data logger were generally taken every 15 minutes for the first 1.5 hours and then every half an hour for the

remainder of the test, which usually ended shortly after the temperature of the black surface reached its peak value.

5.2.3 Results

To assess the correlation between laboratory and in-situ temperature profile results, the in-situ temperature profiles were also obtained for the case of no lime, which acted as a control for comparison reasons, and secondly for the case in which 100g/m^2 of

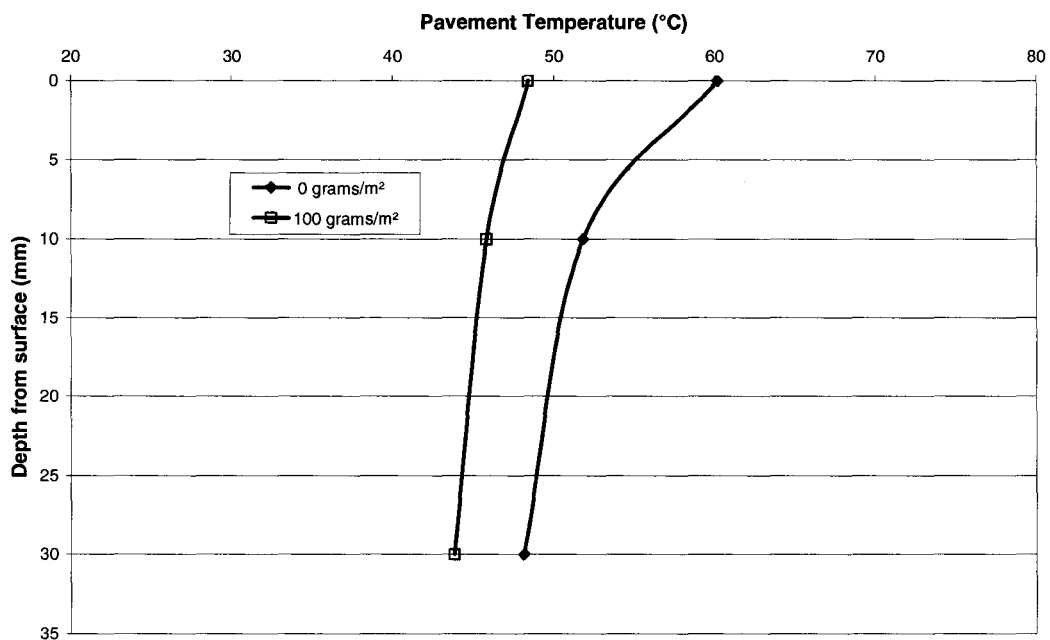


Figure 5-8: Peak Temperature Profiles of Field Site Pavement That is Surface-Modified with Hydrated Lime at 0 and 100g/m^2 Concentrations.

hydrated lime was applied to the surface. Test results corresponding to the two hydrated lime concentrations were plotted as shown in Figure 5-8 with the measurements made with respect to time are summarized in Appendix C

5.2.4 Discussion

The general trend in Figure 5-8 indicates that the temperature decreases with depth, as one might expect. Through the depth, not including the surface, the reduction is seen to be fairly consistent given that the two curves follow approximately the same trend but are only shifted. Readings at the two depths were not necessarily taken during steady state conditions; instead, they were taken at peak surface temperature, which occurred at approximately 4.5 hours after the start of the test, as shown in Figure 4-8. In addition, increased surface temperature requires some time before influencing the temperature measured at deeper points in the pavement structure.

To assess the correlation and closeness between laboratory and field results, the temperature reduction magnitudes corresponding to each hydrated lime amount added were compared. Figure 5-9 relates the temperature profiles of field and laboratory pavements at corresponding depths, ranging between 10 and 30mm, measured from the surface of the pavement for hydrated lime application amounts of 0 and 100g/m². As shown in Figure 5-9, it is evident that there is a strong correlation (i.e. $R^2 = 0.99$) of the best fit line connecting the points. This means that one can further assess the influence of

100g/m² of hydrated lime on the temperature profile of the pavement in a laboratory environment without the need for further field site verification of results.

Even though no thermocouples were placed at depths of 10mm or 30mm in the laboratory prepared samples, the curves of Figure 5-5 were used to interpolate the temperature readings corresponding to the above two depths. The average temperature reduction difference between in-situ and laboratory pavements is observed to be 3.78°C. Despite the difference in temperatures, there is still a strong correlation indicated by a high correlation coefficient value seen in Figure 5-9. This difference is mainly due the variation in temperature conditions between the time of in-situ and laboratory testing, and the possibility of field dosage changes due to wind. In addition, laboratory thermocouples were installed differently when compared to those installed at the field. This 3.78°C difference may reflect the fact that the thermocouples had been installed differently and the conditions at the surface being different. For further comparison, the curves shown in Figures 5-5 and 5-8 were used to approximate temperature reductions at depths between 0 and 30mm, and the results proving the correlation are shown in Figure 5-9.

The general trend indicates that the difference between field site and laboratory temperature reduction due to the addition of hydrated lime is the smallest on the surface, and increases as one moves down deeper into the pavement structure. This is because the surface temperature is primarily controlled by the sunlight, which is the main source of

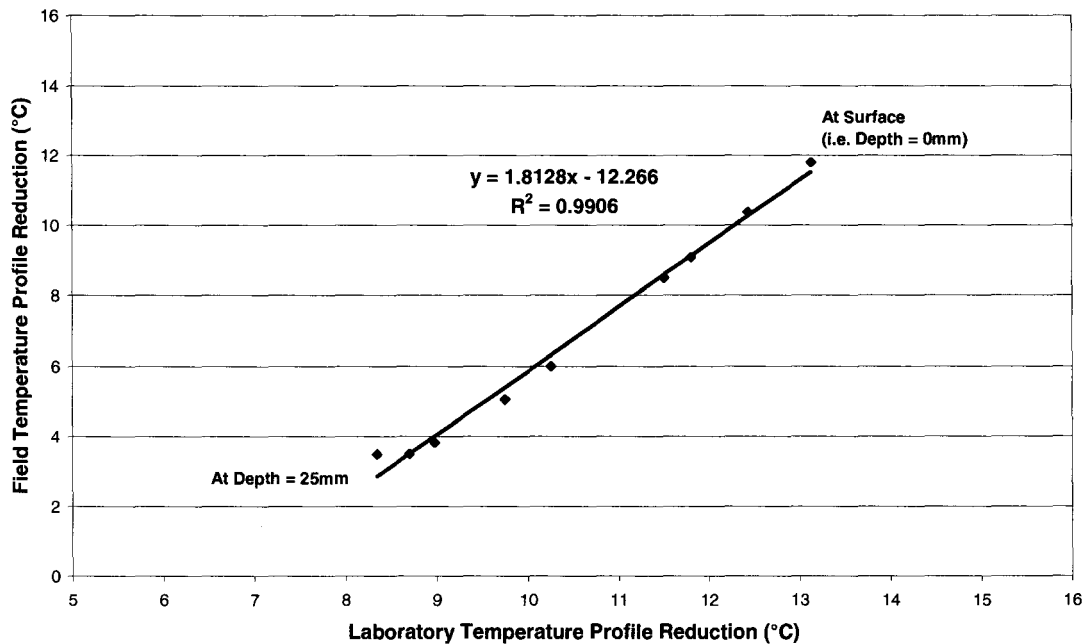


Figure 5-9: Field Site versus Laboratory Temperature Profile Reduction.

heat, therefore any change in weather conditions is directly reflected on the surface temperature difference. On the other hand, the temperature at the bottom of the pavement layer is influenced by not only the temperature profile of the pavement structure affected by the sunlight, but also the temperature of the soil beneath it.

CHAPTER 6

MECHANICAL PROPERTIES OF STUDY HMA MIXES

The temperature reduction due to the surface modification of HMA mixtures with hydrated lime was investigated in Chapter 4. This Chapter discusses the enhancement in the performance of hot mix asphalt (HMA) mixes due to temperature reductions with respect to their mechanical properties. The mechanical properties studied include:

- Fatigue Resistance;
- Rutting Resistance;
- Resilient Modulus; and
- Effective Surface Modulus.

6.1 EQUIPMENT AND PROCEDURES

6.1.1 Nottingham Asphalt Tester (NAT)

High stiffness and good fatigue resistance are required for an asphalt layer to perform well. The most economical way to determine these parameters is to measure them in the laboratory, more specifically by using a Nottingham Asphalt Tester (NAT), which is capable of testing asphalt concrete under controlled stress, strain, and temperature conditions.

The NAT has become a common piece of equipment to evaluate asphalt concrete whether in commercial laboratories, universities, oil companies, regional laboratories and contracting and engineering consulting firms worldwide. It has been shown that NAT test results correlate well with those of other test methods such as the bending beam and wheel tracking [Thom, 2006]. The NAT, shown in Figure 6-1, provides an inexpensive and user-friendly means of measuring and assessing the mechanical properties of asphaltic paving materials on a routine basis. The NAT consists of a loading frame

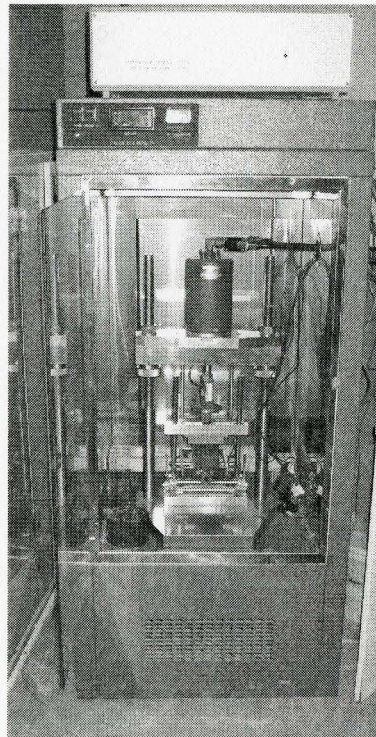


Figure 6-1: The Nottingham Asphalt Tester (NAT)

mounted in a temperature controlled cabinet, with a temperature range of -10°C to $+50^{\circ}\text{C}$. A pneumatic system supplies compressed air to apply a range of loads up to 4.3 kN, which is measured with a load cell whereas deformations are measured using LVDTs (Linear Variable Differential Transducers), with temperature measured via thermocouples. It is designed to derive the maximum information about a material using either cores cut from the road or laboratory prepared specimens. Applications of the NAT include its use in the mix design process, quality control, end-product specification, the assessment of raw materials, failure investigations, and in pavement assessments.

The NAT can be used to carry out a range of tests including the Repeated Load Indirect Tensile Test (RLIT) to measure the resilient modulus of an HMA mix, Static and Dynamic Creep Test, Repeated Load Indirect Fatigue Test (RLIFAT) to measure the fatigue resistance of an HMA mix, and Vacuum Triaxial Test. The NAT can also be used to measure other mechanistic properties of asphaltic material such as its resistance to permanent deformation and the material's Poisson's Ratio.

6.1.1.1 Resilient Modulus Testing

Of particular interest to flexible pavement designers is the resilient modulus (M_r), which is defined as:

$$M_r = \frac{\sigma_d}{\epsilon_{resil}} \quad [6-1]$$

where: σ_d = Repeated axial deviator stress,
 ϵ_{resil} = Recoverable resilient strain.

Resilient modulus M_r , which is required for static analysis of pavement structures, was determined by the Repeated Load Indirect Tensile Test (RLIT), which is a non-destructive test that indirectly measures the resilient modulus of laboratory specimens or thin HMA cores taken from the road. Experience has shown that the stiffness measured with the NAT, via the RLIT test, correlates well with results of the three-point bending test. RLIT is a function of load, deformation, specimen dimensions and assumed Poisson's ratio. If desired, the RLIT control software allows the operator to select a target horizontal deformation (usually 5.0 microns) instead of peak load level for measuring the M_r .

Specimens prepared for this study, which were 100mm (4") in diameter and 30 to 60mm thick, were obtained by coring specimens prepared from samples that were used for the reflective properties study (see Figure 6-2). Once cored, the samples were washed and dried with a cloth to remove all of the dust collected during coring. Thereafter, they were placed outside the NAT all night to drain excess water that resulted from washing. Samples were subsequently placed in the NAT chamber the following day at the target

testing temperature for a period of 24 hours prior to resilient modulus testing. Although the NAT dashboard gauge measures the chamber temperature, a thermocouple was also inserted into the center of a demo sample, having similar dimensions and composition to the tested specimen, and monitored with a thermometer placed outside the NAT chamber to ensure that the sample temperature was also at the target testing temperature.

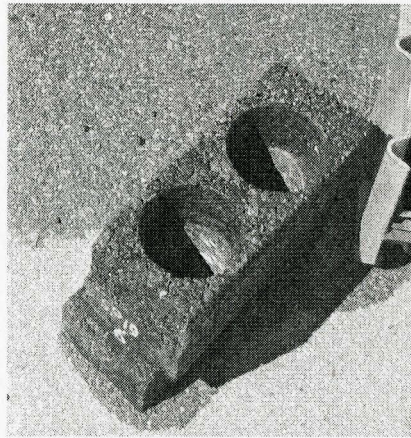


Figure 6-2: Coring of HMA Samples.

The specimens made for testing in the NAT were examined, and the thickness and diameter of each briquette were measured at different locations on the specimen and an average thickness and diameter were inserted into the software as an input. Thereafter, the Repeated Load Indirect Tensile Testing (RLIT) was performed at 10°C, 20°C, and 30°C \pm 0.5°C. The resilient modulus was determined by measuring the resulting

horizontal deformation that results from applying a vertical pulse load through the diameter of a cylindrical specimen; seen in Figure 6-3. For each test, five conditioning pulses were applied to enable the equipment to adjust the load to the requested horizontal diametral deformation (about 5 μm at each of the three testing temperatures). Five load

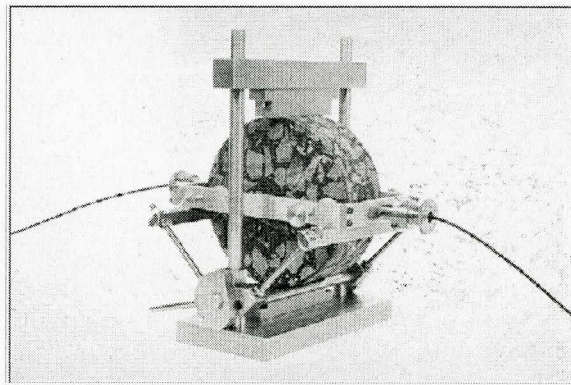


Figure 6-3:
Resilient Modulus Testing Setup, Inside the NAT.

pulses were then applied, with the peak load, peak horizontal diametral deformation and risetime measured for each pulse. The Poisson's ratio was assumed to be 0.25 at 10°C, 0.35 at 20°C, and 0.45 at 30°C, as recommended in the Draft for Development DD213:1993 for the British Standard Institute and in the ASTM D4123-82 [ASTM International, 1994].

6.1.1.2 Fatigue Resistance Testing

The results of the Repeated Load Indirect Fatigue Test (RLIFAT), which is carried out on circular specimens, correlate well with those obtained via the two-point bending test that is carried out on trapezoidal specimens [Irwin and Gallaway, 1973]. The RLIFAT was used in this study to rank mixes in order of their fatigue resistance. RLIFAT, which is carried out at selected strain levels, may also be used for mix design, failure investigation, pavement evaluation and assessment of new materials.

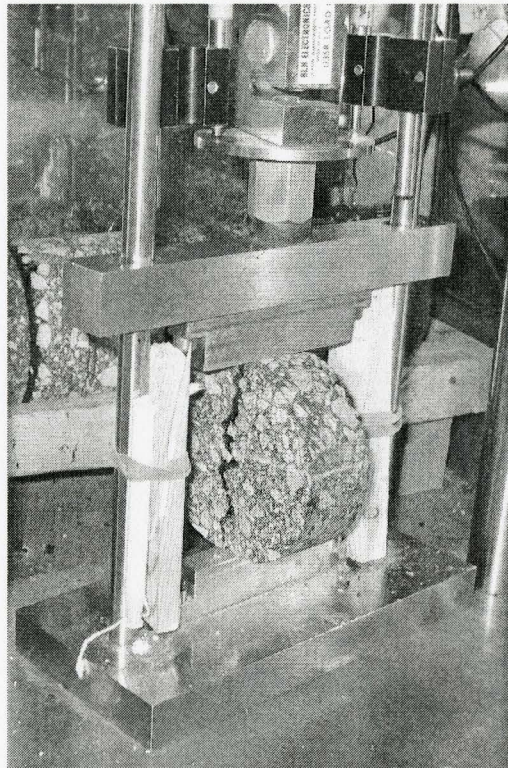
In the Repeated Load Indirect Fatigue Test, the specimens were subjected to repeated load pulses, corresponding to strains of 150, 225, and 300 microstrains, until failure occurred. The corresponding tensile stresses required to carry out the tests were estimated from stress analysis represented by Equation 6-2. These in turn were inserted as an input into the NAT system prior to the start of the testing in order for the NAT to apply the correct load, which would result in the target testing strain value.

$$\sigma = \frac{\varepsilon M_r}{1 + 3\nu} = \frac{2P}{\pi dt} \quad [6-2]$$

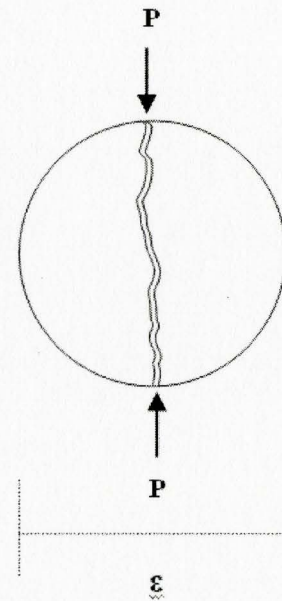
where:

ε	= Average horizontal tensile strain
σ	= Tensile stress at the centre of the specimen (kPa)
ν	= Poisson's ratio
M_r	= Indirect tensile resilient modulus (MPa)
d	= Specimen diameter (mm)
t	= Specimen thickness (mm)

Due to the non-destructive nature of the RLIT test discussed previously, the samples used to measure the resilient modulus of the different HMA mixes were re-used to measure the fatigue life of the mixes. Once the sample being tested was ready, its diameter and thickness were measured at different locations on the specimen and an average diameter and thickness were inserted into the software as input. Before the start



(a)



(b)

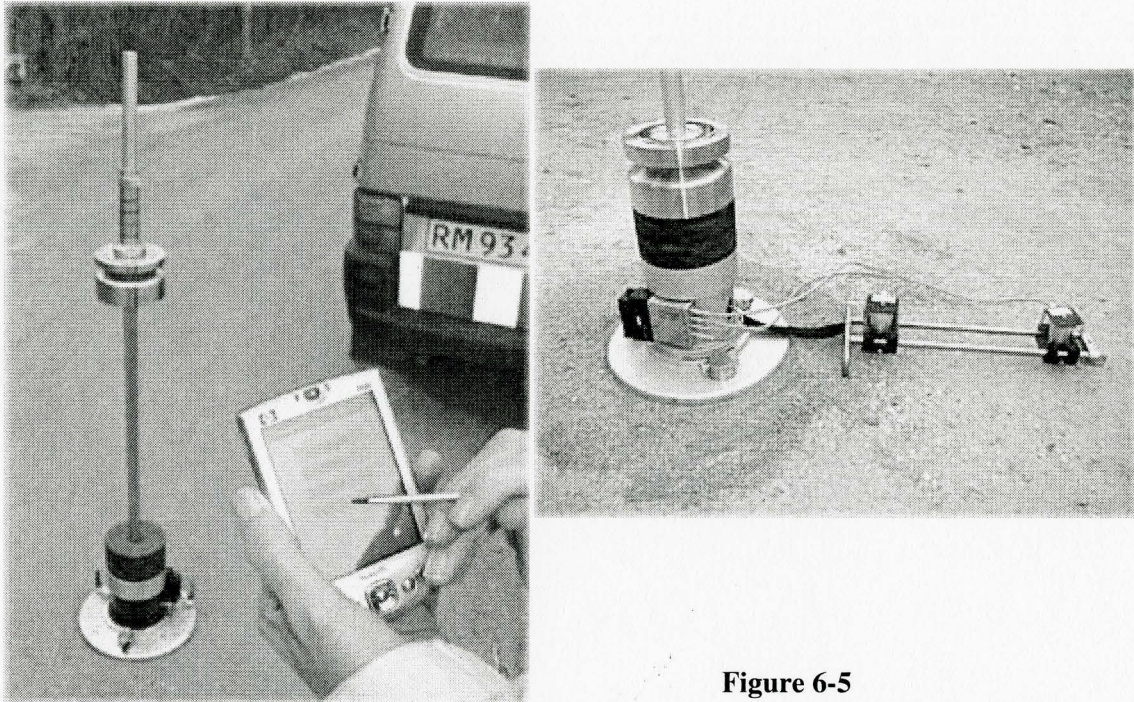
Figure 6-4: (a): Fatigue Resistance Testing Setup, Inside the NAT, (b): Illustration of Specimen Failure in Fatigue.

of the test, which was carried out at a temperature of $20^{\circ}\text{C} \pm 0.5^{\circ}\text{C}$ and a target rise time of 120 milliseconds, 5 conditioning pulses were applied to condition the specimen correctly inside the chamber. The test was then started and the specimen was loaded with pulses until failure, which by definition occurred when a vertical crack developed along the entire diameter of the specimen, as shown in Figure 6-4.

6.1.2 Light Weight Deflectometer (LWD)

Layer moduli are primary inputs to mechanistic pavement design procedures that analyze long-term pavement performance. The Light Weight Deflectometer (LWD), a product of Dynatest International, is a light, portable device that measures the stiffness of construction layers including subgrades, base/subbase courses, and pavements. The LWD, which is an upgrade of the Prima100 PFWD (Portable Falling Weight Deflectometer), was used for this study to determine the in-situ effective surface moduli of newly constructed pavements.

The LWD, shown in Figure 6-5, operates on the same principles as the Falling Weight Deflectometer (FWD), shown in Figure 6-6, but it is small enough to be easily moved and operated by one person. The LWD creates a non-destructive wave through the soil or any compacted layer as a result of the impact of a falling mass (10, 15, or 20 kg)

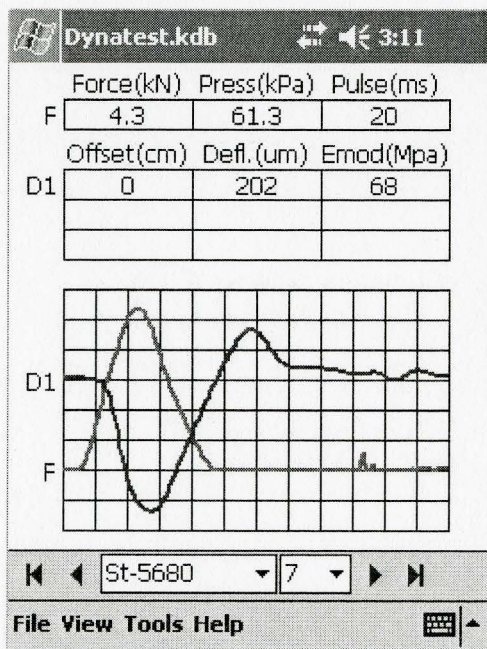
**Figure 6-5**

Top Left:
LWD and Its Bluetooth
Connection Ability.

Left:
Screen Shot of Sample Test
Results.

Top:
Deflections Measured with Three
Sensors.

[Dynatest, 2006]



from a variable drop height (10 to 850mm) onto a 100, 200, or 300mm diameter loading plate that rests on the surface being tested. The LWD uses two types of sensors; a load cell for measuring the impact force from the falling weight, and one to three geophones, shown in Figure 6-5, for tracking the deflection with respect to time via a computerized data acquisition system. This test allows the engineer to back-calculate the effective surface modulus of HMA using the measured deflections and the impact load.

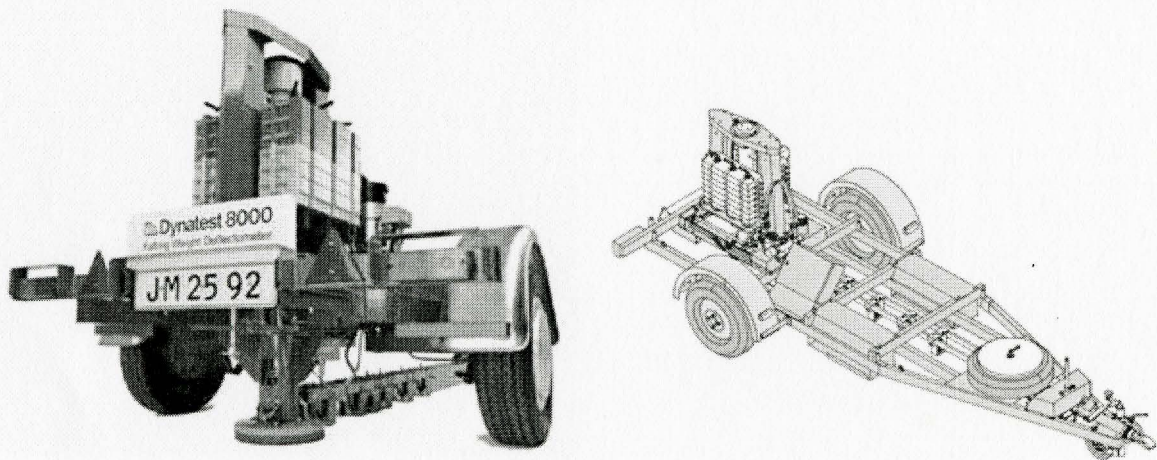


Figure 6-6: Falling Weight Deflectometer (FWD) [Dynatest, 2006].

Field tests were performed on newly laid site, which consisted of HMA that corresponded to the same material that was tested in the laboratory. A small area on a road, which is located at the South West corner of Erin Mills Parkway and Dundas Street in Mississauga, Ontario, was used for testing. A fairly uniform flat $700 \times 800\text{mm}^2$ area in

the middle of the traffic lane, but along the side as shown in Figure 6-7, was marked and used for testing. Tests were carried out at three temperatures on the same day in order to see how the effective surface modulus, as evaluated from system response, changes with temperature. Following the LWD user manual, a large magnitude of pressure was used to ensure that good results could be obtained. In order to maximize the applied pressure, the smallest plate radius was chosen (150mm) together with the largest load (20kg).



Figure 6-7: Section of the Traffic Lane Marked for Testing (Prior to Paving).

Corresponding to each temperature, four load applications were applied to the pavement surface. For further analysis, the testing temperature was measured using a surface temperature measuring device. The first drop of a set was a “seating” load to ensure that the LWD load plate was firmly sitting on the pavement surface. The

following three loads were applied at heights of 127mm (5 inch), 432mm (17 inch) and 686mm (27 inch), respectively. Once the impact load and deflection measurements were made by the LWD, the saved results were transferred to a PC for further analysis using LWD-mod software, which was specifically developed to analyze data obtained using the Light Weight Deflectometer (LWD).

The LWD test results were interpreted using “Maximum Normalized Deflection” and “Back Calculation of Pavement Layer Moduli” methodologies [Miller and Dhillon, 2003]. Maximum Normalized Deflection is measured in the center of the load plate, and is a good indicator of the overall pavement strength. The deflection at this location is a function of the pavement layer stiffness as well as the support capacity of the subgrade. Because deflection is a function of load and because of slight variations in measured load at different testing points and in the homogeneity of the pavement structure, the loading applications were all made at exactly the same point and with the same LWD orientation.

6.1.3 Asphalt Pavement Analyzer (APA)

Urban roadway pavement rutting, particularly at signalized intersections, is of concern and a challenge for those responsible for municipal pavement infrastructure. Agencies have, in recent years, been proactive in trying new strategies for dealing with mitigating this problem. These strategies include the placement of premium hot mix asphalt (HMA) surfacing materials, making use of polymer modified or high performance

grade asphalt binder, stone matrix asphalt (SMA), Superpave mix types, and the use of sulfur extended asphalt modifier. Cities such as Calgary and Lethbridge have recently placed various types of pavement surfacing materials with the objective of assessing performance under in-service conditions. The limited experience with these types of hot mix asphalt materials to date has, however, contributed to using known and proven technologies, rather than the ones that first require proper assessment with regard to their performance. The Asphalt Pavement Analyzer (APA) has been shown to be a useful tool for the assessment of the permanent deformation (rutting) resistance of HMA materials [Uzarowski and Emery, 2000].

The APA has a thermostatically controlled testing chamber designed to test the rutting susceptibility of asphalt aggregate mixtures by applying repetitive linear loads to compacted test specimens through three pressurized hoses via wheels, as shown in Figure 6-8. It can maintain the test temperature and condition its chamber at any set-point between 4° and 72°C, is capable of independently applying loads up to 0.55 kN at a test hose pressure of 827.4 kPa (120 psi) and is capable of simultaneously testing 6 cylindrical or 3 beam samples.

Rut resistance testing was performed in accordance to the AASHTO TP 63-03 guidelines. Tests were carried out using the originally prepared 300 x 125 x 780mm

(Length, Width, Height) rectangular beams described in Chapter 3. Following the APA procedural instructions, specimens are to be preheated in the APA test chamber or a

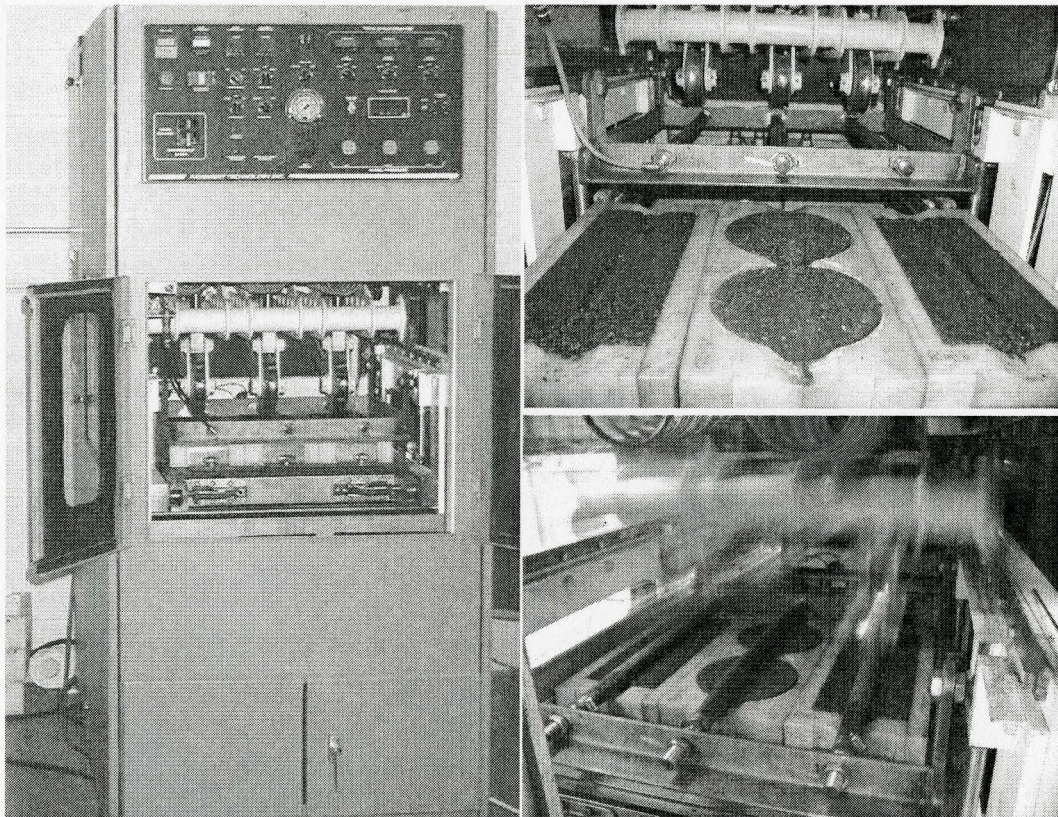


Figure 6-8: *Left: The Asphalt Pavement Analyzer (APA), Right: Testing Setup & Running Test Illustration.*

separate calibrated oven for a minimum of six hours, but are not to be held at elevated temperatures (i.e. greater than the testing temperature) for more than 24 hours prior to testing to reduce asphalt cement age hardening. The preheating procedure adopted in this

study was modified in order to allow for the heat loss while setting up the samples in the APA and getting them ready for testing. This was accomplished by quickly heating

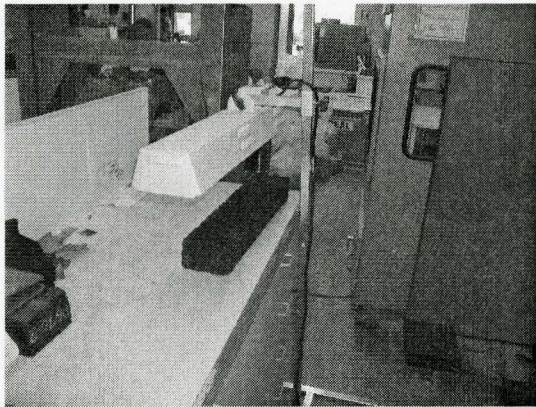


Figure 6-9: Preheating of APA Testing Specimens Using a Curing Lamp.

the surface using a vehicle paint curing lamp, shown in Figure 6-9, until the surface reached a temperature 5°C higher than the testing temperature corresponding to the APA chamber.

Using the APA, the rutting susceptibility of the different HMA mixtures was evaluated by subjecting HMA samples to a “moving wheel load” and measuring permanent deformation at selected points along the wheel path as a function of the number of loading cycles. A pressurized rubber hose was placed between the moving wheel and the HMA sample to approximately simulate traffic loading through tires on a

field pavement. Two rectangular beam samples of the same mix were subjected to 8000 cycles each for higher accuracy of results.

6.2 SUMMARY OF RESULTS

Table 6-1 summarizes the resilient modulus results obtained for the different HMA mixes. The mixes in the table are organized in order of their sensitivity to temperature. One observes that the rate of the resilient modulus reduction of the SP12.5FC2PG64-28 mix is the highest with increasing temperature, whereas the rate of reduction for the SMA mix is the lowest.

Table 6-2 summarizes the rutting results as well as the fatigue life obtained for the different HMA mixes. The mixes in the table are organized in order of their sensitivity to temperature. One observes that the increase in the rate of rutting with increasing temperature is the lowest for SMA mix, whereas the rate for the SP12.5FC2PG64-28 mix is the highest.

Table 6-1: Summary of Resilient Modulus Data vs. Temperature of HMA mixes.

Mix Type	AC Content (%)	Resilient Modulus Testing Temperature (°C)	Resilient Modulus M_r (MPa)	Rate of M_r Decrease (MPa) per 1°C Increase in Temperature
SP12.5FC2PG64-28	4.7	10	8939	155
		20	6858	
		30	5850	
SP19.0	4.5	10	9105	151
		20	8042	
		30	6091	
SP12.5FC2PG70-28 (Polymer Modified)	4.6	10	7522	114
		20	6408	
		30	5235	
SMA	5.8	10	5898	72
		20	4863	
		30	4457	

Table 6-2: Summary of Rutting and Fatigue Life Data vs. Temperature of HMA mixes.

Mix Type	AC Content (%)	Rut Testing Temperature (°C)	Rutting Experienced (mm)	Fatigue Life Testing Strain ϵ	Fatigue Life (No. of cycles to failure) @ 20°C
SP12.5FC2 PG64-28	4.7	52	3.16	225	3100
		58	4.69		
		64	6.57	300	760
		70	7.67		
SP19.0	4.5	52	2.36	150	7558
		58	2.85		
		64	4.13	225	974
		70	4.69		
SP12.5FC2 PG70-28	4.6	52	1.36	225	4189
		58	1.84		
		64	3.27	300	696
		70	3.83		
SMA	5.8	52	1.04	225	9267
		58	1.32		
		64	1.72	300	1357
		70	1.86		

6.3 RESILIENT MODULUS TESTING

The stiffness of asphalt concrete, which is an essential property for analyzing pavement response to traffic loading, is important in determining how stresses and strains are distributed, which in turn influences how well a pavement performs. High stiffness is a good performance characteristic but care must be taken due to the potentially low fatigue resistance of highly stiff HMA mixtures. Stiffness of HMA mixtures depends highly on the temperature (T) of the pavement, and hence the ambient temperature. This section examines and assesses the effect of temperature on the resilient modulus of the different HMA mixtures described in Chapter 2.

Tests conducted on asphaltic concrete, using the RLIT resilient modulus test method, have confirmed temperature to be a major parameter affecting resilient modulus. The $M_r - T$ relationship for a particular mix depends on the asphalt cement content and stiffness, aggregate gradation and actual aggregate employed. In addition, aging of the asphalt cement plays a key role in this $M_r - T$ relationship [Shell Bitumen, 1990].

6.3.1 Factors Affecting Resilient Modulus

The resilient modulus test is widely used. Nevertheless, there are many factors affecting the resilient modulus of asphalt concrete whether measured using the Repeated Load Indirect Tensile (RLIT) test in the NAT or using the two-point bending beam test.

Although M_r is a material property, specimen geometry (thickness and diameter) is an important factor affecting its measured value. The smaller size specimens tend to have a higher resilient modulus than larger ones [Saleh and Ji, 2004]. Mix variables such as the stiffness of the asphalt cement, the AC content of the mix, the percent of air voids (i.e. density), the nature and gradation of the aggregates, the age of the mix and the particle characteristics such as its angularity are significant factors that influence the resilient modulus of asphalt mixtures. The aggregate gradation is a significant factor as the coarser gradation tends to increase the resilient modulus when compared to the fine gradation. The interactions between specimen geometry and aggregate size and the compaction method also play important roles. The larger size specimens tend to be less sensitive to the compaction method and the aggregate gradation when compared to the smaller size specimens. The duration of vertical or deviatoric stress/strain application is another significant factor affecting the resilient modulus due to the visco-elastic nature of bituminous material. Loading time and resilient modulus are inversely proportional; i.e., the shorter the load duration, the higher the resilient modulus and vice versa. Testing temperature, as will later be shown in Figures 6-10 and 6-13, plays a very important role in the determination of the resilient modulus of HMA mixes.

Loading variables such as the loading magnitude, rate, frequency, the rest periods between applications, and the confining stress levels are considered secondary factors affecting the resilient modulus of asphalt mixtures [Saleh and Ji, 2004].

6.3.2 Results and Discussion

Asphalt mixes are visco-elastic. In other words, their mechanical properties depend not only on the temperature at which the load is applied but also on the rate of loading. The complexity of the problem is increased by the heterogeneity of the mix components. The asphalt binder is the component responsible for the visco-plastic properties whereas the mineral skeleton influences the elastic and strength properties of an HMA mix. The great diversity in the nature of the components and the mix compositions makes experimental testing the most suitable way of estimating HMA properties, such as the resilient modulus.

Once the tests were completed, a plot for each mix, representing its laboratory resilient modulus versus the temperature that the mix was tested at, was generated. The curves shown in Figure 6-10 represent the lines of best fit of the data points corresponding to different temperatures. As expected, M_r decreases with increasing temperature.

Referring to Figure 6-10, the resilient modulus is seen to be the greatest for the SP19 and the least for the SMA mixtures, which is attributed to the SMA being the richest in terms of Asphalt Cement (AC) content when compared to the rest of the HMA mixtures studied, whereas the SP19 is the least rich. One observes that the resilient modulus of the SP12.5 FC2 PG64-28 is higher than that of the same mix containing a

PG70-28 performance grade asphalt cement. This is mainly due to the polymer modification present in the PG70-28 AC of the SP12.5 FC2 PG70-28, which makes it more flexible and therefore resistant to fatigue at low temperatures, for instance. Assuming that the rate of M_r reduction remains constant as temperature increases, and making use of the average rates of resilient modulus reduction with increased temperature, one observes that through extrapolation and for pavement temperatures greater than 40°C, the previously-mentioned trends start to change. The SMA becomes the stiffest, whereas the SP12.5FC2 PG64-28 becomes the least stiff. This is because the

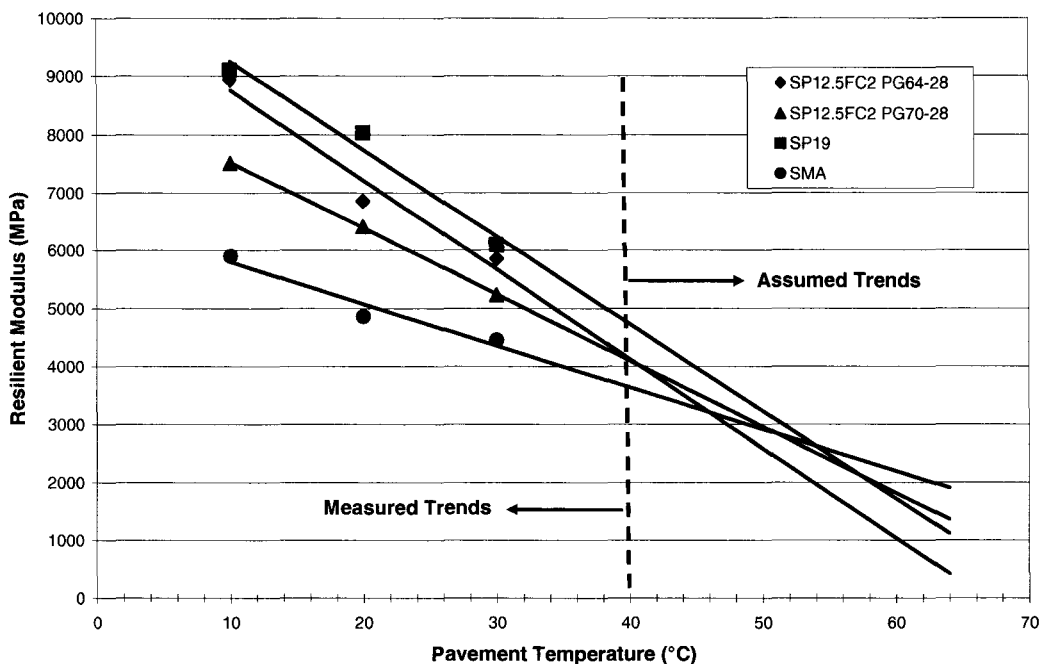


Figure 6-10: Effect of Temperature on Resilient Modulus of HMA Mixes.

average rate of resilient modulus reduction, represented by the average slopes of the lines in Figure 6-10, is the lowest for the SMA and the highest for the SP12.5FC2 PG64-28 mixture. At high temperatures, the polymer modification of the asphalt binder used in the non-modified case; i.e. SP12.5FC2 PG70-28, starts to be effective, making the asphalt binder stiffer, which in turn makes the mix stiffer when compared to the SP12.5FC2 PG64-28. Reduced temperature sensitivity is desirable for a mix to perform well with respect to rutting, for instance.

The reduction in M_r with increasing T is a linear relation as shown by the lines of best fit drawn in Figure 6-10. One finds that at room temperature, a 10°C decrease in temperature increases the resilient modulus by 21%, 19%, 18% and 14% for SP12.5FC2PG64-28, SP19, SP12.5FC2PG70-28 and SMA, respectively. These increases in the resilient modulus were determined using the rate of increase of resilient modulus with decreased temperature. Assuming that similar trends hold at higher temperatures, a reduction in the pavement surface temperature through surface modification via hydrated lime coating would be expected to increase the asphalt binder stiffness, increasing the stiffness of the asphalt concrete.

6.4 EFFECTIVE SURFACE MODULUS FROM LWD TESTING

Nondestructive test (NDT) methods are widely used to evaluate the layer stiffnesses of pavements, which in turn can be used to estimate structural capacity. NDT

methods are preferable over time-consuming and costly destructive methods. The structural capacity of pavement is significantly influenced by the modulus of the hot mix asphalt (HMA) layer, which is a function of temperature that varies diurnally and seasonally.

Detailed pavement field evaluation, particularly the stiffness modulus, should supplement determining laboratory-measured mechanistic properties, since it is important that the values used in further analysis and overlay design are those corresponding to in-situ conditions, and take into account the model used for analysis. The purpose of this section is to evaluate the effect of temperature on the effective surface/stiffness modulus of HMA that is placed in-situ. The HMA studied on site is similar in mix design to the asphalt studied in the laboratory.

6.4.1 Analysis of Results

Back-calculation is a process by which the pavement deflections measured with the LWD at a given load are used to determine the stiffness modulus of the pavement. Back-calculation of pavement stiffness modulus was performed using LWDmod analysis software shown in Figure 6-11. The software models the pavement system as a rigid plate supported by a dense foundation. In general, back calculation uses analytical pavement response models to predict deflections based on a set of given layer thicknesses and modulus values. Given pavement thicknesses, the response models identify, via an

iterative process, the pavement stiffness modulus that produces deflections that are similar to those measured in the field. Once the analysis is over, the software displays the revised set of deflections, which are then used to yield a pavement stiffness modulus of the HMA mix being tested.

File: Data Set 3 Point: Field Mr

Points Show Graphs File Settings Seeds

No. of drops: 3 Next point Previous point

No.	Use	Radius mm	Stress kPa	Distances, mm			Deflections, Micron			Deflections, calc.			Em MPa	Eo MPa	RMS	n
				G1	G2	G3	D1	D2	D3	D1	D2	D3				
1	<input checked="" type="checkbox"/>	150	191	0			98			99			135	500	1.1	
2	<input checked="" type="checkbox"/>	150	136	0			71			71			135	496	0.7	
3	<input checked="" type="checkbox"/>	150	73	0			38			38			135	498	0.4	

Structure and seed values

No. of layers: 2 Deflections

☐ h 150 mm ☒ E 4500 MPa

☒ n 0 ☒ C 100 MPa

☐ Depth to bedrock mm

Results

Calculate point Save

h 150 mm E1 6477 MPa

n 0.00 C 135 MPa

Em 135 MPa

Depth to bedrock mm

New values as seeds

RMS 0.8 % ☒

Calculate project

Stop

Width 3

Steps 3

Alternate 2

Surface Modulus Design

Existing surface modulus 500 MPa Calculate point

Required surface modulus MPa Save

Required thickness mm Calculate project

Notes 100g/m² hydrated lime on surface

Save Notes

Figure 6-11: LWD-mod Analysis Window.

Before proceeding with the analysis and depending on the pavement temperature at the time of testing, the Poisson's ratio (ν) is required as an input. The Poisson's ratio for the testing temperature was obtained from the ν -T graph shown in Figure 6-12, which was produced, as a result of a research completed at McMaster University in the 1970's, for a conventional HL-3 surface mix that is similar in mix design to the SP12.5FC2 PG64-28 surface course tested in the field. It was assumed that the minor differences in the mix designs do not strongly influence ν and therefore, the relationship between dynamic ν and temperature of HL-3 is assumed to apply to the SP12.5 FC2 PG64-28 used for this study.

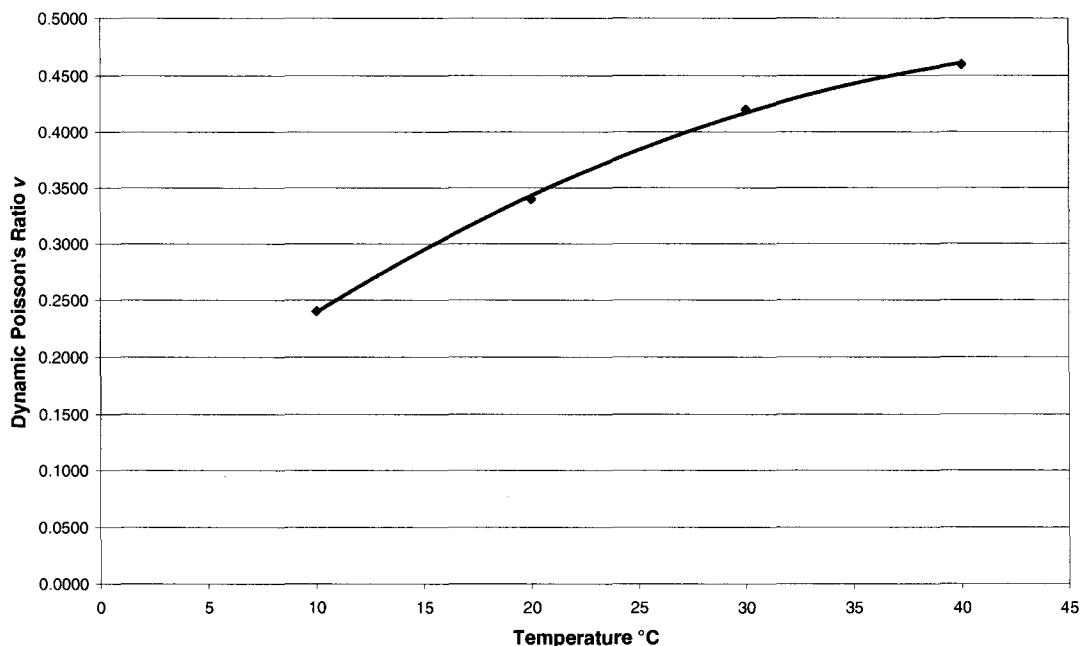


Figure 6-12: Relationship between Dynamic Poisson's Ratio and Temperature
[Lee and Emery, CTAA 1977].

At the start of an analysis, the user must assume an initial estimate for the effective pavement modulus. LWDMod uses the assumed modulus in addition to the layer thickness to start up an iteration procedure in order to find the set of modular values that best fit the measured deflection bowl. These are then printed as the calculated results in the "Results" frame. The iteration procedure is sometimes sensitive to the start up values and therefore it is best to allow the user to enter these values as the first estimate as if he/she knows the actual pavement modulus better than the software. Equations, developed by Boussinesq and Odemark, are manipulated to estimate the modulus from the load and deflection measurements taken directly under the LWD plate.

6.4.2 Results and Discussion

Once the analysis of the results of testing the in-situ SP12.5 FC2 PG64-28 pavement at three different temperatures was completed, a plot representing the field stiffness modulus versus the testing surface temperature was generated, as shown in Figure 6-13. This plot clearly indicates that a linear relation exists between the effective surface modulus E_s and temperature T .

The effective surface modulus values estimated from field results were subsequently compared with resilient modulus values determined in the laboratory. As shown in Figure 6-14, which relates the effective LWD modulus and the elastic NAT resilient modulus, a close linear correlation exists between the two, which implies that if

the resilient modulus of an asphalt concrete mix decreases due to temperature increases, the LWD effective modulus is also expected to decrease.

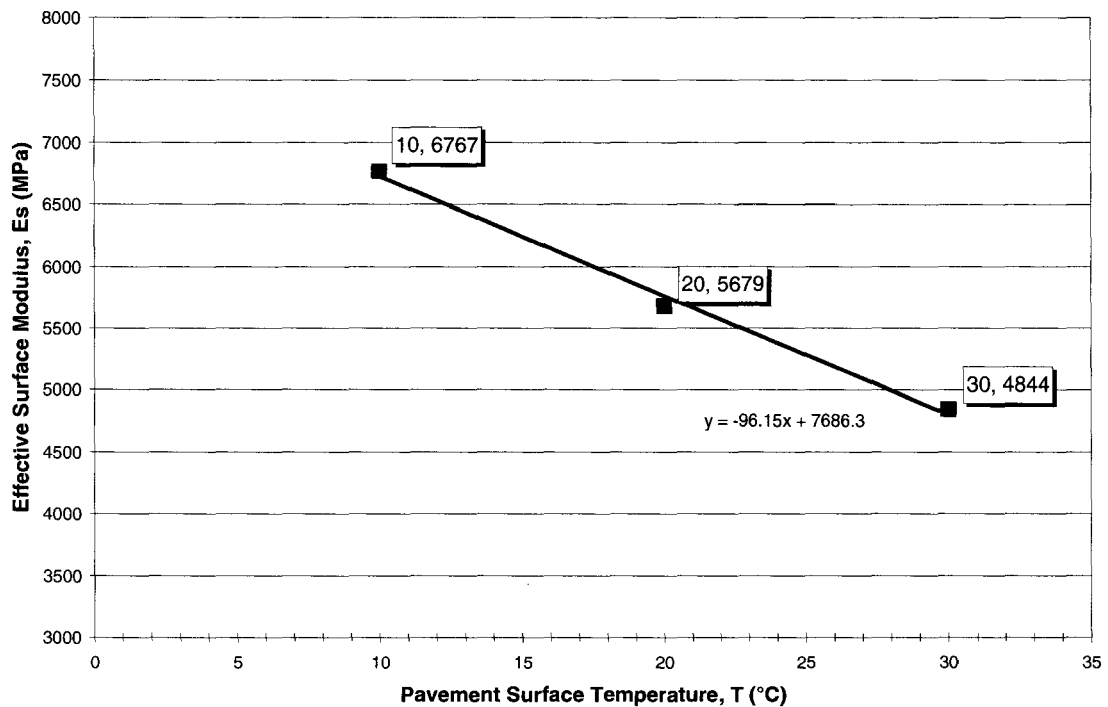


Figure 6-13: In-Situ Effective Surface/Stiffness Modulus versus Surface Temperature.

In general, the LWD test provides a modulus that is different from that obtained in a laboratory setting using the NAT, for instance. This variability is primarily due to the difference in the nature of the method of measurements using the two equipments as well as the difference in testing conditions. The NAT provides a boundary-valued estimate of resilient modulus of a relatively uniform sample under well-defined loading configuration

and temperature conditions. On the other hand, the LWD provides an estimate of the effective modulus E from the response of a non-uniform layered system via a composite behaviour of the entire pavement system comprised of the surface course, the base/subbase, and the subgrade. This variability would also, in part, be a result of the “hidden” joints and cracks below the overlay surface. Referring back to Chapter 2, the asphalt used in the laboratory had an AC content of 4.6% whereas the field asphalt mix had an AC content of 5.2%. This would cause the laboratory results to be higher at low temperatures and the field pavement to be less stiff.

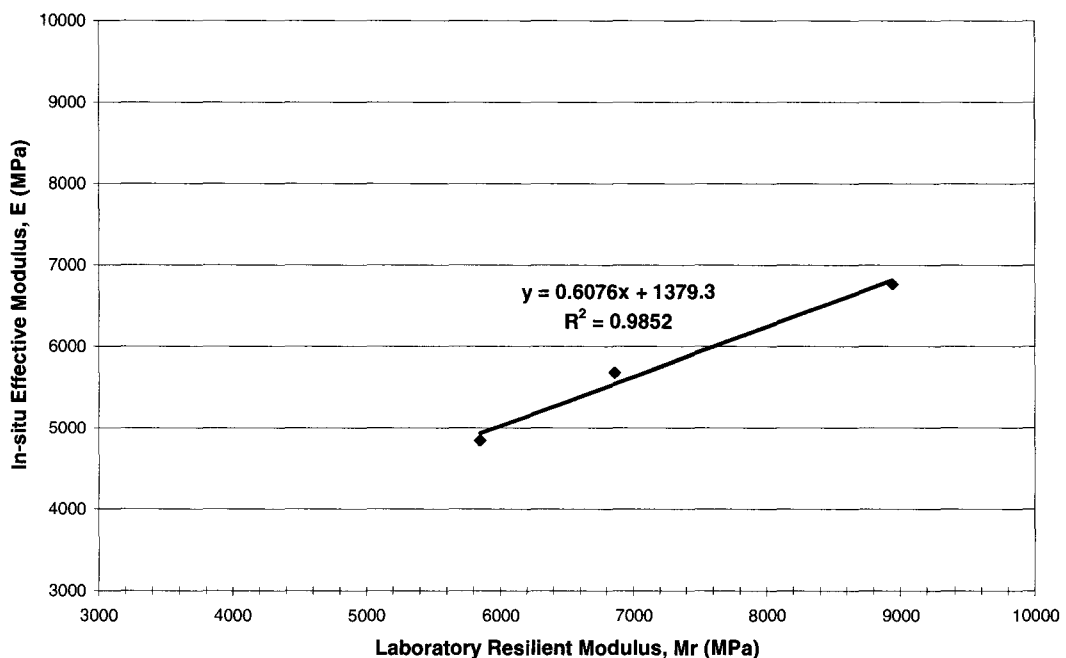


Figure 6-14: Effective LWD Stiffness versus Elastic NAT Resilient Modulus of The SP12.5FC2 PG64-28 HMA Mix.

6.4.3 Effect of Hydrated Lime on Elastic Modulus of HMA Mixes

According to Chapter 4 and assuming reasonable reliability of the data obtained in field and laboratory settings, the addition of 100g/m^2 of hydrated lime on the surface of the SP12.5FC2 PG64-28 pavement reduced the surface temperature by approximately 14°C . The ambient temperature while carrying out the in-situ tests was 36.4°C , which corresponded to a surface temperature of 60.2°C , shown in Figure 5-8. The above-mentioned dosage of hydrated lime therefore reduced the surface temperature of the SP12.5FC2 PG64-28 pavement mix to 46.2°C . Using the curve shown in Figure 6-13 corresponding to in-situ testing of the SP12.5FC2 PG64-28, the reduction in surface temperature from 60.2°C to 46.2°C would increase the effective surface modulus from 1898.1MPa to 3244.2MPa .

6.5 FATIGUE RESISTANCE TESTING

It is well known that pavement surfaces crack over time. They also rut and deteriorate in various other ways. Nevertheless, the principal mode of damage is cracking. It is clear that roads do not crack immediately after the traffic starts but damage accumulates over time due to the many millions of load applications from truck tires and temperature cycles. In other words, road pavements whether asphalt or concrete, undergo fatigue failure. HMA fatigue resistance is directly related to the stiffness of the mix. An increase in the elastic stiffness of a pavement structure improves the load spreading

ability, thus reducing the peak compressive stress transmitted to the subgrade. On the other hand, the fatigue resistance can be affected negatively. The purpose of this section is to report the findings with respect to the fatigue resistance ability of the different HMA mixtures involved in this study.

6.5.1 Results and Discussion

Layers of a flexible pavement structure are subjected to continuous flexing under traffic loading. The magnitude of the strains depends on the overall stiffness and nature of the pavement construction; i.e., the layering. Figure 6-15 shows the fatigue life characteristics of the bituminous mixes of this study. In interpreting the data, it was assumed that Equation 6-3 applies [Irwin and Gallaway, 1973]:

$$N_f = c \epsilon_t^{-m} \quad [6-3]$$

where: N_f = Number of load applications to initiate a fatigue crack,
 ϵ_t = Maximum value of applied tensile strain,
 c and m = Factors depending on the composition and the properties of the mix; m is the slope of the strain-fatigue life line.

HMA fatigue cracking is directly related to the asphalt binder content and stiffness of the concrete. Higher AC contents result in a mix that has a greater tendency

to be more ductile rather than fracture in a brittle fashion under repeated load. The optimum asphalt binder content as determined by mix design should be high enough to minimize fatigue cracking. In addition, the use of an asphalt binder with a lower stiffness increases the mixture's fatigue life by providing greater flexibility. However, the potential for rutting must also be considered in the selection of an asphalt binder to prevent excessive permanent deformations; i.e., asphalt binders with low stiffness tend to have low rutting resistance. The tendency of fatigue not only depends on the AC content and stiffness of the mixture, but also on the relationship between structural layer thickness and loading.

Fatigue tests were performed by applying repetitive loads to a specimen and determining the number of load pulse applications required to induce failure of the specimen. Failure was defined as the point at which the load required to maintain a constant level of strain falls down to 50% of its initial value and not where the sample literally fails; i.e., a functional failure [Irwin and Gallaway, 1973]. Even though samples being tested, as shown in Figure 6-4, failed at the end of the test, their fatigue life was measured according to the above-mentioned criteria relating the initial strain to the failure strain level. The data shown in Figure 6-15 represent best fit lines of the data points collected during the tests for different strain values.

Based on the above discussion and referring to Figure 6-15, fatigue resistance of

the SMA was the greatest whereas the SP19 asphalt concrete was the least resistant, which is attributed to SMA mixes being the richest in Asphalt Content (AC) and therefore the least stiff, whereas the SP19 asphalt concrete was found to be the stiffest

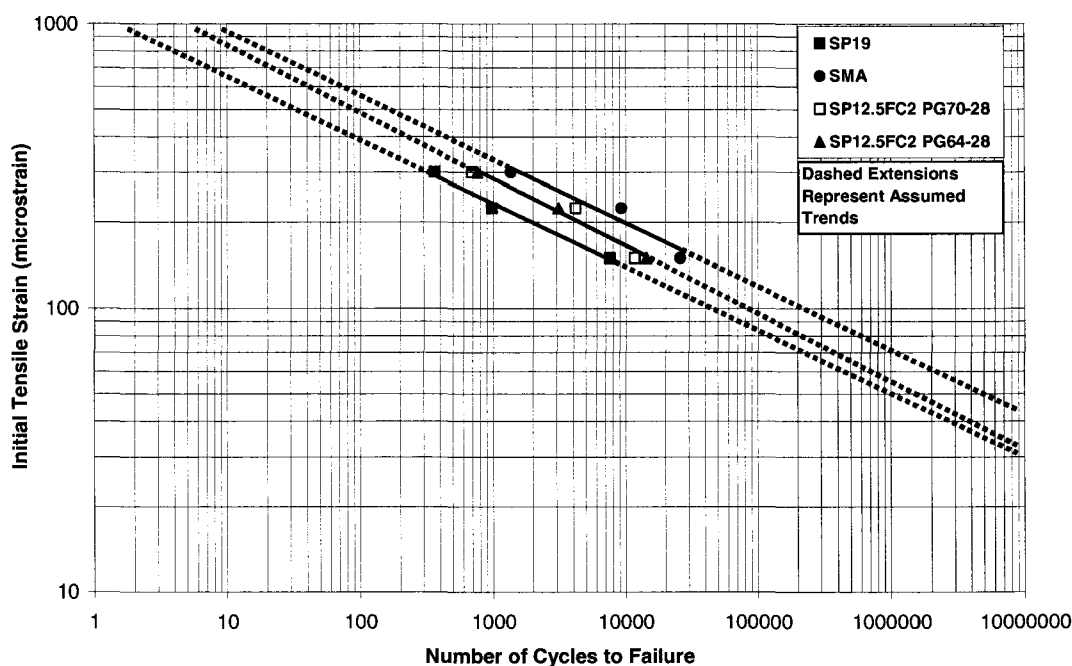


Figure 6-15: NAT fatigue endurance testing of HMA mixes.

due to having the least AC content. Polymer modification of SP12.5FC2 PG70-28 is more active at high temperatures than at low temperatures, therefore, one would expect the fatigue resistance of SP12.5FC2 PG70-28 be higher than SP12.5FC2 PG64-28 but relatively close. Referring to Figure 6-15, the measurements corresponding to SP12.5FC2 PG70-28 are scattered more than for measurements corresponding to SP12.5FC2

PG64-28, which suggests the presence of an outlier between the three measurements in addition to the possibility of experimental error. This explains the reason behind the fact that lines of best fit corresponding to the two mixes are on top of one another. As one might expect, the fatigue life of SP12.5FC2 PG70-28 is a little less than that of SMA, whereas the fatigue life of an SP12.5FC2 PG64-28 mix is a little higher than that of an SP19.0 mix.

Three fatigue tests were performed for each mix. From Figure 6-15, one observes that there are slight variations in the values of m , which is represented by the average slope of the fatigue life lines shown in the figure. For group 1 represented by SMA and SP19 mixes, $m = 5.20 \times 10^{-3}$, whereas for group 2 represented by SP12.5FC2 at both PG grades (i.e. PG64-28 and PG70-28), $m = 5.43 \times 10^{-3}$. The trends shown in the figure indicate that the fatigue life of group 2 is more sensitive to initial strain values than group 1 mixes. Despite the slight variation in sensitivity between the different mixes, the shift in the fatigue resistance line of best fit between mixes is more significant than the slope of the actual lines.

Results obtained indicate that a 75 microstrains reduction in the testing strain from 300 to 225 microstrains results in a change in the number of pulses needed to fail the sample being tested. This reduction in testing strain caused the number of pulses needed to fail mixes to be factored up by 3.5 on average.

6.6 RUT RESISTANCE TESTING

Permanent deformation is characterized by a pavement surface cross section that has permanently changed in shape and is no longer in its designed position. It represents an accumulation of small amounts of non-recoverable deformations that occur each time a load is applied. The most common form of permanent deformation, referred to as rutting, occurs along the wheel paths. There are two main mechanisms that are responsible for rutting.

Firstly, rutting is caused by the lack of strength of the subgrade, subbase, and base, to withstand the large repeated stress being applied to them. For this case, the deformation occurs in the underlying layers rather than in the asphalt layers. It is normally considered a structural problem rather than a material problem. Stiffer paving materials partially reduce this type of rutting. However, there is often not enough pavement strength or thickness to reduce the applied stress to a tolerable level. It may also be caused or aggravated by a pavement layer that has been unexpectedly weakened by the intrusion of moisture [Tarefder, Zaman, Hobson and Toney, 2002].

Secondly, the inability of the pavement surface course to resist the traffic load-induced shear stresses at the surface is another potential cause of rutting that is of most concern to asphalt mix designers. A weak mixture accumulates small permanent deformations with each truck pass and consequently forms a rut characterized by a

downward and lateral movement (shoving) of the mixture. Although rutting may occur in the asphalt surface course, one of its causes can be the weakness of the underlying asphalt course, which is also referred to as the binder course.

Rutting of unstable mixes typically occurs during the summer under high pavement temperatures. While this might suggest that rutting is solely an asphalt cement problem, it is more correct to address rutting by considering the combined resistance of the mineral aggregate and asphalt cement; i.e., rutting is a permanent deformation of the aggregate skeleton due to repeated loading. It is related to insufficient viscosity of the asphalt binder at higher temperatures and lack of stability of the aggregate skeleton.

6.6.1 Factors Influencing Rutting

Hot Mix Asphalt pavements are exposed to daily traffic loading and temperature fluctuations throughout the year from one season to another. HMA pavements being subjected to these conditions often experience rutting by progressive movement of material under repeated loads. High-pressure truck tires and increased wheel loads are primary causes of increased rutting.

Previously conducted studies evaluated the relative weights of rutting parameters based on the rutting performance of HMA. These studies used an Asphalt Pavement Analyzer (APA) and showed that factors such as the binder Performance Grade (PG) and

the test temperature affect the HMA mixture's rutting performance significantly. In general, a HMA produced from a modified binder shows less rutting compared to the HMA produced from unmodified binders. Other factors such as the APA wheel load and hose pressure, and AC content of an asphalt mix were found to have less affect on the rutting performance of the HMA.

As temperature increases, HMA stiffness decreases and therefore, its potential to rut increases. This is attributed to the dependence of the stiffness of HMA on the rheological behaviour of asphalt binder used in the HMA mix, which in turn depends on the temperature. Beside temperature, other environmental factors, such as moisture, influence HMA mixture's rut potential. Moisture weakens the bond between asphalt cement and the aggregates and therefore produces a loss of strength. The gradual loss of strength over a period of time can contribute to the development of lateral flow of HMA materials. As a result, the loss of cohesion due to moisture-induced damage in HMA accelerates the rate of rutting.

6.6.2 Results

In order to study the rutting of HMA at different temperatures, specimens were tested at four temperatures. Three mix designs were studied (SP12.5FC2, SP19, and SMA) to compare their susceptibility to rutting. The effect of asphalt cement Performance Grade (PG) was another variable that was considered. The PG effect was

assessed by testing mix SP12.5FC2 with two different binders, one unmodified (PG 64-28) and the other modified (PG 70-28). The unmodified binder was produced from crude oil having a high level of asphaltiness and is known as base asphalt. The modified binder, on the other hand, typically contains 3-6% styrene-butadiene-styrene (SBS) polymer with base asphalt.

One of the testing temperatures was selected to be 64°C, which is considered to be the maximum temperature of HMA pavements in Ontario during the summer. In order to cover a reasonable range of temperatures encountered during summer conditions, other testing temperatures considered were 52°C, 58°C, and 70°C. Each APA rut test was conducted using 8000 cycles with 445N (100 lb) wheel load and 690 kPa (100 psi) hose pressure, which is assumed to approximate the total load intensity expected in the design life of the pavement. Even though the aim of the study was to monitor the final permanent deformation of each mix at the end of the 8000 testing cycles for each testing temperature, the rutting history was recorded for all tests, and for all testing temperatures. The rutting history for various asphalt concretes, tested at 70°C, is shown in Figure 6-16 with the histories corresponding to the other testing temperatures are summarized in Appendix C.

Once testing of the samples was completed, the results were stored in an excel file for further data analysis. Figure 6-17 summarizes the rutting deflections of the different

HMA mixes that were tested. Each point on the graph represents an average rutting depth of the depths observed from testing 2 samples at the same temperature.

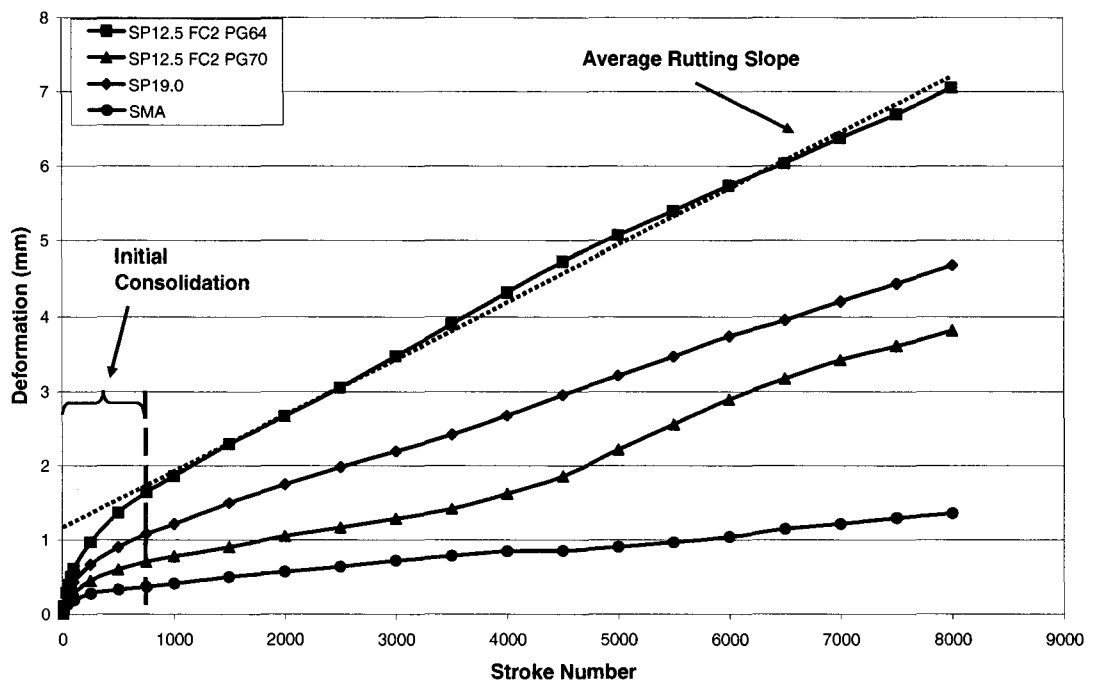


Figure 6-16: Rutting History of HMA Mixes at 70°C.

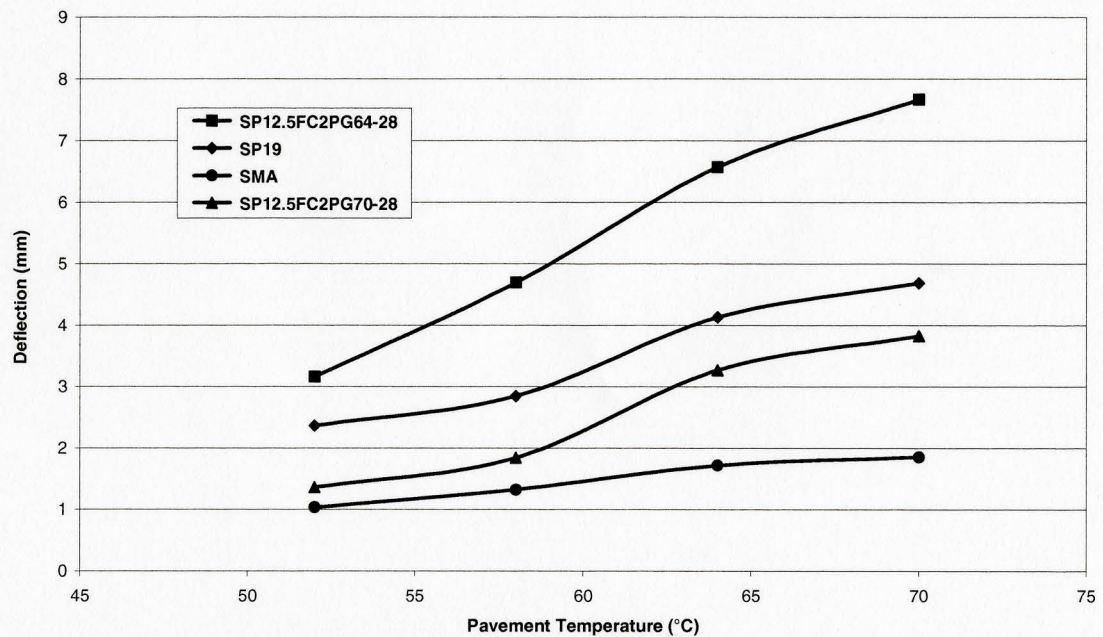


Figure 6-17: Rutting Deformation of HMA Mixes with Temperature at 8000 Cycles.

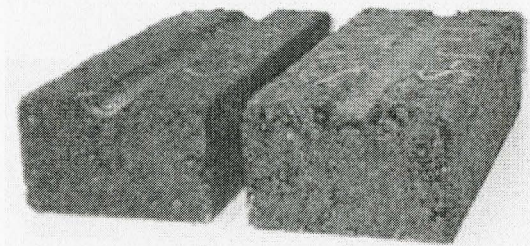


Figure 6-18:
HMA Sample Tested for Rut
Resistance.

6.6.3 Discussion

The performance of urban pavements is often governed by the rutting of asphalt concrete specifically at intersections, bus bays, and routes with considerable truck and

bus traffic, particularly slow moving and standing traffic, which yields higher sustained stress/strain conditions. This distress consequently reduces the service life of the pavement and induces higher operating, maintenance, and rehabilitation costs, as well as safety, which is a concern. Rutting therefore, which is of concern during hot weather, must be dealt with through appropriate asphalt technology and proper construction techniques [Dunn and Donovan, 2004].

The rut resistance of an asphalt concrete pavement is influenced by both aggregate and binder properties. Binder stiffness, which is a function of binder properties, time of loading and temperature, can be related to mix rutting resistance.

To determine the resistance of a bituminous mix to permanent deformation, the low stiffness response of the material at high temperatures or long loading conditions must be analyzed. When the stiffness of the mix is less than 5×10^6 Pa, the mix behaviour is much more complex than it is in the “elastic” range. Under these conditions, the stiffness of the mix not only depends on that of the bitumen and the volume of aggregates, but also other factors including the aggregate grading, its shape, texture and degree of interlocking, and the method and degree of compaction [Vallerga, Tayebali and Monismith, 1995].

The curves in Figure 6-16, represent the rutting trends of the different mixes for up to 8000 cycles at 70°C, with Figure 6-17 summarizing the final permanent deformations experienced at the end of the tests. Average rutting rates were calculated to quantify the resistance of mixes to rutting in terms of the number of cycles required to cause a unit deformation. The corresponding results are summarized in Table 6-3. In general, it is evident that the resistance of the mixes to rutting decreases with an increase in temperature. In other words, the number of cycles required to cause a single millimeter of deformation tends to decrease as the temperature increases. On average, the rutting rate of the mixes studied decreases at temperatures greater than 64°C, which is attributed to the fact that as the mixes deform, they become denser and stiffer, and therefore higher load is required to cause further deformations. As shown in Table 6-4 and referring back to Figure 6-10, one observes that an SMA mix is the slowest in losing its stiffness with increasing temperature, whereas an SP12.5FC2 PG64-28 mix is the fastest. Considering the mixes studies, one can therefore conclude that SMA mixes are the most resistant to rutting whereas SP12.5FC2 PG64-28 mixtures are the least. On the other hand, the curves of the SP19.0 and SP12.5FC2 PG70-28 mixtures lie between the two extremes as shown in Figure 6-17.

A binder's performance grade was also found to be an important factor that influences rutting. In general, an HMA produced from a higher PG binder appears to undergo less rutting when compared to an HMA produced from lower PG binders.

Table 6-3: Relationship between Rutting Rates and Testing Temperature of Different HMA Mixes.

Mix Type	Testing Temperature (°C)	Average Rutting Rate (cycles/mm)
SP12.5 FC2 PG64-28	52	3333
	58	2000
	64	1429
	70	1429
SP12.5 FC2 PG70-28	52	10000
	58	5000
	64	2500
	70	2000
SP19.0	52	5000
	58	3333
	64	2500
	70	2000
SMA	52	12500
	58	10000
	64	10000
	70	10000

As shown in Table 6-4, the SP12.5FC2 mixes have similar AC contents but with two different PG grades; namely PG64-28 and PG70-28.

Due to the difference in asphalt cement PG grades, the rate at which SP12.5FC2 PG64-28 loses its stiffness with increasing temperature is higher than that of SP12.5FC2 PG70-28 mixtures. This is consistent with the observation that SP12.5FC2 PG70-28 mixes show higher rutting resistance than SP12.5FC2 PG64-28 mixes by deforming less with increasing temperature, as shown in Figure 6-17.

Table 6-4: Stiffness Rate of Change with Temperature for Different HMA Mixes.

Mix Type	AC Content (%)	Resilient Modulus M_r (MPa)	Rate of M_r Decrease (MPa) per 1°C Increase in Temperature
SP12.5FC2PG64-28	4.7	8939	155
		6858	
		5850	
SP12.5FC2PG70-28	4.6	7522	114
		6408	
		5235	
SP19.0	4.5	9105	151
		8042	
		6091	
SMA	5.8	5898	72
		4863	
		4457	

6.6.4 Effect of Hydrated Lime on Rutting Resistance of HMA Mixes

Since rutting is an accumulation of very small permanent deformations, one way to increase mixture shear strength is to use a stiffer asphalt cement, which is less ductile at high pavement temperatures. This is assuming that asphalt concrete mixes with higher shear strength are expected to behave more elastically and experience less permanent deformations. Then, when a load is applied, the asphalt cement will act like a rubber band and spring back to its original position rather than deforming permanently. Another way to increase the HMA shear strength is by selecting an aggregate that has a high degree of internal friction; i.e., one that is cubical, has a rough surface texture, and is graded to develop particle-to-particle contact. When a load is applied to the mix, the aggregate particles lock tightly together and function more as a large, single, elastic stone. As with

the asphalt cement, the aggregate acts like a rubber band and springs back to its original shape when unloaded. In that way, no permanent deformation accumulates.

According to Chapter 4, the ambient temperature while carrying out the in-situ tests was 36.4°C, which corresponded to a surface temperature of 60.2°C, as shown in Figure 5-8. As per Chapter 4 and assuming that the data collected is reasonably reliable, modifying the HMA surface with 100g/m² of hydrated lime reduces the surface temperature to 46.2°C, which is an approximate reduction of 14°C. Using the curve shown in Figure 6-17 and corresponding to the SP12.5FC2 PG64-28 mix, the reduction in surface temperature from 60.2°C to 46.2°C would increase the rutting resistance by observing a reduction in the permanent deformation from 5.4 to 2.3 millimeters.

CHAPTER 7

REAL WORLD APPLICATIONS OF HMA SURFACE MODIFICATION

This study provides a laboratorial as well as an in-situ assessment of the influence of placing hydrated lime on the surface of HMA mixes. The purpose of the field testing was to confirm that the effect of the surface modification observed in the laboratory and field site are similar. Using the KENLAYER software [Huang, 2004], this chapter evaluates the surface modification effect on the response of HMA pavement-subgrade system subjected to a truck load on the surface. It is shown that once hydrated lime is placed on the surface of the HMA pavement, the temperature reduction throughout the pavement structure strongly influences the critical stresses and strains by reducing their magnitudes within the pavement.

7.1 PROCEDURE

The study reported in this thesis was carried out during the summertime. To coincide with what has been done throughout the study, two cases were considered. One case was with no lime applied to the surface of a new pavement, which acted as control for comparison, whereas the second included the application of 100g/m^2 of hydrated lime to the surface of the new pavement. To analyze a relatively wide range of temperatures,

three summertime target air temperatures were considered with respect to the stress-strain analysis. The average cool, intermediate, and hot ambient temperatures considered were 23.3°C, 30.4°C, and 36.4°C, respectively. Corresponding to these ambient temperatures, LTPPBind software Version 3.1 was used to obtain black pavement surface temperatures as well as the temperature distribution with depth [FHWA, 2006]. The corresponding average black pavement temperatures obtained were 44.6, 51.0, and 64.2°C, respectively. The temperature distributions are summarized in Table 7-1.

According to the results presented in Chapter 4, the pavement surface modification influences the energy absorptivity of the pavement at the surface as well as the temperature variation with depth, as one might expect. However, the magnitude of the influence varies depending on the reflective properties of the surface. Figure 4-4, which shows the effect of different hydrated lime concentrations on the surface temperature of pavement, together with the three previously mentioned temperatures were used to generate three new pavement temperatures as a result of the surface modification. The surface modified average pavement temperatures were 33.3, 37.6, and 51.2°C, respectively. Corresponding to these three pavement temperatures, temperature profiles of HMA layer containing PG64-28 asphalt cement, presented in Figure 7-1, were obtained using the LTPPBind software.

As previously mentioned, the analysis was performed on black as well as surface modified pavement. When comparing the LTPPBind and study temperature readings for the two scenarios at corresponding depths, as shown in Table 7-2, the two sets are relatively close. This suggests that the profiles predicted by LTPPBind maybe used to describe temperature variations for the problem addressed in this thesis. For consistency between various temperature sets and due to the fact that only one set of study readings is available, readings obtained from LTPPBind were used for the analysis.

The default pavement thickness adopted in LTPPBind is 200mm and therefore, the pavement analyzed was of the same thickness, as shown in Figure 7-1. The HMA layer was subdivided into 5 layers in order to properly capture the temperature influences

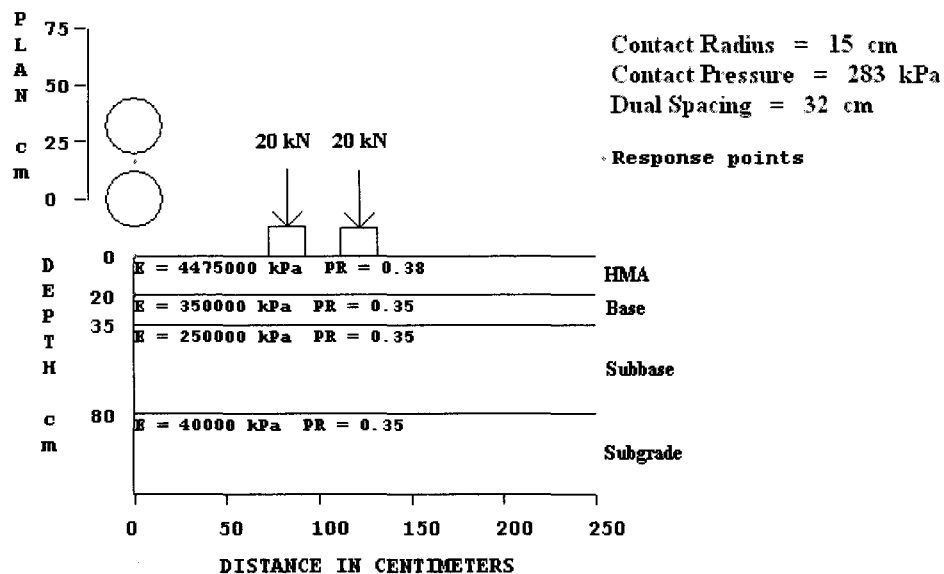


Figure 7-1: KENLAYER Sample Analysis Window.

on the resilient modulus and Poisson's ratio per sub-layer. Given the variation in temperature, each layer was assigned a different resilient modulus and Poisson's ratio in accordance to Figures 6-10 and 6-12, respectively. The HMA was supported by a granular base, subbase, and subgrade with each having an average in-situ thickness and resilient modulus shown in Table 7-1. The above sets of input, summarized in Table 7-1, were entered into the KENLAYER spreadsheet in addition to a 20kN load per tire, which corresponded to the standard 80kN axle loading. The dual tires were spaced at 32cm center-to-center with a contact radius of 15cm. Analyses were completed for six cases corresponding to the different pavement temperatures, yielding stresses, strains, and vertical deflections at pre-selected depths.

For convenience of analysis in practice, HMA is usually not subdivided into smaller layers. Instead, it is considered as one layer. Therefore, the analyses were also completed using average temperatures in HMA and hence average resilient modulus and Poisson's ratio. Analyses with average values were completed to measure the sensitivity of temperature distribution on the performance parameters of HMA. The analysis structure was based on the input sets presented in Table 7-3.

Referring to Figure 7-1, the stresses and strains were predicted directly under the response point, which was chosen to be exactly in the center between the two dual tires shown in the figure (the two circles represent the contact radius of the dual tires). It

Table 7-1: Actual Input Sets Corresponding To Different Summer Day Temperatures.

Air Temperature (°C)	Layer Number	Layer Name	Reading Depth (mm)	Pavement Temperature, Black (°C)	Resilient/Stiffness Modulus, E (MPa) ⁺	Poisson's Ratio, ν [*]	Average E (MPa), ν	Pavement Temperature, 100g/m ² of hydrated lime (°C) #	Resilient/Stiffness Modulus, E (MPa) ⁺	Poisson's Ratio, ν [*]	Average E (MPa), ν
23.3	1	HMA	0	44.6	3416.5	0.372	3640.5,	33.3	5161.8	0.379	5385.8,
			25	41.7	3864.4	0.379	0.375	30.4	5609.7	0.373	0.376
	2	HMA	50	39.7	4173.3	0.381	4289.2,	28.4	5918.6	0.367	6034.5,
			75	38.2	4405.0	0.382	0.382	26.9	6150.3	0.361	0.364
	3	HMA	100	36.9	4605.8	0.382	4683.0,	25.6	6351.1	0.355	6428.3,
			125	35.9	4760.2	0.382	0.382	24.6	6505.5	0.351	0.353
	4	HMA	150	35.0	4899.3	0.382	4961.0,	23.7	6644.5	0.346	6706.3,
			175	34.2	5022.8	0.381	0.381	22.9	6768.1	0.341	0.344
30.4	1	HMA	0	51.0	2428.1	0.345	2652.0,	37.6	4497.7	0.382	4721.6,
			25	48.1	2876.0	0.359	0.352	34.7	4945.6	0.381	0.382
	2	HMA	50	46.1	3184.9	0.367	3300.7,	32.7	5254.5	0.378	5370.3,
			75	44.6	3416.5	0.372	0.369	31.2	5486.2	0.375	0.377
	3	HMA	100	43.3	3617.3	0.375	3694.5,	29.9	5686.9	0.372	5764.2,
			125	42.3	3771.8	0.377	0.376	28.9	5841.4	0.369	0.370
	4	HMA	150	41.4	3910.8	0.379	3972.6,	28.0	5980.4	0.365	6042.2,
			175	40.6	4034.3	0.380	0.380	27.2	6104.0	0.362	0.364
36.4	1	HMA	0	64.2	389.3	0.237	613.3,	51.2	2397.2	0.344	2621.1,
			25	61.3	837.2	0.267	0.252	48.3	2845.1	0.358	0.351
	2	HMA	50	59.3	1146.1	0.285	1262.0,	46.3	3154.0	0.366	3269.8,
			75	57.8	1377.8	0.298	0.292	44.8	3385.6	0.371	0.369
	3	HMA	100	56.5	1578.6	0.308	1655.8,	43.5	3586.4	0.375	3663.7,
			125	55.5	1733.0	0.316	0.312	42.5	3740.9	0.377	0.376
	4	HMA	150	54.6	1872.0	0.322	1933.8,	41.6	3879.9	0.379	3941.7,
			175	53.8	1995.6	0.328	0.325	40.8	4003.4	0.380	0.379
36.4	5	HMA	200	53.1	2103.7	0.332	2103.7,	40.1	4111.6	0.381	4111.6,
							0.332				0.381
	6	Base	-	-	350	0.35	350,	-	350	0.35	350,
							0.35				0.35
	7	Subbase	-	-	250	0.35	250,	-	250	0.35	250,
							0.35				0.35
	8	Subgrade	-	-	40	0.35	40,	-	40	0.35	40,
							0.35				0.35

⁺ Readings from Figure 6-10, ^{*} Readings from Figure 6-12, [#] Readings from Figure 4-4.

should be noted that the vertical stress was found to be the highest directly under the tire and close to the surface of the HMA structure. However, when measured close to the surface of an HMA layer, the vertical stress was not affected by the modification of the surface with hydrated lime. At depths greater than 100mm, analysis confirmed that the vertical stress is the highest between the two dual tires.

Table 7-2: Comparison between LTPPBind and Study Profile Temperatures for Different Hydrated Lime Concentrations (During hot summer day).

Air Temperature (°C)	Depth (mm) *	Black Pavement (0g/m ² of Hydrated Lime)		Modified Pavement (100g/m ² of Hydrated Lime)	
		LTPPBind	Study Reading	LTPPBind	Study Reading
36.4	5	63.5	62.4	50.5	50.7
	25	61.3	57.4	48.3	49.3
	45	59.7	56.8	46.7	48.5
	65	58.3	55.0	45.3	45.8

*Measured from surface.

Table 7-3: Average Input Sets Corresponding To Different Summer Day Temperatures.

Air Temperature (°C)	Layer Number	Layer Name	Average Resilient/Stiffness Modulus, E (MPa) ⁺		Average Poisson's Ratio, ν [*]	
			Black (0 Lime)	100g/m ² Lime	Black (0 Lime)	100g/m ² Lime
23.3	1	HMA	4475.4	6220.7	0.38	0.36
	2	Base	350	350	0.35	0.35
	3	Subbase	250	250	0.35	0.35
	4	Subgrade	40	40	0.35	0.35
30.4	1	HMA	3486.9	5556.5	0.37	0.37
	2	Base	350	350	0.35	0.35
	3	Subbase	250	250	0.35	0.35
	4	Subgrade	40	40	0.35	0.35
36.4	1	HMA	1448.2	3456.0	0.30	0.37
	2	Base	350	350	0.35	0.35
	3	Subbase	250	250	0.35	0.35
	4	Subgrade	40	40	0.35	0.35

⁺ Readings from Figure 6-10, ^{*} Readings from Figure 6-12, [#] Readings from Figure 4-4.

Even though horizontal strains close to the surface of the HMA layer maybe critical with regard to top-down cracking, the analysis was aimed toward those at the bottom of the layer, which are more critical when trying to mitigate fatigue and bottom-up cracking.

In addition to predicting the vertical stresses and strains at various depths as a result of the surface modification of the HMA pavement surface, damage analyses were also completed for the six different cases corresponding to the different pavement temperatures. The analyses included the prediction of the maximum damage ratio, which is defined in Equation 7-1, and the design life of the pavement in years.

$$\text{Maximum Damage Ratio} = \frac{\text{Actual Number of Load Repetitions}}{\text{Allowable Number of Load Repetitions}} \quad [7-1]$$

To minimize the number of variables coming into the analyses, the actual number of load repetitions was kept at one million (1,000,000) for all cases. The maximum damage ratio, which indicates complete failure of the pavement once it reaches a value of 1.0, was calculated based on the allowable number of load repetitions obtained from the results of the analyses.

7.2 RESULTS AND DISCUSSION

The horizontal tensile and vertical strains, as well as the vertical stresses, were obtained for the cases of no lime on a new pavement at the various summertime air temperatures, which acted as controls for comparison purposes, and secondly for the cases in which 100g/m^2 of hydrated lime was applied to the surface. Analysis results for the six different cases, corresponding to the bottom of the HMA layer as well as the top of the subgrade layer, are shown in Figures 7-2, 7-3, 7-4, and 7-5. From the four figures, it is clear that negligible difference in predictions is observed when the HMA is subdivided into smaller layers rather than being considered as one layer. This would suggest that considering the HMA as one layer for simplification of analysis is reasonable.

From Figure 7-2, it is clearly observed that the rate of decrease of vertical stress with decreasing air temperature is the highest when the air is initially at highly elevated temperature. This rate tends to decrease as the initial air temperature being considered decreases. According to the figure, the minimum reduction in vertical stress at the bottom of the HMA layer is found to be 9 kPa occurring during cool summertime temperatures, and a maximum reduction of 32 kPa occurring during hot summertime temperatures. Although the stress magnitudes are much smaller, similar trends are observed at 800mm from the surface, as shown in Figure 7-3. The smaller magnitudes are attributed to the fact that the impact of the load largely vanishes before reaching the subgrade.

Furthermore, it was found that the placement of hydrated lime on the surface of the HMA increases the stiffness of the pavement, and therefore the load is distributed

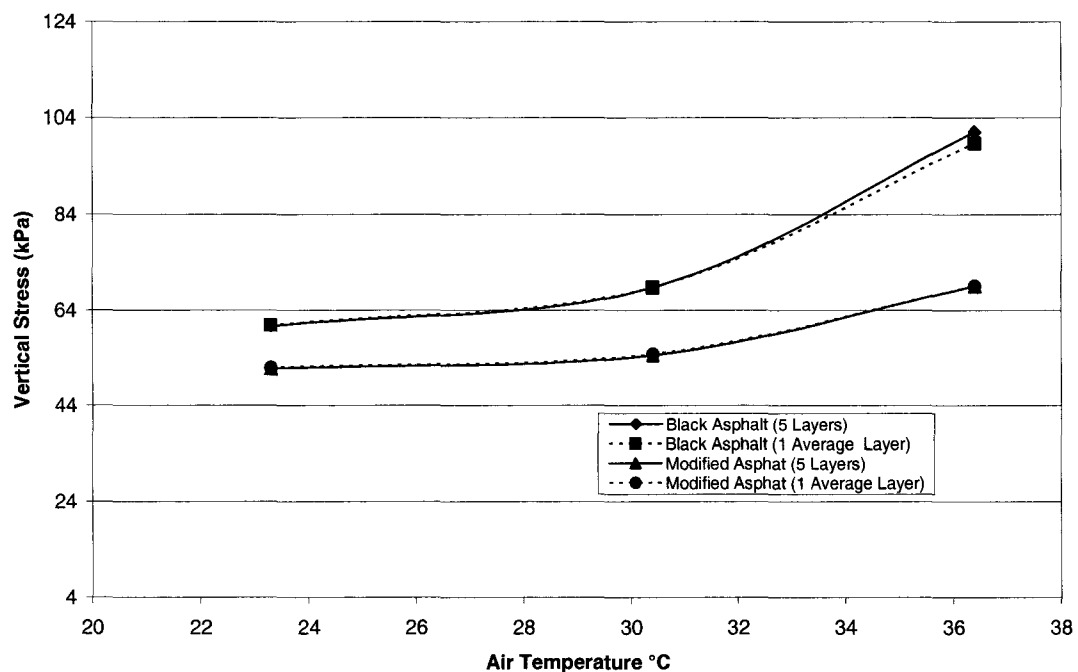


Figure 7-2: Vertical Stress Measured at Bottom of HMA Layer for Black and 100g/m² of Hydrated Lime Modified Pavement vs. Air Temperature.

more uniformly. Nonetheless, hydrated lime showed a positive influence on the reduction of vertical stress at the subgrade level. From Figure 7-3, it is evident that the addition of hydrated lime reduced the vertical stress at the top of the subgrade layer by approximately 0.5 kPa and 1.7 kPa during cool and hot summertime temperatures, respectively. This corresponds to an average stress reduction of 12.75%.

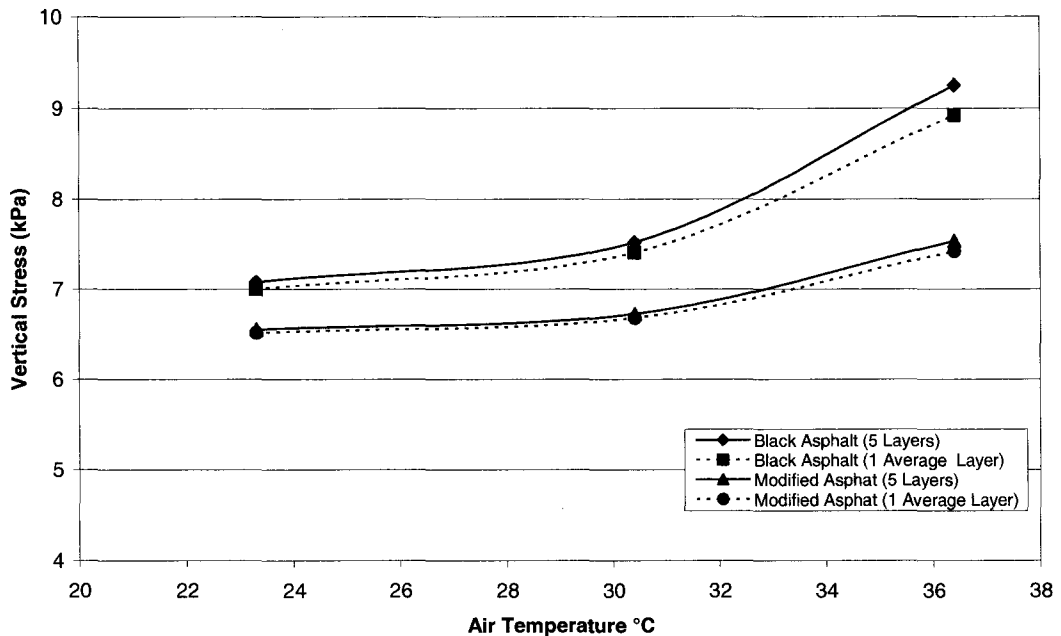


Figure 7-3: Vertical Stress Measured at Top of Subgrade Layer for Black and 100g/m² of Hydrated Lime Modified Pavement vs. Air Temperature.

Trends observed in Figures 7-4 and 7-5 are similar to those shown in Figures 7-2 and 7-3. The effect of temperature on the horizontal and vertical strains is the greatest at highly elevated temperatures and tends to decrease as the air temperature decreases. The hydrated-lime-surface-modification-induced reduction in horizontal strain at the bottom of the HMA layer is important due to increased horizontal tensile strains resulting in increased fatigue cracking, which develops at the bottom of the pavement and propagates upwards. Reducing the pavement temperature through the addition of hydrated lime reduces the horizontal tensile strains, which enhances the fatigue cracking resistance

capabilities of the pavement. The curves shown in Figure 7-4 indicate that the addition of hydrated lime results in an average horizontal strain reduction of 20%.

Both vertical stress and strain at the subgrade surface found to be sensitive to temperature. One observes that the vertical strain, as shown in Figure 7-5, is more sensitive to temperature when initially at highly elevated temperatures than when at low temperatures. High vertical strains at the subgrade level are used as performance parameters for rutting [Asphalt Institute, 1989].

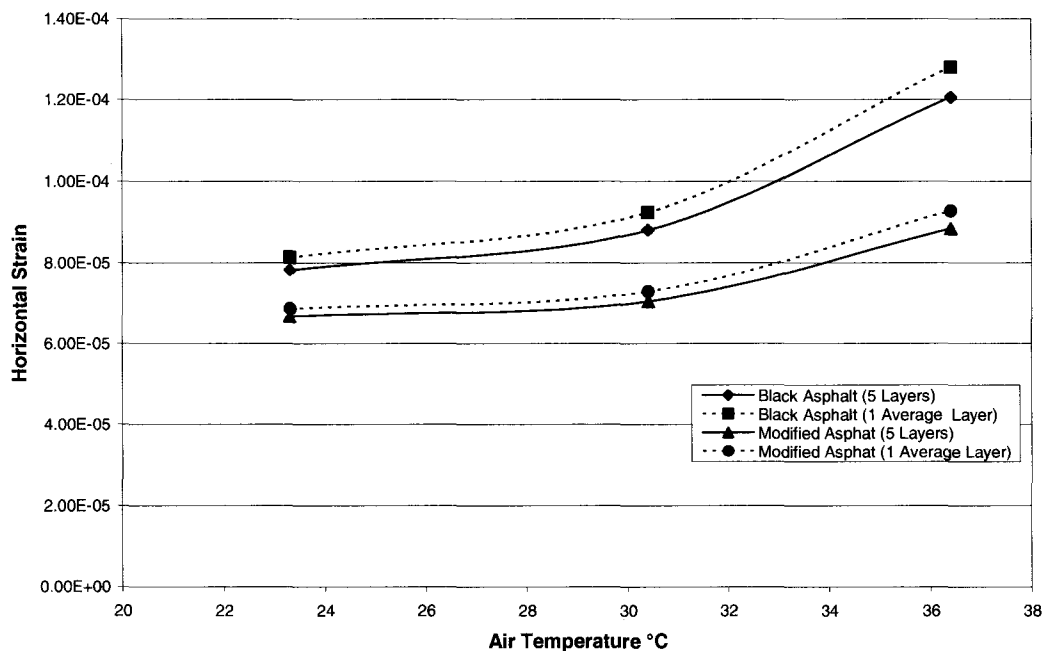


Figure 7-4: Horizontal Strain Measured at Bottom of HMA Layer for Black and 100g/m² of Hydrated Lime Modified Pavement vs. Air Temperature.

Based on trends and Asphalt Institute (AI) correlations, one may conclude that rutting damage increases as temperature increases. Therefore by reducing the vertical strains as a result of reduced pavement temperature, the rutting potential decreases. To quantify the effect of hydrated lime on the vertical strain at the subgrade level, Figure 7-5 indicates an average strain reduction of 12.5%. The percentage is smaller than that for the horizontal strain at the bottom of the HMA layer. This is again attributed to the fact that the load largely vanishes before reaching the subgrade, and therefore the strain at the subgrade level is less sensitive to temperature variations. As per the figure, the maximum

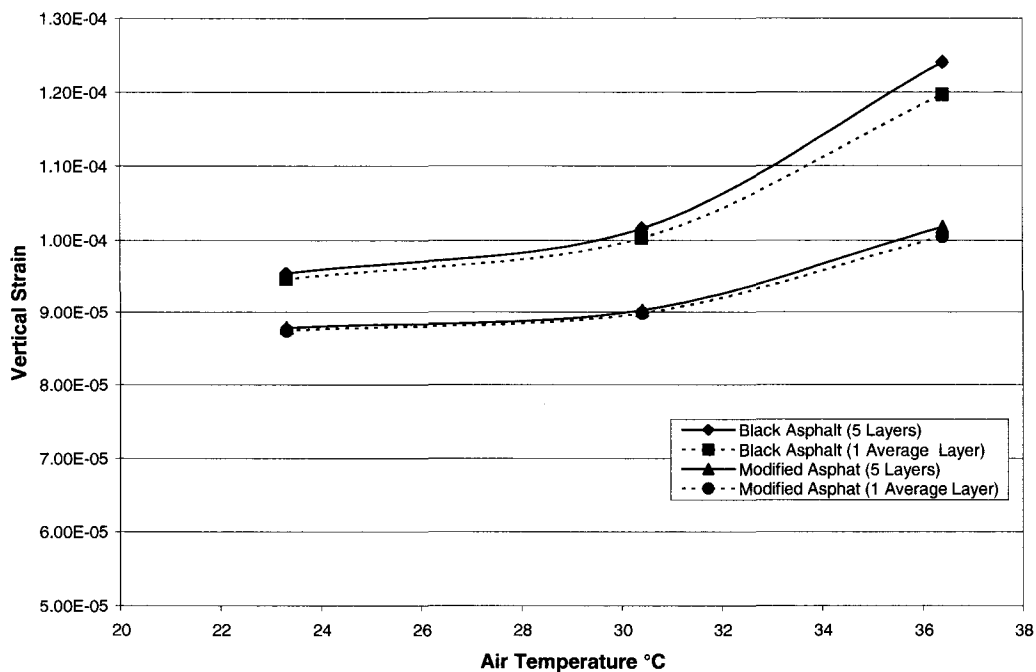


Figure 7-5: Vertical Strain Measured at Top of Subgrade Layer for Black and 100g/m² of Hydrated Lime Modified Pavement vs. Air Temperature.

vertical strain observed is less than 200 μ -strains, which is the maximum amount of strain allowed in practice before a subgrade is considered failed [Emery, 2007].

The purpose of the surface modification of the HMA pavement was to not only enhance the performance of the mixes, but also increase their design life. Using KENLAYER, the HMA was subdivided into 5 layers with each layer being assigned a different resilient modulus and Poisson's ratio based on the temperature variation between the different layers. A damage analysis was completed to assess the influence of hydrated lime on the pavement damage, which is reflected by the maximum damage ratio and the design life of the pavement in years. In practice, analyses are usually completed on single layer HMA with average properties for convenience reasons, therefore, a second analysis was completed to assess the sensitivity of the analysis to the temperature variations within the HMA layer. The allowable numbers of load repetitions are summarized in Table 7-4, which were then used to calculate the maximum damage ratio for the different cases. The results indicate the insensitivity of the analysis to temperature variations. The general trend indicates that the hydrated lime-induced-temperature-reduction increases the number the load repetitions allowed and hence, increases the design life of the pavement. A complete set of analyses results is summarized in Table 7-5.

Table 7-4: Allowable Number of Load Repetitions for All Cases.

Air Temperature (°C)	Allowable Number of Load Repetitions			
	Black		100g/m ² Lime	
	5 Layers HMA	1 Layer HMA	5 Layers HMA	1 Layer HMA
23.3	2.519E+7	2.483E+7	3.318E+7	3.297E+7
30.4	2.046E+7	2.026E+7	3.030E+7	2.987E+7
36.4	1.297E+7	1.465E+7	2.031E+7	2.014E+7

Table 7-5: Damage Analyses Results.

Air Temperature (°C)	Maximum Damage Ratio				Design Life (Yrs)			
	Black		100g/m ² Lime		Black		100g/m ² Lime	
	5 Layers HMA	1 Layer HMA	5 Layers HMA	1 Layer HMA	5 Layers HMA	1 Layer HMA	5 Layers HMA	1 Layer HMA
23.3	0.040	0.040	0.030	0.030	25.19	24.83	33.18	32.97
30.4	0.049	0.049	0.033	0.033	20.46	20.26	30.30	29.87
36.4	0.077	0.068	0.049	0.050	12.97	14.65	20.31	20.14

From the Table 7-5, the corresponding results based on 5 layers and 1 layer analyses are relatively close. This confirms that the analysis is relatively insensitive to the configuration of the system being analyzed. Due to the placement of hydrated lime on the surface of HMA, both the damage ratio and the design life of the structure are positively influenced. Based on the 5 layers analysis, surface modification of pavement reduced the damage ratio and the design life of the pavement by an average of 30 and 45%, respectively. When compared to the analysis completed considering 1 HMA layer, the damage ratio and the design life of the pavement were reduced by an average of 28 and 40%, respectively

CHAPTER 8

CONCLUSIONS AND RECOMMENDATIONS

This study investigated the thermal behaviour of hot mix asphalt, and assessed the mechanical properties of HMA that are directly affected by the surface and profile temperatures.

A 100g per one square meter dosage of hydrated lime was found to be the optimum concentration to be applied to a HMA surface in order to achieve maximum surface and profile temperatures reduction per gram of lime while avoiding the placement of excessive ineffective material. This dosage, placed on laboratory and in-situ samples, resulted in surface and profile temperatures reduction of approximately 14°C. The reduction in temperature led to improving the fatigue resistance of HMA mixes and also their temperature-sensitive mechanical properties including the resilient modulus and rut resistance as measured using the NAT and the APA, respectively. Being related to temperature, an increase in resilient modulus and rutting resistance, as a result of the temperature reduction, was observed. This increase varied depending on the HMA mixture being considered. The study also characterized the different mixes and organized them in relation to one another with respect to their resilient modulus with temperature, fatigue resistance, and their rutting susceptibility with temperature. Mixes studied were

designed differently but variables such as AC content and Performance Grade (PG) were also assessed using mixes of relatively similar designs.

It was observed, as expected, that AC content as well as its stiffness greatly influenced the resilient modulus of HMA. In other words, mixes with higher AC contents showed a more ductile behaviour when compared to those that have lower content. This is attributed to the fact that asphalt cement is a visco-elastic material. On the other hand, with increasing temperature, AC rich mixes tend to lose their stiffness modulus at a lower rate than those that are low in AC content. The Performance Grade (PG) of the asphalt cement was stipulated to be another factor contributing to the resilient modulus of asphalt mixes. Due to the polymer modification of higher PG grades, they not only improved the stiffness behaviour of the mix, but also reduced the rate at which the stiffness of a mix decreased with increasing temperature. Fatigue resistance of a mix was found to be inversely related to its resilient modulus. At low temperatures, stiff mixes have low fatigue resistance, and less stiff mixes survive longer before low temperature fatigue cracks develop.

Rutting was found to be directly related to temperature and therefore, the higher the temperature, the more the rutting. Rutting is directly related to the resilient modulus of HMA and therefore, mixes that were stiffer at high temperatures were found more

capable of resisting rutting, and vice versa. On the other hand, mixes that had a high rate of decrease of stiffness with increasing temperature showed a high rate of increase of rutting depth as temperature increased, and vice versa. Being related to resilient modulus, increasing the PG grade of asphalt cement used in a mix increased its rutting resistance. Usually, the increased richness of AC content decreases the rutting resistance of the mix at high temperatures, but if accompanied by a high percentage of 100% crushed stones, like in Stone Mastic Asphalt (SMA), its rutting resistance could increase.

The placement of hydrated lime on the surface of HMA mixes enhances the performance of pavements as well as reduces the size of maintenance required as a result of reduced damage. When performing the damage analyses, it was found that hydrated lime would extend the design life of a pavement. The addition of lime reduced the temperature of the pavement at all levels and therefore reduced its damage ratio, for a given number of load applications, by approximately 30%. Reducing the damage ratio means that the pavement survives longer and hence its design life was increased by approximately 40%.

In concluding this thesis, I would like to present some recommendations for future studies:

- An in-situ testing program should be conducted in which temperature is monitored during the four to five months of summertime and also during the winter months in order to assess the influence of hydrated lime on the de-icing process once it is placed on the surface of HMA mixes.
- In-situ testing program should be conducted with thermocouples embedded into the pavement rather than vertically installed into the pavement.
- Rutting tests should be completed in APA on samples, which have temperature gradient through depth.

REFERENCES

- Akbari, H., “Cool Construction Materials Offer Energy Savings and Help Reduce Smog”, Copied Document from JEGEL, 1995.
- Anderson, P., MacInnis, K. and Moore, G., “Stone Mastic Asphalt (SMA)-A Solution to Mitigate Rutting at Heavy Traffic Intersections and Bus Lanes”, Canadian Technical Asphalt Association Proceedings of the 47th Annual Conference, CTAA 2002, Calgary, Alberta, Polyscience Publications Inc., 2002. Page 199.
- Asphalt Institute (AI), “Chapter 10.2: The Asphalt Handbook: Soil-Subgrade Strength Evaluation Methods”, Manual Series No. 4 (MS-4), 1989 Edition. Page 419.
- Asphalt Institute (AI), “Performance Graded Asphalt Binder Specification and Testing”, Superpave Series No. 1 (SP-1), Asphalt Institute, 2003.
- Asphalt Institute (AI). “Performance Graded Asphalt Binder Specification and Testing”, Superpave Series No. 2 (SP-2), Asphalt Institute, 2003.
- ASTM Standards, “Standard Test Method for Percent Air Voids in Compacted Dense and Open Bituminous Paving Mixtures”, ASTM International, November 1994.
- Bhutta, S.A. and Davidson, K., “Rheological Properties of Modified and Unmodified Asphalt Cements”, Canadian Technical Asphalt Association Proceedings of the 45th Annual Conference, CTAA 2000, Winnipeg, Manitoba, Polyscience Publications Inc., 2000. Page 80.
- Birgisson, B., Roque, R., Drakos, C., Novak, M.E. and Ruth, B.E., “Mechanisms of Instability Rutting in Hot Mix Asphalt Pavements”, Canadian Technical Asphalt Association Proceedings of the 47th Annual Conference, CTAA 2002, Calgary, Alberta, Polyscience Publications Inc., 2002. Page 135.
- Bosscher, P. J., Bahia, H.U., Thomas, S. and Russell, J.S., “The Relation Between Pavement Temperature and Weather Data: A Wisconsin Field Study To Verify the Superpave Algorithm”, Transportation Research Board 77th Annual Meeting, Washington, D.C., January 11-15, 1998.

Brule, B., “Polymer-Modified Bitumens: Proposals for Performance Specifications”, Canadian Technical Asphalt Association Proceedings of the 44th Annual Conference, CTAA 1999, Quebec City, Quebec, Polyscience Publications Inc., 1999. Page 241.

Cabrera, J.G. and Dixon, J.R., Performance and Durability of Bituminous Materials, Second Edition, E & FN Spon, 1996. Page 55, 99.

Canadian Strategic Highway Research Program (C-SHRP), “ASPHALT: Current Issues and Research Needs”, Transportation Association of Canada, October 2000.

Carslaw, H.S. and Jaeger, J.C., “Linear Flow of Heat in The Solid Bounded by Two Parallel Planes”, Conduction of Heat in Solids, Second Edition, Oxford University Press, 1959.

Dunn, L. and Donovan, H.B., “Asphalt Mix Rutting Susceptibility Study”, Canadian Technical Asphalt Association Proceedings of the 49th Annual Conference, CTAA 2004, Toronto, Ontario, Polyscience Publications Inc., 2004. Page 497.

Dynatest International “Dynatest 3031 LWD Light Weight Deflectometer”, 2006.
[<http://www.dynatest.com>]

Emery, J., “Why Live with Ruts and Cuts?”, Canadian Technical Asphalt Association Proceedings of the 49th Annual Conference, CTAA 2004, Toronto, Ontario, Polyscience Publications Inc., 2004. Page 479.

Emery, J., “Evaluation and Mitigation of Top-Down Cracking”, JEGEL Document, 2004.

Emery, J., “Vertical Strain at Subgrade Level”, Defense Conversation, April 18, 2007.

Federal Highway Administration (FHWA), “LTPPBind V3.1”, Long Term Pavement Performance Program, United States Department of Transportation, October 2nd, 2006.
[<http://www.ltpbind.com>]

Hornby, A.S., “Oxford Advanced Learner’s Dictionary of Current English, Revised and Updated”, Oxford University Press, Oxford, 1974.

Huang, Y.H., “KENLAYER”, Pavement Analysis and Design, Second Edition, Pearson Education Inc., Upper Saddle River, NY, 2004.

Incropera, F.P. and DeWitt, D.P., “Fundamentals of Heat Transfer”, John Wiley & Sons, Inc., New York, 1981.

IPP & T., “Troubleshooting with Infrared Thermometry”, Copied Document from JEGEL, October 2004.

Irwin, L.H. and Gallaway, B.M., “Influence of Laboratory Test Method on Fatigue Test Results for Asphaltic Concrete”, Copied Document from JEGEL, 1973.

John Emery Geotechnical Engineering Limited (JEGEL) Data Sheets, “Mix Designs”, JEGEL Document, 2005.

Kandil, K., Hassan, Y. and Abd El Halim, A.O., “Effect of Pavement Overlay Characteristics on Pavement’s Long-Term Performance”, Canadian Technical Asphalt Association Proceedings of the 45th Annual Conference, CTAA 2000, Winnipeg, Manitoba, Polyscience Publications Inc., 2000. Page 287.

Kennepohl, G., Aurilio, V., Uzarowski, L., Emery, J. and Lum, P., “Ontario’s Experience with SMA and Performance to Date”, Canadian Technical Asphalt Association Proceedings of the 44th Annual Conference, CTAA 1999, Quebec City, Quebec, Polyscience Publications Inc., 1999. Page 495.

Khattak, M., Yuan, F., Mohammad, L. and Abadie, C., “A Case Study: In-Situ Layer Moduli of Pavements Using Nondestructive Testing”, Copied Document from JEGEL, 2004.

Lee, M.A. and Emery J.J., “Characterizing Asphaltic Concrete”, Canadian Technical Asphalt Association Proceedings of the 22nd Annual Conference, CTAA 1977.

Lee, M.A. and Emery J.J., “Improved Methods for Characterizing Asphaltic Concrete”, Canadian Technical Asphalt Association Proceedings of the 22nd Annual Conference, CTAA 1977.

Lesueur, D. and Little, D., “Hydrated Lime as an Active Filler in Bitumen”, Paper presented at the 78th Annual Meeting of the TRB, Washington, D.C., January 1999.

Lesueur, D. and Little, D.N., “Effects of Hydrated Lime on Rheology, Fracture and Aging of Bitumen”, Transportation Research Report 1661, Transportation Research Board, 1999.

Little, D.N. and Epps, J.A., “The Benefits of Hydrated Lime in Hot Mix Asphalt”, Report for National Lime Association, 2001.

Little, D.N., “Fundamentals of the Stabilization of Soil with Lime”, Bulletin 332, National Lime Association, 1987.

Little, D.N., “Laboratory Testing Asphalt Mixtures Incorporating Crushed River Gravel Stockpile Treated with Lime Slurry”, prepared for Chemical Lime Corporation, Texas Transportation Institute, 1994.

Little, D.N., “Hydrated Lime as a Multi-Functional Modifier for Asphalt Mixtures”, Presented at the HMA in Europe Lhoist Symposium, Brussels, Belgium, October 1996.

Long Term Pavement Performance Program LTPP, “Design Pamphlet for the Determination of Layered Elastic Moduli for Flexible Pavement Design in Support of the 1993 AASHTO Guide for the Design of Pavement Structures”, Publication No. FHWA-RD-97-077, September 1997.

Lunardini, V.J., “Heat Transfer in Cold Climates”, U.S. Army Cold Regions Research and Engineering Laboratory, Hanover, N.H., Litton Educational Publishing, Inc., New York, 1981.

McIntosh, G.B., “Infrared Thermography”, Electrical Business Newspaper, December 2004.

Miller, L.J. and Dhillon, P., “Stone Mastic Asphalt (SMA)-Hot Mix for High Stress Pavement Applications”, Canadian Technical Asphalt Association Proceedings of the 48th Annual Conference, CTAA 2003, Halifax, Nova Scotia, Polyscience Publications Inc., 2003. Page 253.

Mohseni, A. and Symons, M., “Effect of Improved LTPP AC Pavement Temperature Models on Superpave Performance Grades”, Transportation Research Board 77th Annual Meeting, Washington, D.C., January 11-15, 1998.

National Lime Association, “Hydrated Lime - Solution for High Performance Hot Mix”, National Lime Association Paper, October 2001.

National Lime Association, “Hydrated Lime - More than Just a Filler”, National Lime Association Paper, May 2001.

National Lime Association, “Using New Pavement Design Procedures for HMA Mixtures Modified with Hydrated Lime”, National Lime Association Paper, 2004.

National Lime Association, “Lime Terminology, Standards & Properties”, National Lime Association Fact Sheet, May 2004.
[<http://www.lime.org>]

National Lime Association, “How to Add Hydrated Lime to Asphalt: An Overview of Current Methods”, National Lime Association Paper, September 2003.

Omega Canada, “Fine Gage Bare Wire and Insulated Thermocouples”, 2002.
[<http://www.omega.ca/shop/subsectionsc.asp?subsection=A02&book=Temperature>]

OPSS, “Ontario Provincial Standards for Roads and Public Works”, Ontario Provincial Standards Specifications, OPSS 1003, Ontario Ministry of Transportation, Downsview, Ontario, April 2005.

OPSS, “Ontario Provincial Standards for Roads and Public Works”, Ontario Provincial Standards Specifications OPSS 1151, Ontario Ministry of Transportation, Downsview, Ontario, April 2005.

OPSS, “Field Requirement for Compaction,” Ontario Provincial Standards Specifications, OPSS 310, Ontario Ministry of Transportation, Downsview, Ontario, April 2005.

Pavement Design Course Notes, 4G03, “Asphalt Technology: Stone Mastic Asphalt (SMA)”, McMaster University, January 2005.

Petersen, J.C., Plancher, H. and Harnsberger, P.M., “Lime Treatment of Asphalt to Reduce Age Hardening and Improve Flow Properties”, AAPT, Volume 56, 1987.

Petersen, J.C., “Lime Treated Pavements Offer Increased Durability”, Lime Notes, Issue Number 3, Fall 1988.

Potts, J.M., “An Investigation of the Thermal Stresses within Soderberg Electrodes”, Masters of Engineering Thesis, McMaster University, Hamilton, Ontario, Appendix 5, 1999.

Roberts, F.L., Kandhal, P.S., Brown, E.R., Lee, K.W. and Kennedy, T.W., Hot Mix Asphalt Materials, Mixture Design and Construction, Second Edition, NAPA Research and Education Foundation, 1996.

Saleh, M. and Ji, S.J., “Factors Affecting Resilient Modulus”, Copied Document from JEGEL, 2004.

Shell Bitumen, “Chapter 15: The mechanical properties of bituminous mixes”, Shell Bitumen Handbook, 1990. Page 235.

St-Jacques, M. and Brosseaud, Y., “A Case Study: Coloured Bituminous Wearing Courses in France, Overview of Uses”, Copied Document from JEGEL, 2001.

Tarefder, R.A., Zaman, M., Hobson, K. and Toney, R., “Evaluation of Relative Weights of Rutting Parameters”, Canadian Technical Asphalt Association Proceedings of the 47th Annual Conference, CTAA 2002, Calgary, Alberta, Polyscience Publications Inc., 2002. Page 119.

Tarrer, R., “Use of Hydrated Lime to Reduce Hardening and Stripping in Asphalt Mixes”, 4th Annual ICAR Symposium, Atlanta, Georgia, 1996.

The Toronto Star, “Paler Roofs Pitched To Fight Heat”, July 22nd, 2005.

Transportation Association of Canada TAC, “Moisture Damage of Asphalt Pavements and Antistripping Additives”, 1997.

Thom, N., “Asphalt Cracking: A Nottingham Perspective”, Nottingham Centre for Pavement Engineering, University of Nottingham, November 26, 2006
[http://www.civil.uminho.pt/cec/revista/Num26/n_26_pag_75-84.pdf]

Uzarowski, L. and Emery, J., “Use of The Asphalt Pavement Analyzer for Asphalt Mix Design and Evaluation”, Canadian Technical Asphalt Association Proceedings of the 45th Annual Conference, CTAA 2000, Winnipeg, Manitoba, Polyscience Publications Inc., 2000. Page 382.

Vallerga, B.A., Tayebali, A.A. and Monismith, C.L., “Early Rutting of Asphalt Concrete Pavement Under Heavy Axle Loads in Hot Desert Environment: Case History”, 1995.

Wikipedia Encyclopedia, “Albedo”, December 29, 2006.
[<http://en.wikipedia.org/wiki/Albedo>]

Wikipedia Encyclopedia, “Constantan”, April 18, 2007.
[<http://en.wikipedia.org/wiki/Constantan>]

Yoder, E.J. and Witczak, M.W., Principles of Pavement Design, Second Edition, John Wiley & Sons Inc., New York, 1975. Page 24, 243.

APPENDIX A

SAMPLE CALCULATION

The following is a sample calculation used to estimate the initial amount (mass) of asphalt material to be used in order to yield the targeted percent of air voids of the specimen once it is produced.

Targeted Specimen Dimensions:

- Length = 300 mm
- Width = 125 mm
- Height = 78 mm

Maximum Theoretical Relative Density of the Asphalt Mix being used:

- MRD = 2.528

Targeted Percent of Air Voids:

- Percent Compaction of MRD = 93
- % Air Voids = $100 - 93 = 7$

Initial Mass of Material to yield Target Properties:

- $300 * 125 * 78 * 0.93 * 2.528 = 6876.8$ grams.
- The calculated mass was rounded to 6880 grams for added convenience of weighing the material, and to also allow for the small amount of material lost on the weighing dish and on the pan after transferring the material to the compaction mould.
- Prepared specimens were tested for actual percent of air voids.
 - If % Air voids_{actual} > % Air voids_{target}, more material was added.
 - If % Air voids_{actual} < % Air voids_{target}, some material was removed.
 - A trial-and-error process was used to estimate the amount of material added or removed.

APPENDIX B

TESTING PROCEDURES

1. Testing of Air Voids

- Before starting the test, the water in the pail had to be at room temperature (25°C).
- The sample tested was weighed in air (A_1) and then placed in the water pail on a pan hanging from the scale. The sample had to be completely covered with water and kept submerged for five minutes. Once this time was over, the scale reading representing the weight of the sample in water was recorded (B_1).
- The sample was then taken out of the water and the excess surface water was wiped with a towel to put the sample in a saturated surface dried (SSD) condition. The sample was then placed on the scale to take the SSD weight reading (A_2).
- The following calculations were made using the maximum theoretical relative density of the mix (MRD) to obtain the percent voids of the sample.
 - $B_2 = \text{Volume} = A_2 - B_1$
 - $C = \text{Bulk Relative Density} = A_1/B_2$
 - $\text{Percent of Air Voids} = [(MRD - C)/MRD]*100$

2. Resilient Modulus Testing in the NAT

In general, the specimen setup procedural instructions are as follows:

- The specimen was placed centrally within the cradle formed by the alignment jig crossbars and the lower loading strip.
- The LVDTs were retracted in the yoke using the knurled adjusters and the yoke was placed centrally over the specimen so that it rests on the alignment jig crossbars.
- Using the four brass and nylon clamping screws, the yoke was clamped to the specimen so that the specimen is centrally located within, and parallel to the yoke.
- The subframe crosshead was taken and slid down the subframe slidebars until the top loading strip was centrally located on the specimen and made sure that the slide bars were centrally located in the crosshead slots.
- The half ball bearing was placed in the conical hole in the subframe crosshead and the load cell centrally on the ball bearing located at the top of the subframe crosshead.
- The fatigue resistance test computer software was run.
- Specimen information such number and the file name where the data is to be stored were inserted.

- The diameter and thickness of the specimen being tested were measured at different locations on the specimen and an average diameter and thickness were inserted into the software as input.
- The temperature the specimen being tested at was set to either 10°C, 20°C, or 30°C \pm 0.5°C.
- The target rise time was set to 120 milliseconds and the average deflection to 5 μ m.
- Before the start of the test, five conditioning pulses were run to settle the specimen correctly inside the chamber. A reading of roughly 120 for the rise time and 5 μ m for the average deflection obtained as a result of the five conditioning pulses indicates that the test is being run correctly and it is fine to proceed.
- The test was then started and the results of five testing pulses (rise time, average deflection, and resilient modulus) were saved after which an average was calculated and displayed on the screen.

3. Fatigue Resistance Testing in the NAT

In general, the specimen setup procedural instructions are as follows:

- The specimen was placed centrally within the cradle formed by the alignment jig crossbars and the lower loading strip.

- The subframe crosshead was taken and slid down the subframe slidebars until the top loading strip was centrally located on the specimen and made sure that the slide bars were centrally located in the crosshead slots.
- The half ball bearing was placed in the conical hole in the subframe crosshead and the load cell centrally on the ball bearing located at the top of the subframe crosshead.
- The LVDT's were tied to the slide bars above the top loading strip and made sure they were resting on the circular loading plate placed over the half ball bearing transferring the load to the subframe crosshead. This was to measure the vertical deformation of the specimen in response to the vertical loading through the timely pulses.
- The fatigue resistance test computer software was run. Specimen information such number and the file name where the data is to be stored were inserted.
- The diameter and thickness of the specimen being tested were measured at different locations on the specimen and an average diameter and thickness were inserted into the software as input.
- The temperature the specimen being tested at was set to $20^{\circ}\text{C} \pm 0.5^{\circ}\text{C}$.
- The target rise time was set to 120 milliseconds.
- Before the start of the test, five conditioning pulses were run to settle the specimen correctly inside the chamber. A reading of roughly 120 for the rise indicated that the test was being run correctly and it is fine to proceed.

- The test was then started and the specimen was loaded with pulses until failure represented by vertical crack along the entire diameter of the specimen. The complete set of raw data including the deformation and the number of pulses to failure were automatically saved to an Excel file.

4. Rutting Resistance Testing in the APA

In general, the specimen setup procedural instructions are as follows:

- Set the hose pressure gap reading to 700 ± 35 kPa (100 ± 5 psi). Set the load cylinder pressure reading for each wheel to achieve a load of 445 ± 22 N (100 ± 5 lbf).
- Stabilize the testing chamber temperature at the temperature selected for testing the specimens at.
- Secure preheated, molded specimens in the APA. The preheated APA chamber should not be open more than six minutes when securing the test specimens into the machine.
- In order to create a temperature gradient within the sample along the vertical direction, the surface of the specimens being tested was preheated using a vehicle paint curing lamp to a temperature that was 5°C higher than the testing temperature equal to that pre-set in the APA chamber. This was to allow for

any heat loss while setting up the samples in the APA and getting them ready for testing.

- Place the samples in the testing moulds and push the sample holding tray in and secure it. Close the chamber doors, and allow ten minutes for the temperature to re-stabilize prior to starting the test.
- Start the APA testing software on a computer attached to the machine and input the specimens' information.
- Apply fifty cycles to seat the specimens before the initial measurements.
- Set the preset counter to 8000 cycles.
- Start the test. When the test reaches 8000 cycles, the APA will stop, and the load wheels will automatically retract.
- The testing results, which include the rut depth for each cycle number, are automatically saved into the computer in the form of an Excel file for future analysis and manipulations.

APPENDIX C

COLLECTED RAW DATA**1. Profile Temperature Monitoring****Table 1:** Summary of Laboratory Temperature Profile Readings
for Different Hydrated Lime Amounts with Time.

Time (Hours)	Temperature (°C) of Black (Unmodified) Pavement at Various Depths*				Temperature (°C) of Pavement Modified with 100g/m ² of Hydrated Lime at Various Depths*			
	5 mm	25 mm	45 mm	65 mm	5 mm	25 mm	45 mm	65 mm
0.00	30.10	26.20	21.80	17.20	21.80	17.30	22.40	14.40
0.08	31.90	28.80	24.30	19.40	23.90	19.80	24.60	16.80
0.50	37.50	35.00	31.10	27.70	29.40	26.50	29.10	22.60
0.75	39.80	36.80	34.40	30.50	32.20	29.60	31.90	26.00
1.00	40.40	37.10	35.70	37.80	33.20	30.80	32.50	27.20
1.50	41.20	37.30	35.90	38.00	33.70	31.50	32.60	28.70
2.00	43.90	39.20	38.60	39.50	34.60	33.00	33.70	28.70
2.50	44.10	39.70	39.30	40.90	37.20	35.30	36.50	32.20
3.25	47.40	40.50	46.40	42.50	38.70	36.70	38.50	33.60
4.00	49.90	43.90	49.70	43.50	41.20	39.70	39.50	36.90
4.75	53.40	45.80	50.80	45.80	43.30	41.70	41.40	38.00
5.25	61.10	55.30	56.20	54.30	49.80	49.20	48.40	45.30
6.00	62.40	57.40	56.80	55.00	50.70	49.30	48.50	45.80

* Measured from pavement surface.

Table 2: Summary of In-situ Temperature Profile Readings
for Different Hydrated Lime Amounts with Time.

Time (Hours)	Temperature (°C) of Black (Unmodified) Pavement at Various Depths*		Temperature (°C) of Pavement Modified with 100g/m ² of Hydrated Lime at Various Depths*	
	10 mm	30 mm	10 mm	30 mm
0.00	35.00	28.70	28.10	30.70
0.08	36.80	30.40	29.60	32.20
0.25	37.30	31.70	29.60	32.50
0.50	39.20	34.60	31.10	33.60
0.75	42.40	37.70	33.50	36.00
1.00	42.80	38.80	34.00	36.30
1.25	43.80	40.00	34.50	36.40
2.00	46.20	42.20	36.10	38.40
2.75	47.60	43.60	37.10	39.20
3.50	48.00	43.90	40.20	39.60
4.50	50.40	46.10	44.00	42.10
5.00	51.8	48.1	45.8	43.8

* Measured from pavement surface.

2. Rutting Histories from Testing in the APA

Table 3: Rutting History of all Mixes at 52°C.

Cycle Number	Average Permanent Deformation (mm)			
	SP12.5FC2PG64-28	SP12.5FC2PG70-28	SP19	SMA
0	0.0000	0.0000	0.0000	0.0000
200	0.5210	0.2501	0.3729	0.3031
400	0.6698	0.3091	0.4997	0.3844
600	0.7756	0.3646	0.5598	0.4250
800	0.8488	0.3925	0.6564	0.4607
1000	0.9087	0.4296	0.7132	0.4705
2000	1.1342	0.5896	0.9474	0.6164
4000	1.5602	0.8533	1.3707	0.7822
6000	2.2152	1.0917	1.8735	0.9233
8000	2.8093	1.3666	2.3616	1.0392

Table 4: Rutting History of all Mixes at 58°C.

Cycle Number	Average Permanent Deformation (mm)			
	SP12.5FC2PG64-28	SP12.5FC2PG70-28	SP19	SMA
0	0.0000	0.0000	0.0000	0.0000
200	0.1692	0.3186	0.3767	0.2697
400	0.2983	0.4325	0.5307	0.3222
600	0.4300	0.5050	0.6155	0.3651
800	0.6036	0.5599	0.6823	0.4185
1000	0.7487	0.6007	0.7483	0.4661
2000	1.5838	0.8368	0.9942	0.6114
4000	2.8439	1.1770	1.4525	0.8951
6000	3.7524	1.5107	2.0987	1.1132
8000	4.6942	1.8465	2.8475	1.3170

Table 5: Rutting History of all Mixes at 64°C.

Cycle Number	Average Permanent Deformation (mm)			
	SP12.5FC2PG64-28	SP12.5FC2PG70-28	SP19	SMA
0	0.0000	0.0000	0.0000	0.0000
200	1.1778	0.4283	0.6561	0.3763
400	1.5985	0.5660	0.9078	0.4732
600	1.8997	0.6489	1.0558	0.5340
800	2.1270	0.7409	1.1820	0.6109
1000	2.3451	0.8086	1.2885	0.6682
2000	3.3296	1.0492	1.6865	0.8540
4000	4.9133	1.6236	2.6148	1.1439
6000	6.2442	2.4921	3.4486	1.4179
8000	7.3846	3.2642	4.1351	1.7108

Table 6: Rutting History of all Mixes at 70°C.

Cycle Number	Average Permanent Deformation (mm)			
	SP12.5FC2PG64-28	SP12.5FC2PG70-28	SP19	SMA
0	0.0000	0.0000	0.0000	0.0000
200	0.8789	0.4082	0.6029	0.2682
400	1.2243	0.5807	0.8446	0.3156
600	1.4973	0.6446	0.9710	0.3492
800	1.6782	0.6982	1.1018	0.3778
1000	1.8650	0.7804	1.2163	0.4137
2000	2.6665	1.0532	1.7488	0.5716
4000	4.3156	1.6267	2.6757	0.8484
6000	5.7383	2.8967	3.7475	1.0447
8000	7.0551	3.8223	4.6743	1.3619